Toll signaling enhances mosquito antiplasmodial immunity by promoting differentiation of hemocytes to the Megacyte lineage

Ana Beatriz Barletta Ferreira[1], Banhisikha Saha[1], Nathanie Trisnadi[1#], Gianmarco Raddi[1#], and Carolina Barillas-Mury[1*].

[1]Laboratory of Malaria and Vector Research, National Institute of Allergy and Infectious Diseases, National Institutes of Health, Rockville, MD 20852.

[#] Present address: Nathanie Trisnadi, Atropos Therapeutics Inc., San Carlos, California, USA. Gianmarco Raddi, School of Clinical Medicine, University of Cambridge, Cambridge CB2 0SP, UK, CRUK Cambridge Institute, Cambridge CB2 0RE, UK.

* Correspondence should be addressed to: cbarillas@niaid.nih.gov (CB-M)

Abstract

Activation of Toll signaling in *Anopheles gambiae*, by silencing Cactus, eliminates *Plasmodium* ookinetes by enhancing local release of hemocytes-derived microvesicles that promote activation of the mosquito complement-like system. A new effector hemocyte subpopulation of large granulocytes, the megacytes, was recently identified. We report that Cactus silencing dramatically increases the proportion of megacytes, from 5 to 79% of circulating granulocytes. Transcriptomic and morphological analysis, as well as *in situ* hybridization and expression of cell-specific markers, indicate that Cactus silencing triggers granulocyte differentiation into megacytes. Megacytes are very plastic cells that can extend long filopodia and tend to form clusters *in vivo*. Moreover, megacytes are massively recruited to the basal midgut surface in response to bacterial feeding and *Plasmodium* infection. We propose that Toll signaling promotes differentiation of granulocytes to the megacyte lineage, a major cellular effector of antibacterial and antiplasmodial immunity.

Introduction

Ookinete traversal of the *Anopheles gambiae* midgut disrupts the peritrophic matrix, a chitinous network that surrounds the blood meal, and that normally prevents bacteria of the gut microbiota from coming in direct contact with epithelial cells (Kumar et al., 2010). Contact of midgut epithelial cells with bacteria, or their immune elicitors, triggers the release of prostaglandin E2 (PGE2), which attracts hemocytes to the basal surface of the midgut (Barletta et al., 2019). *Plasmodium* ookinete midgut traversal also causes irreversible damage to invaded cells and triggers a strong caspase-mediated nitration response (Han et al., 2000, Oliveira Gde et al., 2012, Trisnadi and Barillas-Mury, 2020). Hemocytes patrolling the midgut undergo apoptosis and

38 release hemocyte-derived microvesicles (HdMv) if they come into contact with an area of the
39 midgut basal lamina that has been nitrated (Castillo et al., 2017). HdMv release promotes local
40 activation of the mosquito complement-like system (Castillo et al., 2017), a major final effector of
41 antiplasmodial immunity that binds to the parasite's surface and forms a complex that ultimately
42 lyses the ookinete (Blandin et al., 2004).

43 Overactivation of *Toll* signaling in *A. gambiae* mosquitoes by silencing *Cactus*, an inhibitor
44 of this pathway (Frolet et al., 2006), elicits a very strong complement-mediated immune response
45 that eliminates *Plasmodium berghei* ookinetes (Frolet et al., 2006). Hemocytes mediate this
46 enhanced immune response, as transfer of *Cactus*-silenced hemocytes into naïve mosquitoes
47 recapitulates the phenotype of systemic *Cactus* silencing (Ramirez et al., 2014). Furthermore,
48 cactus silencing increases HdMv release in response to ookinete midgut invasion (Castillo et al.,
49 2017), indicating that hemocytes are more reactive to *Plasmodium* infection. However, the
50 mechanism by which activation of the *Toll* pathway enhances hemocyte responses to *Plasmodium*
51 is not clear.

52 Hemocytes are classified into three cell types, prohemocytes, oenocytoids and
53 granulocytes, based on their morphology. However, single cell RNA sequencing (sc-RNAseq)
54 analysis of *An. gambiae* hemocytes identified several novel subpopulations of granulocytes based
55 on their transcriptional profiles, and defined molecular markers specific for hemocyte
56 subpopulations (Raddi et al., 2020). Furthermore, Lineage analysis revealed that regular
57 granulocytes derive from prohemocytes and can further differentiate into distinct cell types,
58 including dividing granulocytes, and two final effector cells, megacytes and antimicrobial (AM)
59 granulocytes (Raddi et al., 2020). Here explore the role of Toll signaling on mosquito hemocyte
60 differentiation and their response to infection with bacteria and *Plasmodium* parasites.

Results

Cell dynamics of mosquito granulocytes

Megacytes are present in low abundance (~1-2% of hemocytes) in sugar fed females. They are large cells, five times larger than regular granulocytes, and express a specific transmembrane protein marker (TM7318) (Raddi et al., 2020). Regular granulocytes (Fig. 1A) reach an average diameter of 14.2 μm (Fig. 1B) when they spread over a glass surface, while the average diameter of megacytes is 28.6 μm ($p<0.0001$, Unpaired T-test) (Fig. 1A and 1B). Granulocyte cellular dynamics were evaluated by live imaging of perfused hemocytes *in vitro* as they adhered and spread on a glass surface. Hemocytes were labeled *in vivo*, through systemic injection of adult females with a red lipophilic dye (Vybrant CM-DiI) that accumulates on intracellular vesicles. A green, fluorescent probe (Cell Mask) was added after perfusion to label the plasma membrane. Both regular granulocytes and megacytes attached to the glass surface and spread fully within one hour (Videos S1-S4). Megacytes already have a larger cell diameter when they first attach to glass (Fig. 1C, upper panel and Video S3), and exhibit a peripheral "halo", corresponding to an area of extended thin cytoplasm cell, almost devoid of vesicles (Fig. 1C, upper panel and Video S3). Lateral views revealed that, initially, megacytes have a large nucleus and a voluminous cytoplasm in the central region of the cell that flattens dramatically as the cell "spreads" over the glass surface (Fig. 1C, lower panel and Video S4). In contrast, the central region of regular granulocytes remains unchanged in (Fig. 1D, lower panel and Video S2) and the periphery of the cell exhibits a modest increase in diameter as the cell spreads along the surface (Fig. 1D, upper panel and Video S1).

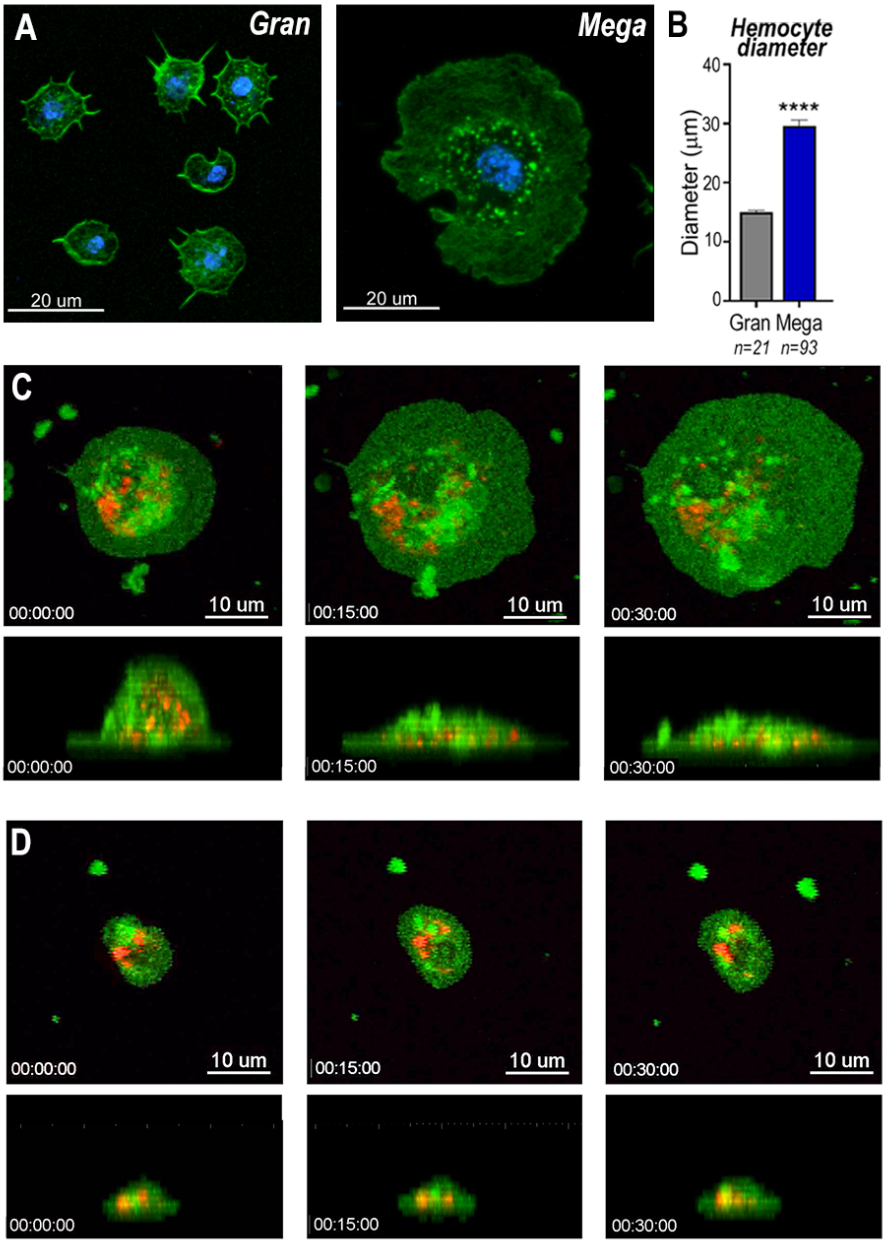

Fig.1: Megacyte and granulocyte cell dynamics. (A) Regular granulocytes and megacytes from *An. gambiae* females spread on a glass surface. Actin, green (phalloidin) and nuclei, blue (Hoechst). Scale bar: 20um. (B) Granulocyte diameter of sugar-fed mosquitoes after spreading on a glass surface. Error bars represent mean± SEM. Unpaired t-test. ****P≤0.0001. (C) Live imaging time-lapse of a megacyte spreading in a glass surface for 30 minutes. Plasma membrane stained in green and microvesicles in red. Top (XY) and lateral view (XZ) of a megacyte. Scale Bars: 10um and 5um, respectively. (D) Live imaging time-lapse of a megacyte spreading on a glass surface for 30 minutes. Top (XY) and lateral view (XZ) of a regular granulocyte. Scale Bars: 10um and 5um, respectively.

Effect of *Toll* signaling activation on mRNA markers of granulocyte populations.

The effect of *Toll* signaling on hemocyte differentiation was explored by silencing Cactus, an inhibitor of the Toll pathway. Hemocytes that adhered to glass (mostly granulocytes) or that remain in suspension (mostly prohemocytes and oenocytoids) were collected 4 days post-injection from *dsLacZ* control and *dsCactus*-injected females. Bulk sequencing of cDNA libraries generated between 16.2 and 25.3 million fragments that mapped to the *Anopheles gambiae* AgamP4.9 transcriptome. Only transcripts with 10 or more reads were included in the analysis, resulting in a total of 9,421 unique transcripts (Accession E-MTAB-11252). Glass-bound and unbound hemocyte samples were analyzed together, because the differences in expression between ds*LacZ* *vs* ds*Cactus*-silenced hemocytes explained 81% of the variance between the four experimental groups (Fig. S1A and S1B). Differential expression (DE) analysis of *Cactus*-silenced hemocytes using the DESeq2 software, identified 1071 differentially expressed genes (Q-value < 0.001), of which 407 were upregulated (log2 fold change >2), while 664 were downregulated (log2 fold change < -2) (Fig 2A).

The effect of Cactus silencing on expression of the transcripts that define the different hemocyte clusters established by (sc-RNAseq) (Raddi et al., 2020) was analyzed (Tables S1 and S2), to establish whether there was a significant effect on the relative abundance of specific hemocytes subpopulations. Overall, 23 oenocytoid markers, 2 from prohemocytes and 57 from granulocytes were differentially expressed between dsLacZ and dsCactus hemocytes (Tables S1 and S2). Most differentially expressed oenocytoid markers 22/23 (95%) were down-regulated, while one of the prohemocyte markers was up-regulated and the second one down-regulated (Fig. 2B). The number of down-regulated granulocyte markers 28/57 (49%) was very similar to that of up-regulated ones 29/57 (51%). However, detailed analysis of granulocyte subpopulations

114 revealed that most up-regulated markers 18/29 (62%) correspond to megacytes, while most down-
115 regulated markers correspond to regular granulocytes 21/28 (75%). This suggests that ds*Cactus*
116 silencing increases the proportion of circulating megacytes, at the expense of a reduction in regular
117 granulocytes.
118
119
120
121
122
123
124
125
126
127
128
129
130
131
132
133
134
135
136

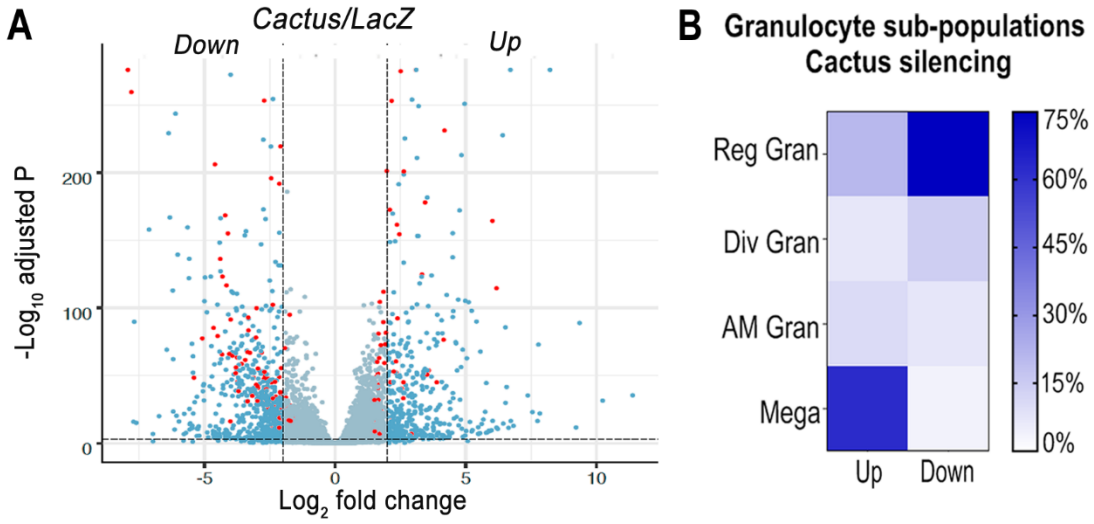

Fig.2: Effect of *Toll* pathway activation on mRNA markers of granulocyte populations. (A) Differential expression of Cactus dsRNA knockdown. From a total of 9421 filtered genes. Volcano plot of DE genes in Cactus silenced hemocytes compared to LacZ control filtered for log2 fold change > 2 and Q-value <0.001. Dark blue dots on the right represent upregulated DE genes and on the left the downregulated ones. Red dots show genes that are hemocytes specific markers. Complete list of up and down regulated genes is listed in Tables S1 and S2. (B) Percentage of granulocyte sub-population markers up and downregulated in Cactus silenced hemocytes. Complete list of up and down regulated genes for each hemocyte subpopulation is in Tables S1 and S2.

158 **Cactus silencing promotes granulocyte differentiation into megacytes**

159 Cactus silencing did not significantly increase the proportion of total circulating
160 granulocytes, based on hemocyte counts by light microscopy (Ramirez et al., 2014), suggesting
161 that the observed enhanced immune response could be due to functional changes in hemocytes.
162 The morphology of hemocytes perfused from *Cactus*-silenced females was analyzed using
163 fluorescent probes to stain the actin cytoskeleton and the nucleus. *Cactus* silencing dramatically
164 increased the proportion of large granulocytes (diameter > 40 μm), presumably megacytes, from
165 5.3% to 79.2% ($p<0.0001$, X^2 test) (Fig. 3A and B), in agreement with the observed increase in
166 up-regulated megacyte-specific markers in the transcriptomic analysis of Cactus-silenced
167 hemocytes (Fig. 2B). Interestingly, megacytes from *Cactus*-silenced mosquitoes (Fig. 3A) and are
168 even larger (average diameter of 47 μm after spreading in a glass surface) than megacytes from
169 dsLacZ controls (average diameter of 30 μm) (Figure 3C and D). *In situ* RNA hybridization of
170 dsCactus granulocytes with a fluorescent probe for the megacyte-specific marker TM7318,
171 confirmed that the proportion of TM7318-positive granulocytes was much higher (80%) in Cactus-
172 silenced females than in dsLacZ controls (4%) ($p<0.0001$, X^2 test) (Fig. 3E and F), providing direct
173 evidence that overactivation of *Toll* signaling triggers a dramatic increase in the proportion of
174 circulating megacytes. Expression analysis of the TM7318 marker in perfused hemocyte samples
175 confirmed that mRNA levels were 42-fold higher in dsCactus hemocytes than the dsLacZ control
176 group ($p<0.001$, T-test) (Fig. 3G), while a modest increase (2.8-fold) in FBN50 mRNA, a marker
177 of antimicrobial (AM) effector granulocytes, was observed ($p<0.0001$, T-test). Conversely,
178 expression of FBN11228, a marker of regular granulocytes, decreased by 30-fold in circulating
179 hemocytes of Cactus-silenced mosquitoes (Fig. 3G). The changes in the relative abundance of

mRNAs from cell-specific markers in dsCactus-hemocytes coincides with the observed changes in hemocyte morphology and the *in situ* hybridization and transcriptomic data (Fig. 3G).

The relative increase in megacytes in *Cactus*-silenced *An. gambiae* females could be due to enhanced megacyte proliferation or to increased differentiation of regular granulocytes into megacytes. The effect of *Cactus*-silencing on granulocyte proliferation was evaluated by quantitating the proportion of hemocytes that incorporated Bromodeoxyuridine /5-bromo-2'-deoxyuridine (BrdU), a thymidine analog. The proportion of BrdU+ hemocytes that adhered to glass (mostly granulocytes) in *dsCactus* mosquitoes (51%, n=694 cells) is not significantly different from *dsLacZ* controls (52%, n=410 cells) (Fig. S2A and B). BrdU fluorescence intensity (RFU) is also not significantly different between *dsLacZ* and *dsCactus* hemocytes (Fig. S2C). However, the ratio of BrdU fluorescence intensity to nuclear volume is significantly lower in *dsCactus* hemocytes (Fig. S2D). This indicates that the increase in nuclear volume in megacytes does not involve DNA replication. These observations, together with the increase in the proportion of megacytes in *dsCactus* females, at the expense of other regular granulocytes (Fig. 2B and 3G), indicate that activation of *Toll* signaling promotes differentiation of granulocytes towards the megacyte lineage.

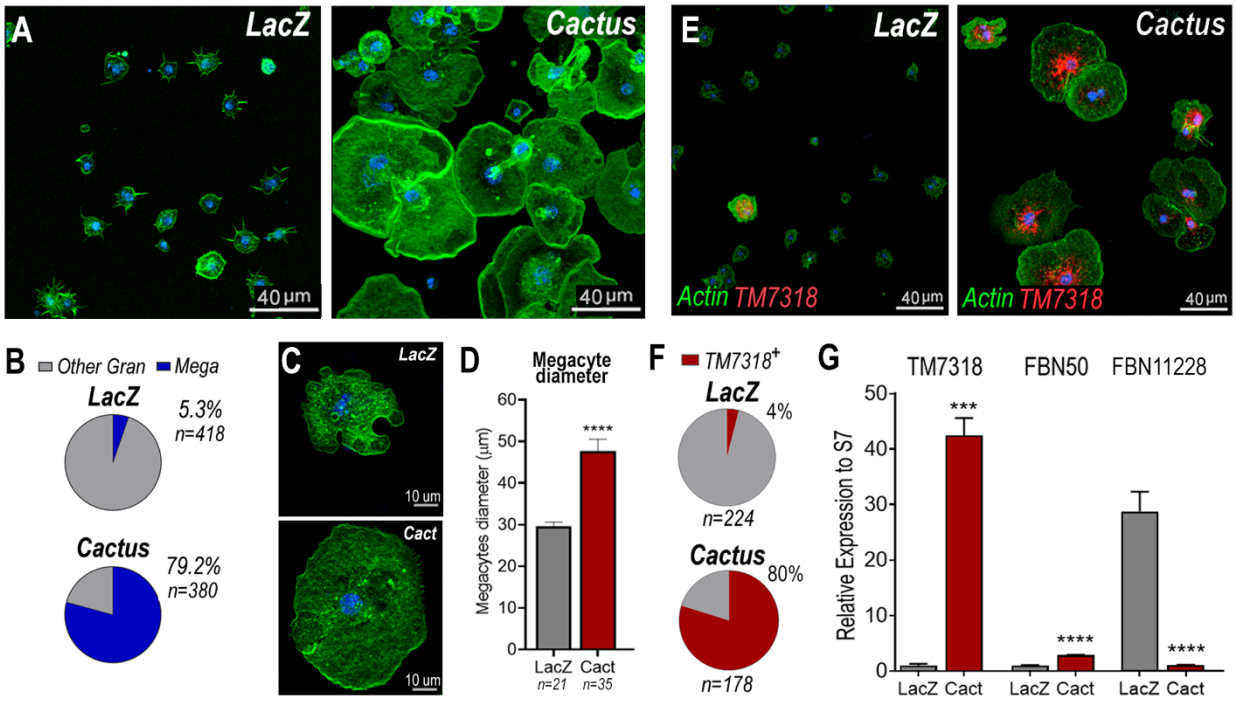

Fig.3: Cactus silencing promotes granulocyte differentiation into megacytes. (A) *An.gambiae* hemocytes in LacZ control and Cactus attached to a glass surface. Actin is showing in green and nuclei in blue. Scale Bar: 40um. (B) Percentage of megacytes among all granulocytes in dsLacZ and dsCactus mosquitoes. Percentages were compared using X^2 test. ****P≤0.0001. (C) Megacyte in control LacZ mosquitoes (upper) and in Cactus-silenced mosquitoes (lower). Actin is showing in green, and nuclei is in blue. Scale Bar: 10um. (D) Diameter of megacytes from LacZ control and Cactus-silenced mosquitoes. Error bars represent mean± SEM. Unpaired t-test. ****P≤0.0001. (E) RNA *in situ* hybridization for megacyte specific marker TM7318. Actin is showing in green (phalloidin), TM7318 mRNA in red and the nuclei in blue (Hoechst). Scale bar: 40um. (F) Percentage of TM7318 positive cells in LacZ and Cactus silenced granulocytes. Percentages were compared using X^2 test. ****P≤0.0001. (G) Relative mRNA expression of hemocyte specific markers in LacZ control and Cactus hemocytes for transcriptome validation. Megacyte marker (TM7318), antimicrobial granulocytes (FBN50) and regular granulocytes (FBN11228). Gene expression was normalized using RpS7 expression. Error bars represent mean ± SEM. Unpaired t-test, ****P≤0.0001.

Toll signaling-mediated megacyte differentiation is partially dependent on LL3

Single cell sequencing revealed high expression of the LPS-induced TNFα transcription factor (LITAF)-like 3 (LL3) mRNA in megacytes, and LL3-silencing abrogated the ability of hemocytes to respond to systemic injection of HDF-containing hemolymph (Raddi et al., 2020). The potential interaction between of LL3 and Toll-mediated megacyte differentiation was explored by co-silencing Cactus and LL3 by dsRNA injection. LL3 silencing alone had no significant effect in the proportion of megacytes (Fig. S3). As expected, Cactus-silencing greatly increased the proportion of megacytes from 1% in the dsLacZ control to 68% ($p<0.0001$, X^2 test); while co-silencing LL3 and Cactus resulted in an intermediate phenotype, with a partial, but significantly, reduction in the proportion of megacytes from 68% to 34.3% ($p<0.0001$, X^2 test) (Fig. S3B). This indicates that Toll-mediated differentiation of regular granulocytes into megacytes is partially dependent on LL3, and suggests that there may be an alternative LL3-independent pathway that remains to be identified.

Characterization of megacyte *in vivo* dynamics and ultrastructure

The effect of *Cactus* silencing on granulocyte dynamics was evaluated *in vivo*, through live imaging within adult female mosquitoes. Female mosquitoes were imaged for 2h, one day after blood feeding on a healthy mouse. Hemocytes were visualized by systemic injection of Vybrant CM-DiI, a fluorescent lipophilic dye that is preferentially taken up by granulocytes. Circulating hemocytes in dsLacZ females (presumably normal granulocytes) have a smaller diameter than those of dsCactus females (Videos S5 and S6) (Fig. 1A and B) and they seldom come in contact with each other as they patrol the basal surface of the midgut (Video S5). Hemocytes from dsCactus females (presumably megacytes) are larger and have a spindle shape (Fig.1A and B,

247 Videos S3 and S4). They appear to have higher plasticity, as they can readily stretch their
248 cytoplasm and they often come into contact with each other (Videos S6). The plasticity of
249 dsCactus megacytes was confirmed by *in vitro* live imaging of perfused hemocytes labeled by
250 systemic injection of Vybrant CM-DiI and green Cell Mask. Some megacytes from dsCactus
251 mosquitoes projected long thin filopodia towards other megacytes (Video S7). This process was
252 not observed in regular granulocytes or in megacytes from the dsLacZ controls. Taken together,
253 our live imaging data indicates that, in addition to their larger diameter (Fig. 3C and D), dsCactus
254 megacytes are also more active, have increased plasticity as they patrol the midgut (Video S6),
255 and greater tendency to interact with each other and form clusters (Videos S6 and S7).

256 The detailed ultrastructure of megacytes was explored using Transmission Electron Microscopy
257 (TEM). Hemocytes from Cactus silenced females were collected by perfusion, allowed to settle
258 and fixed in suspension. As expected, the maximum diameter of hemocytes fixed while in
259 suspension was smaller than when they were allowed to spread on a glass surface. Regular
260 granulocytes were still significantly smaller (6-10 µm) than megacytes (15-20 µm), with nuclei
261 that are also proportionally smaller (Fig. 4A and B). Extensive electrodense areas are observed in
262 the nuclei of megacytes, probably corresponding to the nucleolus. Large numbers of cytoplasmic
263 vacuoles that contain abundant amorphous material are observed, as well as an extensive
264 mitochondrial network (Fig. 4A and B). Mitochondrial organization of perfused hemocytes was
265 further investigated using Mitotracker staining. Mitochondria of regular granulocytes have a
266 punctate pattern with strong staining on individual organelles (Fig. 4D). In contrast, megacytes
267 exhibit a more diffuse and extensive mitochondrial network (Fig. 4E). It is noteworthy that large
268 membrane-bound mitochondria-like extracellular structures and small vesicles are often observed

269 "budding off" from the surface of dsCactus megacytes (Fig. 4B-C), but not from regular
270 granulocytes (Fig. 4A).

271

272

273

274

275

276

277

278

279

280

281

282

283

284

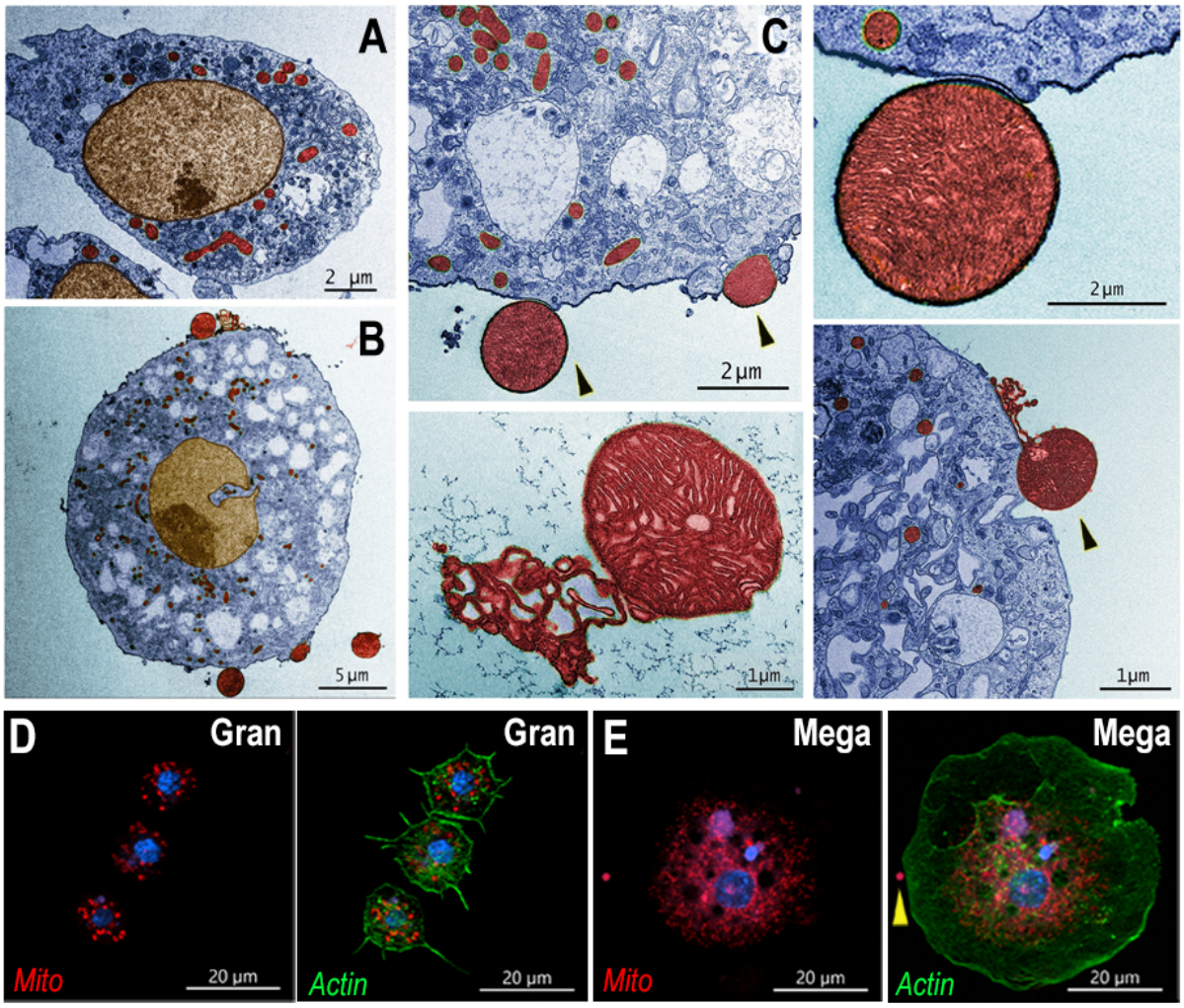

Fig.4: Ultrastructure of megacytes in Cactus-silenced mosquitoes. (A) Transmission Electron Microscopy (TEM) of regular granulocytes from Cactus-silenced mosquitoes. Scale Bar: 2um. (B) TEM of megacytes from Cactus-silenced mosquitoes. Scale Bar: 5um. (C) Extracellular giant mitochondria-like structures (black arrows). Close-up of a mitochondria-like structure (lower center). Scale Bars: 2um and 1um. TEM images were digitally colorized, cytoplasm is shown in blue, mitochondria in red and nuclei in golden yellow. (D) Mitotracker staining in regular granulocytes. Scale Bar: 20um. (E) Mitotracker staining in Cactus-megacytes. Actin is stained in green (phalloidin), mitochondria is in red (mitotracker) and nuclei in blue (Hoechst). Yellow arrow indicates an extracellular mitochondrion like structure outside of a megacyte. Scale bar: 20um.

Megacytes associate with the basal surface of the midgut in response to bacterial feeding and *Plasmodium berghei* infection

We have shown that the direct contact of bacteria with epithelial cells, before the peritrophic matrix is formed, triggers PGE2 release and attracts hemocytes to the basal surface of the midgut (Barletta et al., 2019). Hemocyte recruitment to the midgut in dsCactus females was explored by feeding them a BSA protein meal containing bacteria. As expected, bacterial feeding attracted hemocytes to the midgut in both dsCactus and dsLacZ control females (Fig. 5A and B). However, there are important differences in hemocyte recruitment. In dsLacZ females, hemocytes attach to the midgut basal lamina individually or in doublets (Fig.5A), while hemocytes from dsCactus females form large clusters on the basal midgut surface, with multiple hemocytes in very close association (Fig.5B and C). dsCactus hemocytes on the midgut surface have the characteristic morphology of megacytes, with a larger cytoplasm and nuclei than those from dsLacZ females (Fig. 5B and C). Accumulation of actin was often observed in the boundaries where hemocytes from dsCactus females come in direct contact as they form clusters (Fig. 5D).

The recruitment of granulocyte subpopulations to the midgut of dsCactus females, in response to both bacterial feeding and *P. berghei* infection, was analyzed by quantitation of mRNA transcripts of cell-specific hemocyte markers in dissected mosquito midguts. TM7318 mRNA levels increased dramatically in dsCactus midguts after bacterial feeding (250-fold increase) relative to dsLacZ control ($p=0.0022$, Mann-Whitney test) (Fig. 5E), indicative of extensive megacyte recruitment. A significant, but more modest increase in FBN50 (5-fold) ($p=0.0152$, Mann-Whitney test) a marker of antimicrobial granulocytes, was also observed (Fig. 5E). Although hemocytes undergo apoptosis as they release HdMv in response to *P. berghei* midgut invasion, a strong increase in TM7318 mRNA associated with the midgut of dsCactus infected

females (50-fold increase) ($p=0.0022$, Mann-Whitney test), relative to dsLacZ controls (Fig. 5F) was still detected. FBN50 levels were also significantly higher (10-fold increase) ($p=0.0043$, Mann-Whitney test), although the increase was not as robust as that of the megacyte-specific marker (Fig. 5F).

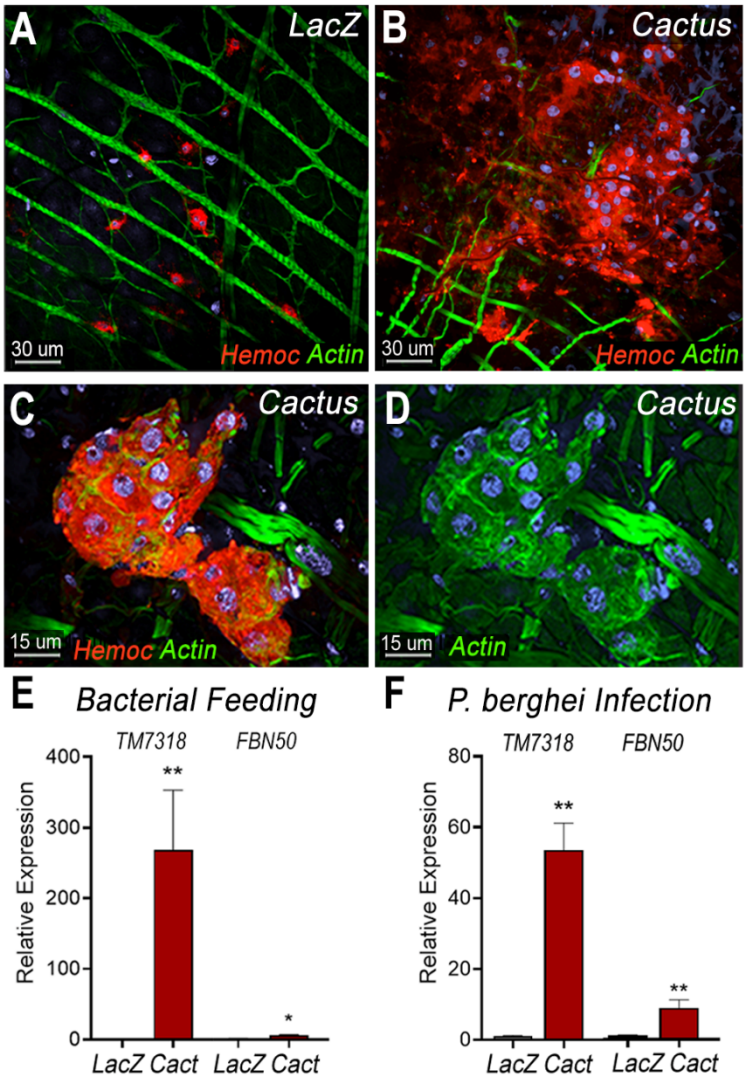

344

345 **Fig. 5: Bacterial feeding and *Plasmodium berghei* infection increase megacyte association to**
346 **the midgut basal surface.** (A) Effect of bacterial feeding in LacZ-injected controls on hemocytes
347 associated to the midgut basal surface. (B) Effect of Cactus silencing on the hemocytes associated
348 to the basal surface of the midgut 4 hours post bacterial feeding. (A) and (B) Scale Bar: 30um. (C)
349 and (D) Hemocyte cluster attached to the midgut surface in Cactus-silenced mosquitoes 4 hours
350 post bacterial feeding. Scale bar: 15um. (A-D) Midgut actin is showing in green (phalloidin),
351 hemocytes (stained with Vybrant CM-DiI) in red and nuclei in blue (Hoechst). (E) Relative mRNA
352 levels of effector hemocyte markers in the midgut 4 hours after bacterial feeding in LacZ and
353 Cactus-silenced mosquitoes. Scale bar: 15um. (F) Relative mRNA levels of effector hemocyte
354 markers in the midgut 26 h post *P.berghei* infection (post-invasion) in LacZ and Cactus-silenced
355 mosquitoes. TM7318, as a megacyte marker and FBN50, as an antimicrobial granulocyte. Error
356 bars in (E) and (F) represent mean ± SEM. Unpaired t-test, *P≤0.05, **P≤0.01.
357

358

Discussion

The dramatic phenotype of Toll pathway overactivation by silencing Cactus expression, which results in complete elimination of *P. berghei* parasites by the mosquito complement system, was documented more than fifteen years ago (Frolet et al., 2006). Furthermore, the observations that the transfer of dsCactus hemocytes recapitulated the phenotype in recipient mosquitoes (Ramirez et al., 2014) and that Cactus silencing greatly increased in HdMv release in response to *Plasmodium* midgut invasion (Castillo et al., 2017), clearly indicated that hemocytes are key players of this enhanced antiplasmodial response. However, the mechanism by which Toll signaling enhanced hemocyte responses to *Plasmodium* infection remained a mystery.

Transcriptomic analysis indicated that Cactus silencing increased the proportion of circulating megacytes, at the expense of a reduction in regular granulocytes (Fig. 2). This was confirmed by morphological analysis, *in situ* hybridization and mRNA quantitation of hemocyte-specific markers, TM7318 (megacytes) and FBN11228 (regular granulocytes). We provide direct evidence that, besides being larger, megacytes also have higher plasticity and can greatly extend their cytoplasm and flatten their nucleus as they spread on a glass surface (Fig. 1C).

The lack of DNA replication and the concomitant reduction in the proportion of regular granulocytes, indicates that Toll activation increases the proportion of circulating megacytes by promoting final differentiation of granulocytes to the megacyte lineage. Besides the dramatic increase in circulating megacytes, Cactus silencing also results in megacytes that are even larger and more plastic than megacytes from dsLacZ controls. Co-silencing Cactus and the transcription factor LL3 partially reduced megacyte differentiation, suggesting that this transcription factor participates in the differentiation process, but there may be other LL3-independent mechanisms involved.

382 Fine ultrastructural analysis revealed that the cytoplasm of megacytes exhibits extensive
383 large vacuolar structures filled with amorphous material, as well as small vesicles and
384 mitochondria-like structures that are secreted from the cell membrane. In vertebrates,
385 mitochondrial extrusion has been recently documented as a trigger of inflammation. Activated
386 platelets release their mitochondria, both within microparticles or as free organelles; and secreted
387 phospholipase A2 IIA can hydrolyze the membrane, releasing inflammatory mediators, such as
388 lysophospholipids, fatty acids, and mitochondrial DNA, that promote leukocyte activation.
389 Furthermore, extracellular mitochondria also interact directly with neutrophils *in vivo*, and
390 trigger their adhesion to the endothelial wall (Boudreau et al., 2014). Activated monocytes
391 release mitochondria, and their proinflammatory effect on endothelial cells is determined by the
392 activation status of the monocytes that released them. It has been proposed that free
393 mitochondria could be important mediators of cardiovascular disease by inducing activation of
394 type I IFN and TNF signaling (Puhm et al., 2019).
395 Large numbers of megacytes are recruited to the midgut of dsCactus females in response
396 to bacterial feeding, forming extensive clusters of cells that are in close contact with each other,
397 indicating that Toll activation also results in functional differences in the way these cells interact.
398 *Plasmodium* midgut invasion triggered strong recruitment of megacytes to the basal surface of the
399 midgut, in agreement with the documented increase in HdMv release in proximity to epithelial
400 cells invaded by ookinetes (Castillo et al., 2017). We recently described specific subsets of
401 mosquito granulocytes based on single-cell transcriptomic analysis (Raddi et al., 2020). Here we
402 present a functional characterization of megacytes, a newly described subpopulation of final
403 effector granulocytes and provide direct evidence of their recruitment to the basal surface of the
404 mosquito midgut when bacteria are allowed to come in contact with epithelial cells. We propose

405 that Toll signaling promotes hemocyte differentiation into the megacyte lineage, and that the
406 dramatic increase in the proportion of circulating megacytes mediates the observed increase in
407 HdMv (Castillo et al., 2017), resulting in enhanced complement activation that ultimately
408 eliminates *P. berghei* ookinetes. Activation of Toll signaling in mosquitoes appears to also trigger
409 the release of free mitochondria-like structures by megacytes, suggesting that these could be an
410 ancient systemic danger signal that promotes immune activation.
411

412 **Data Availability**

413 The raw data and detailed information on individual experiments and number of replicates are
414 available at Supplementary tables file.
415

416 **Acknowledgments**

417 This work was supported by the Intramural Research Program of the Division of Intramural
418 Research Z01AI000947, NIAID, National Institutes of Health. We thank Kevin Lee, Yonas
419 Gebremicale and André Laughinghouse for insectary support, and Asher Kantor for editorial
420 assistance.
421

422 **Author Contributions**

423 Experiments were designed by A.B.F.B., N.T., B.S., G.R. and C.B.M., carried out by A.B.F.B.
424 B.S., N.T., and analyzed by A.B.F.B., N.T., B.S., G.R. and C.B.M. A.B.F.B. and C.B.M. wrote
425 the paper.
426
427

Declaration of Interests

The authors declare no competing financial interests.

References

BARLETTA, A. B. F., TRISNADI, N., RAMIREZ, J. L. & BARILLAS-MURY, C. 2019. Mosquito Midgut Prostaglandin Release Establishes Systemic Immune Priming. iScience, 19, 54-62.

BLANDIN, S., SHIAO, S. H., MOITA, L. F., JANSE, C. J., WATERS, A. P., KAFATOS, F. C. & LEVASHINA, E. A. 2004. Complement-like protein TEP1 is a determinant of vectorial capacity in the malaria vector Anopheles gambiae. Cell, 116, 661-70.

BOUDREAU, L. H., DUCHEZ, A. C., CLOUTIER, N., SOULET, D., MARTIN, N., BOLLINGER, J., PARE, A., ROUSSEAU, M., NAIKA, G. S., LEVESQUE, T., LAFLAMME, C., MARCOUX, G., LAMBEAU, G., FARNDALE, R. W., POULIOT, M., HAMZEH-COGNASSE, H., COGNASSE, F., GARRAUD, O., NIGROVIC, P. A., GUDERLEY, H., LACROIX, S., THIBAULT, L., SEMPLE, J. W., GELB, M. H. & BOILARD, E. 2014. Platelets release mitochondria serving as substrate for bactericidal group IIA-secreted phospholipase A2 to promote inflammation. Blood, 124, 2173-83.

CASTILLO, J. C., FERREIRA, A. B. B., TRISNADI, N. & BARILLAS-MURY, C. 2017. Activation of mosquito complement antiplasmodial response requires cellular immunity. Sci Immunol, 2.

FROLET, C., THOMA, M., BLANDIN, S., HOFFMANN, J. A. & LEVASHINA, E. A. 2006. Boosting NF-kappaB-dependent basal immunity of Anopheles gambiae aborts development of Plasmodium berghei. Immunity, 25, 677-85.

451 HAN, Y. S., THOMPSON, J., KAFATOS, F. C. & BARILLAS-MURY, C. 2000. Molecular
452 interactions between Anopheles stephensi midgut cells and Plasmodium berghei: the time bomb
453 theory of ookinete invasion of mosquitoes. EMBO J, 19, 6030-40.
454 KUMAR, S., MOLINA-CRUZ, A., GUPTA, L., RODRIGUES, J. & BARILLAS-MURY, C.
455 2010. A peroxidase/dual oxidase system modulates midgut epithelial immunity in Anopheles
456 gambiae. Science, 327, 1644-8.
457 LOVE, M. I., HUBER, W. & ANDERS, S. 2014. Moderated estimation of fold change and
458 dispersion for RNA-seq data with DESeq2. Genome Biol, 15, 550.
459 MOLINA-CRUZ, A., DEJONG, R. J., ORTEGA, C., HAILE, A., ABBAN, E., RODRIGUES, J.,
460 JARAMILLO-GUTIERREZ, G. & BARILLAS-MURY, C. 2012. Some strains of Plasmodium
461 falciparum, a human malaria parasite, evade the complement-like system of Anopheles gambiae
462 mosquitoes. Proc Natl Acad Sci U S A, 109, E1957-62.
463 OLIVEIRA GDE, A., LIEBERMAN, J. & BARILLAS-MURY, C. 2012. Epithelial nitration by a
464 peroxidase/NOX5 system mediates mosquito antiplasmodial immunity. Science, 335, 856-9.
465 PUHM, F., AFONYUSHKIN, T., RESCH, U., OBERMAYER, G., ROHDE, M., PENZ, T.,
466 SCHUSTER, M., WAGNER, G., RENDEIRO, A. F., MELKI, I., KAUN, C., WOJTA, J., BOCK,
467 C., JILMA, B., MACKMAN, N., BOILARD, E. & BINDER, C. J. 2019. Mitochondria Are a
468 Subset of Extracellular Vesicles Released by Activated Monocytes and Induce Type I IFN and
469 TNF Responses in Endothelial Cells. Circ Res, 125, 43-52.
470 RADDI, G., BARLETTA, A. B. F., EFREMOVA, M., RAMIREZ, J. L., CANTERA, R.,
471 TEICHMANN, S. A., BARILLAS-MURY, C. & BILLKER, O. 2020. Mosquito cellular immunity
472 at single-cell resolution. Science, 369, 1128-1132.

473 RAMIREZ, J. L., GARVER, L. S., BRAYNER, F. A., ALVES, L. C., RODRIGUES, J.,
474 MOLINA-CRUZ, A. & BARILLAS-MURY, C. 2014. The role of hemocytes in Anopheles
475 gambiae antiplasmodial immunity. J Innate Immun, 6, 119-28.
476 RAUDVERE, U., KOLBERG, L., KUZMIN, I., ARAK, T., ADLER, P., PETERSON, H. &
477 VILO, J. 2019. g:Profiler: a web server for functional enrichment analysis and conversions of gene
478 lists (2019 update). Nucleic Acids Res, 47, W191-W198.
479 TRISNADI, N. & BARILLAS-MURY, C. 2020. Live In Vivo Imaging of Plasmodium Invasion
480 of the Mosquito Midgut. mSphere, 5
481
482

Material and Methods

Mosquitoes and mouse feeding

Anopheles gambiae mosquitoes (G3 strain – CDC) were reared at 28ºC, 80% humidity under a 12h light/ dark cycle and kept with 10% Karo syrup solution during adult stages. For mosquito infections with *Plasmodium berghei,* we used the transgenic GFP *P.berghei* parasites (ANKA 2.34 strain) kept by serial passages into 3-4 weeks old female BALB/c mice (Charles River, Wilmington, MA) starting from frozen stocks. Mouse infectivity was evaluated before feeding by parasitemia levels from Giemsa-stained thin blood films and *in vitro* microgamete exflagellation counting. Briefly, one microliter of tail blood was mixed with 9ul of gametocyte activating medium (RPMI 1640 with 25mM HEPES + 2mM glutamine, Sodium Bicarbonate 2g/L, 100uM xanthurenic acid, 50ug/ml hypoxanthine). After 10 minutes of incubation exflagellations were quantified using a 40X objective by phase contrast. Four to five-day old mosquitoes were fed when mice reached 3-5% parasitemia and 2-3 exflagellation per field. To feed blood-fed control mosquitoes, three- to four-week-old uninfected mice were used. Following feeding, both control and infected mosquitoes were maintained at 19ºC, 80% humidity and 12h light/dark cycle until the day of dissection.

Ethics statement

Public Health Service Animal Welfare Assurance #A4149-01 guidelines were followed according to the National Institutes of Health Animal (NIH) Office of Animal Care and Use (OACU). These studies were done according to the NIH animal study protocol (ASP) approved by the NIH Animal Care and User Committee (ACUC), with approval ID ASP-LMVR5.

Perfused hemocytes live imaging

Three-day-old adult females were injected with Vybrant DiI (1:10 water diluted, ThermoFisher Scientific, Waltham, MA, USA) on one side of the thorax. The next day, mosquitoes were injected with 69 nL of either dsCactus or dsLacZ at 3 µg/µL on the other side of the thorax. After 4 days, hemocytes were ready for perfusion or mosquitoes were used for in vivo live imaging as described below. Mosquitoes were cold-anesthetized and, using forceps, a small cut was made in the abdomen. Transfer buffer (95% Schneider media + 5% citrate buffer) was injected at the thorax and 10-15 µL of hemolymph was harvested at the cut-site. This was repeated for 5-7 mosquitoes and collected in a microcentrifuge tube stored on ice. To stain the plasma membrane of hemocytes we used CellMask green plasma membrane stain stock solution (C37608, Invitrogen, Waltham, MA, USA) and for the nuclei we used the Hoechst 33342 Solution (20mM) (ThermoFisher Scientific, Waltham, MA, USA). Two microliters of fluorescent label solution (58 µL H2O + 1 µL Cell Mask stock + 1µL Hoechst stock) was added for every 20 µL of perfusion and 100 µL of this mixture was mounted on an ibidi µ-Slide 18 Well Glass Bottom slide. Cells were allowed to settle for 30 minutes then imaged. Images were taken on a Leica SP5 confocal microscope using a 63x 1.4 NA oil objective with 405 nm wavelength laser (at 3% transmission) for Hoechst, 488 nm (5%) for Cell Mask, and 561 nm (3%) for DiI. Pinhole was set to 1 AU and frame average was 12. Z-intervals of 1-2 µm encompassing the full cell height was taken every 5 minutes for 2 hours.

Bacterial artificial feeding

We used a bacterial mixture obtained from the midguts of the Anopheles gambiae G3 from our colony (Barletta et al., 2019). A pre-inoculum was set up in LB media from the frozen stocks containing the bacterial mixture and allow to grow overnight at 28°C, 250rpm in a shaker incubator. At the day of the experiment, the pre-inoculum was diluted in fresh LB media and allowed to grow for 2 hours in the same condition described above. Briefly, after 2 hours of growth,

528 bacteria were washed with sterile PBS to remove toxins and the concentration of the culture was
529 estimated based on the Optical Density (OD) of the culture. At 600nm, 1OD was considered the
530 equivalent of 10^9 bacteria/mL. Three-to-four day mosquitos were fed a sterile 10% sucrose
531 solution containing antibiotics (Penicillin, 100U/mL and Streptomycin, 100ug/mL) for 2 days
532 prior the bacterial feeding. Control group was fed with a sterile 10% Bovine Serum Albumin
533 (BSA) solution in HBSS without calcium and magnesium and the bacteria group was fed with the
534 same solution containing 4 x 10^9 bacteria per feeder. Mosquitoes were dissected 6 hours post
535 feeding for visualization of hemocytes attached to the midgut basal surface.
536 *Hemocyte collection, morphology staining and quantification*
537 Hemocytes were collected by perfusion using anticoagulant buffer (60% Schneider medium, 30%
538 citrate buffer, pH 4.5 and 10% FBS), pH was adjusted to 7-7.2 after mixing all the components.
539 After perfusion, hemocytes were placed in a µ-slide angiogenesis chamber (ibidi GmbH,
540 Gräfelfing, Germany) and were allowed to settle for 15 minutes. Cells were fixed for an hour at
541 room temperature by adding 16% paraformaldehyde (PFA) solution in anticoagulant buffer to a
542 final concentration of 4%. Following fixation cells were washed with PBS 0.1% Triton and
543 incubated for 30 minutes at room temperature with 1U of phalloidin (Alexa Fluor 488, Molecular
544 Probes, ThermoFisher Scientific, Waltham, MA, USA) and 20 µM Hoechst 33342 (405, Molecular
545 Probes, ThermoFisher Scientific, Waltham, MA, USA), both diluted in PBS 0.1% Triton. Cells
546 were then placed in mounting media for storage by adding 2 drops of Prolong Gold Antifade
547 Mountant (Molecular Probes, ThermoFisher Scientific, Waltham, MA, USA). For determination
548 of proportion of megacytes upon Cactus silencing, the hemocytes were imaged, the diameter of
549 every cell was measured and classified as granulocytes (cell diameter >12.5-25 µm) or megacytes
550 (cell diameter >25 µm) as mentioned before. The total number of granulocytes and megacytes

obtained from hemolymph pooled from 16-20 mosquitoes was noted and the percentage of megacytes amongst granulocytes was determined for each sample. Data from three independent biological replicates were used to plot the graphs.

Measurement and categorization of the hemocytes by size

The mosquito hemolymph was collected and the hemocytes were allowed to attach on a coated well of 15µm chamber slide. For each well 8-10 mosquitoes were bled and for every sample, bleeding was done in two wells with a total of 16-20 mosquitoes. Post attachment, the hemocytes were fixed with 4% p-formaldehyde and stained with Phalloidin and DAPI to visualize the morphology. Images were taken for at least 10 random fields for each well and the images were used to measure the cell diameter using Imaris software. Using the "Pairs" option of "Measurement points" tool in the software, the largest diameter of every cell was determined. For categorizing the hemocytes into different subtypes, the following size reference was followed for every image analysis. Cells with diameter ranging from 4-7.5µm were classified as prohemocytes, >7.5 µm-12.5 µm as oenocytoids, >12.5-25 µm as granulocytes and >25 µm as megacytes.

dsRNA synthesis

Three-to-four day old female *An.gambiae* females were cold-anesthetized and injected with 69nl of a 3ug/ul dsCactus or dsLacZ control. Double-stranded RNA for *Cactus* (AGAP007938) was synthesized by *in vitro* transcription using the MEGAscript RNAi kit (Ambion, ThermoFisher Scientific, Waltham, MA, USA). DNA templates were obtained by PCR using *An.gambiae* cDNA extracted from whole body sugar-fed females. A 280-bp fragment was amplified with primers containing T7 promoters (F-**TAATACGACTCACTATAGGG**TAACACTGCGCTTCATTTGG and R- **TAATACGACTCACTATAGGG**GCCCTTTTCAATGCTGATGT), using an annealing temperature of 58ºC. Double-stranded RNA for LacZ was synthetized by amplifying a 218-bp

574 fragment from LacZ gene clones into pCRII-TOPO vector using M13 primers to generate a dsRNA
575 control as previously described (Molina-Cruz et al., 2012).

576 *RNA extraction and bulk RNAseq library preparation*

577 Hemocytes were collected as previously described above. In short, *An.gambiae* females were
578 perfused using anticoagulant buffer and immediately transferred to a glass tube for attachment.
579 After one hour, hemocytes that did not attach to the glass tube were collected and transferred to a
580 1.5 ml microcentrifuge containing 800ul of TRIZOL LS reagent (Invitrogen, Waltham, MA,
581 USA), that correspond to the unbound fraction enriched mainly by prohemocytes and oenocytoids.
582 Hemocytes that attached to the glass surface were washed twice with PBS and resuspended in 1mL
583 of TRIZOL LS reagent (Invitrogen, Waltham, MA, USA), this corresponds to the bound fraction,
584 mainly enriched by granulocytes. Hemocytes were then lysed in TRIZOL reagent for 15-30
585 minutes at room temperature to allow for full dissociation, then stored at 4ºC overnight and then
586 at -20C until RNA extraction. The homogenate of hemocyte samples were transferred to Phase
587 Lock Gel Heavy 2 mL tubes (QuantaBio, Beverly, MA, USA) that had been pre-spun for 1500
588 RCF for 1 minute, and allowed to incubate for 5 minutes at room temperature. 100 uL of
589 chloroform (200 uL per 1 mL TRIZOL or TRIZOL plus media) was added, the tubes capped, and
590 then vigorously shaken for 15 seconds. Samples were then centrifuged for 12,000 RCF, 10
591 minutes, 4ºC. If the clear, aqueous phase was still mixed with TRIZOL matrix then 100 uL more
592 of chloroform was added, and the samples again mixed vigorously and spun as before. The aqueous
593 phase was then transferred to a fresh 1.5 mL Eppendorf tube and the RNA precipitated by adding
594 0.25 mL of isopropyl alcohol (500 mL per 1 mL TRIZOL reagent used). 20 uL of glycogen (5 mg
595 / mL) were also added to aid in precipitation and pelleting. Samples were mixed by repeated
596 inversion 10 times, incubated for 10 minutes at room temperature, and then spun at 12,000 RCF,

10 minutes, 4ºC. All the supernatant was removed, and the RNA pellets washed twice with 75% ethanol (minimum 1 mL of ethanol per 1 mL of TRIZOL used). Each time the samples were mixed by vortexing and centrifuged 7,500 RCF, 5 minutes, 4C. At the end, the supernatant was removed and samples air-dried until almost dry, but not completely (still translucent). RNA was resuspended with 30 uL of RNAse free water, pipetting a few times to homogenize and then incubating at 55ºC for 10 minutes to completely resuspend. Samples were then stored at -20C until library preparation by Bespoke Low-Throughput Team at the Wellcome Sanger institute. Total RNA quantity was assessed on a Bioanalyser and ranged from 300 ng to 39 ng. mRNA was then isolated with the NEBNext Poly(A) mRNA magnetic isolation module. RNA-seq libraries were prepared from mRNA using the NEBNext Ultra II Directional RNA Library Prep Kit for Illumina (New England Biolabs) as by manufacturer instructions, except that a proprietary Sanger UDI (Unique Dual Indexes) adapters / primer system was used. Furthermore, Kapa Hifi polymerase rather than NEB Q5 was employed. For bulk RNAseq sequencing samples libraries were run on the Illumina HiSeq 4000 instrument with standard protocols using a 150-cycle kit set to a 75bp paired-end configuration. Libraries supplied at 2.8 nM and loaded with a loading concentration of 280 pM.

Bulk RNA-seq bioinformatic analysis

Sequencing reads in CRAM format were fed into a personal BASH pipeline to convert cram files to fastq using biobam's bamtofastq program (Version 0.0.191) (Raddi et al., 2020). Forward and reverse fastq reads in paired mode were aligned to the A. gambiae AgamP4.3 reference genome using hisat2 (Version 2.0.4) and featureCounts (Version 1.5.1) with recommended settings. Count matrices were combined before downstream data processing and analysis within R version 3.5.3 (RStudio version 1.0.153). Downstream normalization, differential expression analysis and

620 visualization were done with DESeq2 R package (Version 1.18.1) (Love et al., 2014). Base factor
621 was defined as the LacZ, unbound condition. Data was normalized by making a scaling factor for
622 each sample. First the log(e) of all the expression values were taken, then all rows (genes) were
623 averaged (geometric average). Genes with zero counts in one or more samples were filtered out
624 and the average log value from log (counts) for all genes was subtracted. Finally, the median of
625 the ratios calculated as above for each sample was computed and raised to the e to make the scaling
626 factor. Original read counts were divided by the scaling factor for each sample to get normalized
627 counts. Then, the dispersion for each gene was estimated, and a negative binomial generalized
628 linear model fitted. P values for the differential expression analysis were adjusted for multiple
629 testing using the Bonferroni correction. Genes were considered as differentially expressed in
630 Cactus knockdown compared to LacZ control if they had an adjusted P value < 0.001 (Wald T-
631 test) and a log2 fold change > 2. Gene lists with vectorbase IDs were converted to gene annotations
632 with g:Profiler (Raudvere et al., 2019). g:Profiler utilizes Ensembl as its primary data source and
633 is anchored to its quarterly release cycle. g:GOSt was used to perform functional enrichment
634 analysis on input gene lists to map the data onto enriched biological processes or pathways. In
635 addition to Ensembl, also KEGG, Reactome, WikiPathways, miRTarBase, and TRANSFAC
636 databases were used. Functional enrichment is evaluated with a cumulative hypergeometric test
637 with g:SCS (Set Counts and Sizes) multiple testing correction (adjusted P value reported only <
638 0.05). Gene lists were ordered on log-fold changes.

639 *Transmission Electron Microscopy (TEM)*

640 Hemocytes were collected by perfusion using anticoagulant buffer, described above and they were
641 allowed to settle on Thermanox™ coverslips (Ted Pella, Redding, CA) for 15 minutes at room
642 temperature then fixed 2.5% glutaraldehyde in 0.1 M sodium cacodylate buffer overnight at 4°C,

643 and then post-fixed 1hr with 1.0% osmium tetroxide/0.8% potassium ferricyanide in 0.1 M sodium
644 cacodylate buffer, washed with buffer then stained with 1% tannic acid in dH2O for one hour.
645 After additional buffer washes, the samples were further osmicated with 2% osmium tetroxide in
646 0.1M sodium cacodylate for one hour. The samples were then washed with dH2O and additionally
647 stained overnight with 1% uranyl acetate at 4°C, dehydrated with a graded ethanol series, and
648 embedded in Spurr's resin. Thin sections were cut with a Leica UC7 ultramicrotome (Buffalo
649 Grove,IL) prior to viewing at 120 kV on a FEI BT Tecnai transmission electron microscope
650 (Thermo fisher/FEI, Hillsboro, OR). Digital images were acquired with a Gatan Rio camera
651 (Gatan, Pleasanton, CA).

652 *Mitotracker staining*

653 Hemocytes were perfused with anticoagulant buffer, described above. Cells were incubated at
654 room temperature for 15 minutes for spreading. Then washed three times with 95% Schneider
655 media, 5% citrate buffer to remove most of the serum from the cells. Hemocytes were placed with
656 200nM Deep Red Mitotracker 644/665 which is retained after fixation (Molecular Probes,
657 ThermoFisher Scientific, Waltham, MA, USA) diluted in 95% Schneider media, 5% citrate buffer.
658 Cells were incubated for 45 minutes at room temperature in the dark, then washed with PBS and
659 fixed with 4% Paraformaldehyde in PBS for 15 minutes at room temperature. Hemocytes were
660 then counterstained with phalloidin and Hoechst as described above.

661 *TM7318 in situ hybridization (ISH)*

662 The ISH protocol includes a permeabilization step with a protease treatment, which compromises
663 the cell morphology. To evaluate the morphology of hemocytes and RNA expression by ISH, we
664 used a two-step protocol to image morphology first and then proceed to image the probes,
665 described in (Raddi et al., 2020). Hemocytes collected by perfusion four days after dsCactus

injection, fixed and stained with Alexa 488 phalloidin (actin) as described above. Ten random fields of each well were imaged using a tile scan "mark and find" tool, where coordinates of the field are recorded and can be restored to image the same cells later. Then, hemocytes were subjected to ISH using RNAscope multiplex fluorescent reagent kit v2 assay (cat# 323110, ACDBio, Abingdon, United Kingdom) following the manufacturer's instructions. TSA based fluorophores Opal 4- color automation IHC kit (cat # NEL801001KT, PerkinElmer, Waltham, MA, USA) was used for the development of fluorescence (Opal 620 – C3). A specific RNA probe for TM7318 (cat# 543201-C3; Aga-Transmembrane-C3) designed by ACDBio was used to stain specifically megacytes. At the end of the ISH protocol, hemocytes were placed in prolong gold and re-imaged using the "mark and find" tool to recall the positions of the morphology pictures. Images were merged using Imaris 9.3.1 (Bitplane, Concord, MA, USA). Each well was imaged taking 12 fields per well. Post imaging, the cell diameter of every cell was measured by Phalloidin stain as described previously and the total number of granulocytes were determined for each sample. Amongst the granulocytes and larger cells (cells with diameter >12.5), the number of cells positive for the TM7318 probe were counted and their percentage was determined for both the control and Cactus silencing.

Confocal microscopy and Tile scan imaging

Confocal images were captured using a Leica TCS SP8 (DM8000) confocal microscope (Leica Microsystems, Wetzlar, Germany) with either a 40x or a 63x oil immersion objective equipped with a photomultiplier tube/ hybrid detector. Hemocytes were visualized with a white light laser, using 498-nm excitation for Alexa 488 (phalloidin); 588-nm excitation for Opal620 (TM7318 probe) and Vybrant DiI (hemocytes); 644-nm excitation for Deep Red Mitotracker (Mitochondria) and a 405-nm diode laser for nuclei staining (Hoechst 33342). Images were taken using sequential

mode and variable z-steps. For combined morphology and in RNA in situ hybridization, we used tile scan "mark and find" tool included in LASX software to capture the same areas of the slide before and after the hybridization. Image processing and merge was performed using Imaris 9.3.1 (Bitplane, Concord, MA, USA) and Adobe Photoshop CC (Adobe Systems, San Jose, CA, USA).

RNA extraction, cDNA synthesis and qPCR analysis

An. gambiae hemocytes were collected as described above four days after dsRNA injection (dsLacZ and dsCactus). Hemolymph pools of 20 mosquitoes (5ul/ each mosquito) were placed directly into 800ul of TRIzol LS reagent (ThermoFisher Scientific, Waltham, MA, USA). For midgut RNA extraction, pools of 20 midguts were homogenized directly in 1mL TRIzol reagent. RNA extraction was carried out as described above in the section *RNA extraction and bulk RNAseq library preparation.* Total extracted RNA was resuspended in nuclease free water and one microgram was used for cDNA synthesis using the Quantitect reverse transcription kit (Qiagen, Germantown, MD, USA) following the manufacturer's instructions. Quantitative PCR (qPCR) was used to measure FBN11228 (AGAP011228), TM7318 (AGAP007318) and FBN50 (AGAP005848) gene expression in hemocytes cDNA. We used the DyNamo SYBR green qPCR kit (ThermoFisher Scientific, Waltham, MA, USA) with target specific primers and the assay ran on a CFX96 Real-Time PCR Detection System (Bio-Rad, Hercules, CA, USA). A 139-bp fragment was amplified for FBN11228 (F- CCAGCATCGGTACAACGGAA and R- AAGCTCGTGTTTTCGTGCTG). A 150-bp fragment was amplified for TM7318 (F- AAAACATCCAGAAACACGCC and R- GGATTCCGGTTAAGTCCACC). A 92-bp fragment was amplified for FBN50 (F- ATCACAAGGTTCCGGCTATG and R- CGTTGGTGTAGGTGAGCAGA). Relative expression was normalized against An. gambiae ribosomal protein S7 (RpS7) as internal standard and analyzed using the ΔΔ Ct method (ref –

712 Livak and Schmittgen, 2001; Pfaffl, 2001). RpS7 (AGAP010592) primers sequences were: F-
713 AGAACCAGCAGACCACCATC and R – GCTGCAAACTTCGGCTATTC. Statistical analysis
714 of the fold change was performed using Unpaired t-test (GraphPad, San Diego, CA, USA). Each
715 independent experiment was performed with three biological replicates (three pools of 20
716 mosquitoes) for each condition.

717 *In vivo live imaging*

718 Mosquitoes were prepared the same way for imaging of perfused hemocytes and injected with
719 Vybrant DiI cell labelling (ThermoFisher Scientific, Waltham, MA, USA) for both dsCactus and
720 dsLacZ. After 4 days, mosquitoes were starved in the morning and then fed on a BALB/c mouse
721 in the afternoon. Imaging took place the next day at 18-20 hours post-bloodmeal. Mosquitoes were
722 imaged as previously described (Trisnadi and Barillas-Mury, 2020). Briefly, 5-10 mosquitoes with
723 legs and head removed were placed between a coverslip and glass slide with craft putty as a spacer.
724 Images were taken on a Leica SP5 confocal microscope using a 40x 1.25 NA oil objective with
725 561 nm (3%) for Vybrant DiI. A z-stack with 1 µm intervals was taken to include hemocytes
726 circulating in the hemolymph to the midgut lumen. The z-stack was taken every 1 minute for 1-2
727 hours.

728 *Visualizing hemocytes attached to the midgut basal lamina*

729 To preserve hemocyte-midgut bound, midguts were quick fixed using a higher concentration of
730 fixative injected straight into the hemolymph of the mosquito (207nl of 16% paraformaldehyde).
731 To stain hemocytes, the day before the dsRNA treatment (dsLacZ and dsCactus), three-to-4-day-
732 old mosquitoes were injected with 69nl of a 100uM solution Vybrant CM-DiI cell labelling
733 solution (ThermoFisher Scientific, Waltham, MA, USA), final concentration in the hemolymph
734 (approximately 3.5uM). Engorged mosquitoes fed with 10% BSA solution containing bacteria

735 were anesthetized and injected with 207nl of 16% paraformaldehyde, rested 40 seconds before
736 midgut dissection in 4% paraformaldehyde solution. After dissected, midguts were placed in ice-
737 cold PBS and opened longitudinally, and the bolus was removed. Clean opened tissues were then
738 fixed overnight at 4^{o}C in 4% paraformaldehyde. The following day, midguts were washed twice
739 with PBS, blocked for 40 minutes with PBS containing 1% BSA and washed twice with the same
740 solution. For actin and nuclei staining, midguts were incubated for 30 minutes at room temperature
741 with 1U of phalloidin (Alexa Fluor 488, Molecular Probes, Waltham, MA, USA) and 20uM
742 Hoechst 33342 (405, Molecular Probes, Waltham, MA, USA), both diluted in PBS. Tissues were
743 mounted in microscope slides using Prolong Gold Antifade mounting media (Molecular Probes,
744 Waltham, MA, USA). Hemocytes were visualized by confocal microscopy and the number of
745 hemocytes per midgut in each biological condition was also analyzed.
746
747
748

Supplemental Information

Toll signaling enhances mosquito antiplasmodial immunity by promoting differentiation of hemocytes to the Megacyte lineage

Ana Beatriz Barletta Ferreira[1], Banhisikha Saha[1], Nathanie Trisnadi[1#], Gianmarco Raddi[1#], and Carolina Barillas-Mury[1*].

[1]Laboratory of Malaria and Vector Research, National Institute of Allergy and Infectious Diseases, National Institutes of Health, Rockville, MD 20852.

[#] Present address: Nathanie Trisnadi, Atropos Therapeutics Inc., San Carlos, California, USA. Gianmarco Raddi, School of Clinical Medicine, University of Cambridge, Cambridge CB2 0SP, UK, CRUK Cambridge Institute, Cambridge CB2 0RE, UK.

* Correspondence should be addressed to: cbarillas@niaid.nih.gov (CB-M)

Supplementary figures

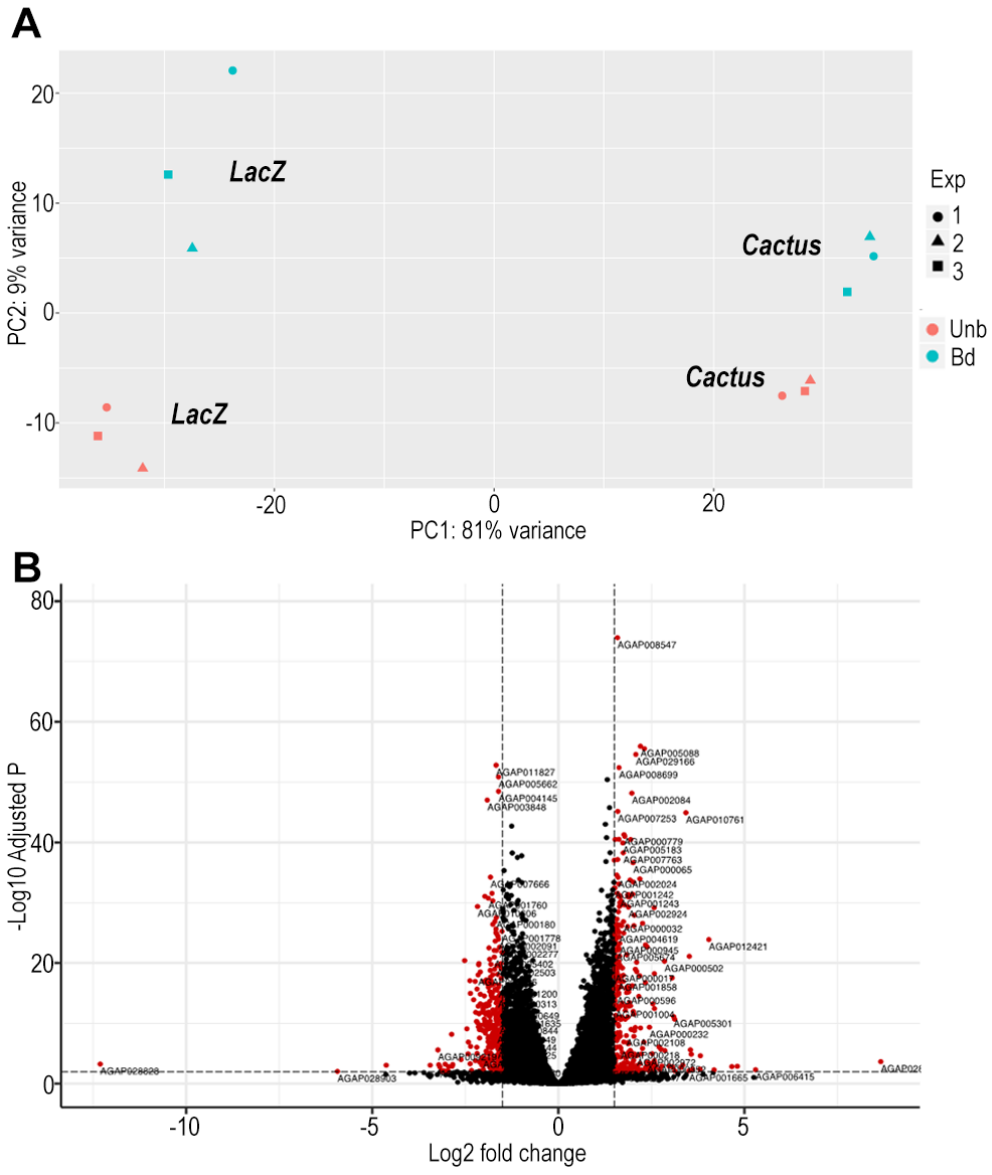

Supplementary Figure 1. Quality control of dsCactus knockdown bulk RNA seq and Differential expression between bound and unbound fractions. (A) PCA plot showing first and second principal component of dsRNA Cactus and control LacZ knock-down, for bound and unbound hemocyte fractions. Cactus and LacZ cluster separately, and so do bound and unbound hemocyte fractions. Bd = bound. UnB = unbound. One, two and three represent different biological replicates for each condition. (B) From a total of 9421 filtered genes (B) Volcano plot of DE genes between bound and unbound hemocytes filtered for log2 fold change >1.5 and Q-value <0.01.

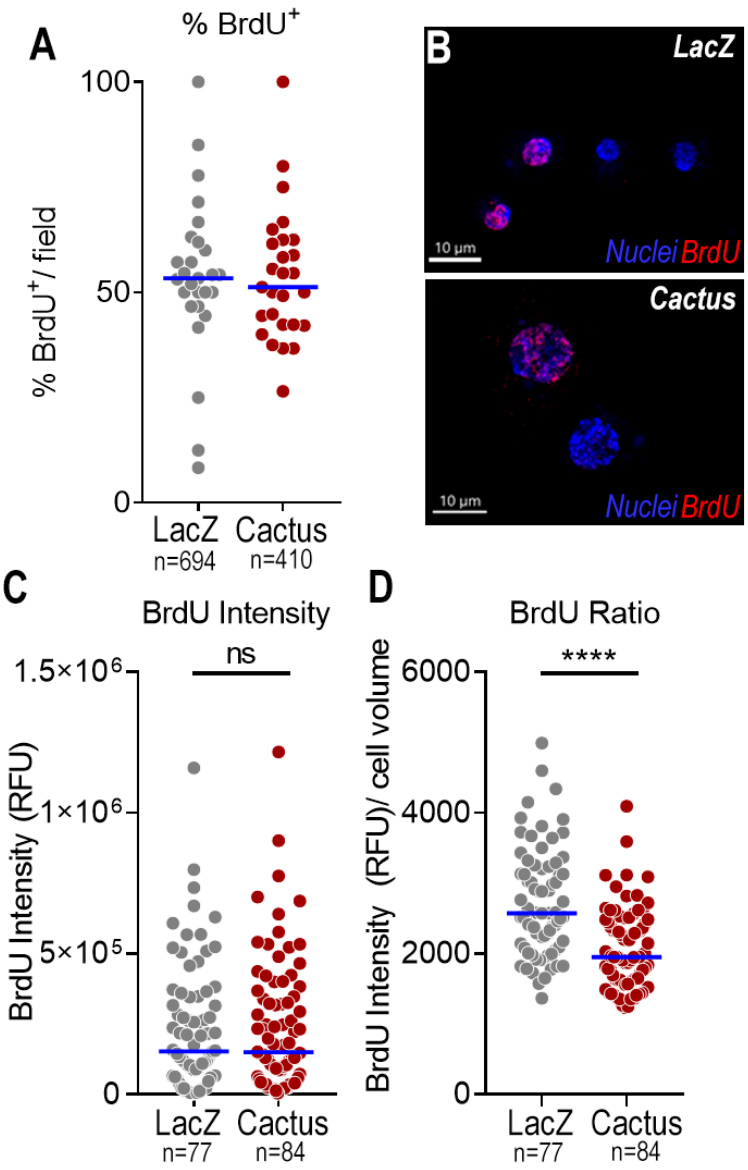

Supplementary Figure 2. Toll activation controls megacyte differentiation and not proliferation. (A) Percentage of $BrdU^+$ hemocytes in dsLacZ and dsCactus mosquitoes 4 days after silencing. (B) Representative pictures of positive BrdU nuclei in LacZ and Cactus hemocytes. Nuclei is in Blue and BrdU is showing in Red. Scale Bar: 10um. (C) BrdU fluorescence intensity (Relative fluorescent units) in hemocytes from dsLacZ and dsCactus female mosquitoes. (D) Ratio between BrdU fluorescence intensity (Relative fluorescent units) and cell volume calculated based on the fluorescence of the nuclei (Hoechst staining). Quantification of cells was performed from 2 independent experiments. In each experiment 10 fields were collected, counted, and analyzed for BrdU staining. Blue bar in A, C and D represent medians. Mann-Whitney t-test, ****$p<0.0001$, ns – nonsignificant.

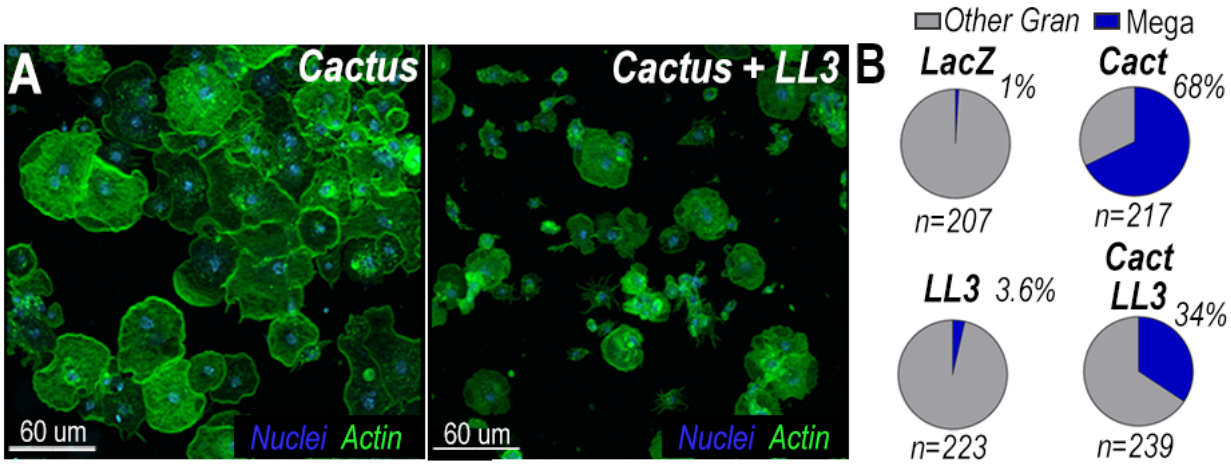

Supplementary Figure 3. LL3 partially mediates megacyte differentiation through Toll signaling. (A) dsCactus and double silenced dsCactus + dsLL3 hemocytes perfused 4 days after silencing. Actin is showing in green and the nuclei in blue. Scale Bar: 60um. (B) Percentage of megacytes among all granulocytes in response to co-silencing of dsCactus and dsLL3. Percentages were compared using X^2-test, $p < 0.0001$ and calculated from 2 independent experiments. In each experiment 10 fields per condition were counted.

Video S1. Front view (XY) of a regular granulocyte from *An.gambiae* mosquito female. Showing in red is the microvesicle staining and in green the plasma membrane. Scale Bar: 10um. Hemocyte was imaged for 1 hour in intervals of 5 minutes.

Video S2. Side view (XZ) of a regular granulocyte from An. gambiae mosquito female. Showing in red is the microvesicle staining and in green the plasma membrane. Scale Bar: 5um. Hemocyte was imaged for 1 hour in intervals of 5 minutes.

Video S3. Front view (XY) of a megacyte from An. gambiae mosquito female. Showing in red is the microvesicle staining and in green the plasma membrane. Scale Bar: 10um. Hemocyte was imaged for 1 hour in intervals of 5 minutes.

Video S4. Side view (XZ) of a megacyte from An. gambiae mosquito females Showing in red is the microvesicle staining and in green the plasma membrane. Scale Bar: 5um. Hemocyte was imaged for 1 hour in intervals of 5 minutes.

Video S5. *In vivo* hemocyte patrolling activity in dsLacZ mosquitoes. Hemocytes stained in red were imaged through the cuticle of the mosquito for 1 hour and 20 minutes. Scale Bar: 30um.

Video S6. *In vivo* hemocyte patrolling activity in dsCactus mosquitoes. Hemocytes stained in red were imaged through the cuticle of the mosquito for 1 hour and 20 minutes. Scale Bar: 30um.

Video S7. DsCactus megacyte dynamics *in vitro*. Perfused hemocytes from dsCactus mosquitoes. Plasma membrane is showing in green, microvesicles in red and nuclei in blue. Scale Bar: 20um.

Table S1. List of upregulated genes in Cactus silenced hemocytes

Table S2. List of downregulated genes in Cactus silenced hemocytes

Table S1.

Upregulated genes by Cactus Knockdown									
Accesion Number	Name	Description	baseMean	log2FoldChange	lfcSE	stat	pvalue	padj	Hemocyte type
AGAP007343	LYSC2	C-type lysozyme	150003.6078	11.38985051	0.890888229	12.78482547	1.9931E-37	3.07315E-36	
AGAP011920	AGAP011920	eupolytin	147.2376396	10.24020054	0.850232306	12.04400311	2.08583E-33	2.77551E-32	
AGAP002842	AGAP002842	CLIPD1 protein	908.0228542	9.35826901	0.461470828	20.27922121	1.96213E-91	1.31101E-89	
AGAP006674	AGAP006674	chymotrypsin-like protease (Precursor)	162.6513041	9.223197473	1.269757003	7.263750031	3.76504E-13	1.82743E-12	
AGAP000188	AGAP000188	Uridine phosphorylase [Source:UniProtKB/TrEMBL;Acc:Q7PFX7]	35514.58459	8.223334693	0.206853775	39.75433709	0	0	
AGAP010771	AGAP010771	nan	212.6244713	7.835796021	0.779798413	10.04848932	9.32865E-24	8.12248E-23	
AGAP028044	CPLCP23	cuticular protein (putative) CPLCP23	568.6912146	7.782049203	0.423632051	18.36983107	2.29124E-75	1.07392E-73	
AGAP028137	CPLCP17	cuticular protein (putative) CPLCP17	23.15155164	7.748117482	0.894497512	8.661977679	4.63649E-18	3.05885E-17	
AGAP009728	AGAP009728	ficolin	96.0328881	7.552158704	0.734283475	10.2850724	8.22802E-25	7.47504E-24	
AGAP012936	nan	nan	771.7781334	7.376956435	0.577741905	12.76860197	2.45525E-37	3.76725E-36	
AGAP010256	AGAP010256	nan	24.41954606	6.826258554	0.892933963	7.644751838	2.09349E-14	1.10678E-13	
AGAP004497	AGAP004497	nan	140.0929815	6.723899197	0.776063174	8.664113205	4.55041E-18	3.00416E-17	
AGAP009489	AGAP009489	Cytidine deaminase [Source:UniProtKB/TrEMBL;Acc:Q7QG43]	26454.65472	6.710199366	0.127644774	52.56932305	0	0	
AGAP002007	AGAP002007	reticulon/nogo receptor	10.82279296	6.638250029	0.923462513	7.188434759	6.55383E-13	3.1326E-12	
AGAP029133	AGAP029133	nan	150.5264926	6.565219163	0.474005189	13.8505217	1.26291E-43	2.4232E-42	
AGAP011980	AGAP011980	nan	120.7652387	6.522865768	0.556577551	11.71959911	1.0115E-31	1.25882E-30	
AGAP008341	AGAP008341	serine/threonine-protein kinase Chk2	412.0975372	6.519154025	0.327414123	19.9110349	3.265E-88	2.10682E-86	
AGAP028008	CPLCP19	cuticular protein (putative) CPLCP19	26.32277697	6.433828174	0.790844224	8.13539251	4.10606E-16	2.42528E-15	
AGAP004115	AGAP004115	cystinosin	4407.482278	6.413747248	0.197665013	32.44755943	5.8634E-231	3.0689E-228	
AGAP007150	AGAP007150	nan	11.35455667	6.222639299	0.900634018	6.909176395	4.87476E-12	2.19108E-11	
AGAP001002	AGAP001002	Toll protein	116127.845	6.177628682	0.268236101	23.03056397	2.3037E-117	2.7825E-115	Megacytes
AGAP013210	AGAP013210	Down syndrome cell adhesion molecule-like protein 1	104.7167101	6.1774525	0.853967007	7.233830448	4.69558E-13	2.2674E-12	
AGAP000473	AGAP000473	Aa_trans domain-containing protein [Source:UniProtKB/TrEMBL;Acc	32.72500638	6.030795595	0.694109812	8.688532407	3.67151E-18	2.43244E-17	
AGAP011226	AGAP011226	nan	2959.788347	6.023113599	0.218447016	27.5724233	2.3834E-167	5.2219E-165	Megacytes
AGAP028013	CPLCP25	cuticular protein (putative) CPLCP25	9.869237005	5.98271328	0.911017367	6.567068309	5.13155E-11	2.15342E-10	
AGAP028178	CPLCP13	cuticular protein (putative) CPLCP13	9.845746458	5.903622512	0.934991859	6.314089748	2.71756E-10	1.07617E-09	
AGAP012544	CASPS14	short caspase 14	9.247569773	5.88732349	0.910161253	6.468440042	9.90198E-11	4.0489E-10	
AGAP006982	AGAP006982	nan	7.337402519	5.814868909	0.975476518	5.961054728	2.50615E-09	9.02885E-09	
AGAP013142	AGAP013142	nan	213.6895269	5.786289236	0.403777627	14.33038596	1.41333E-46	2.93929E-45	
AGAP028156	CPLCP14	cuticular protein (putative) CPLCP14	6.344508639	5.780752493	0.982548003	5.883430098	4.0185E-09	1.42164E-08	
AGAP006368	Obp69	odorant-binding protein 69	42.20555312	5.74398315	0.556557706	10.32055273	5.68947E-25	5.26527E-24	
AGAP001508	AGAP001508	nan	5677.718823	5.67371698	0.63276711	8.966516896	3.06039E-19	2.14843E-18	
AGAP010833	CLIPB14	CLIP-domain serine protease	350.1728028	5.609302809	0.696698509	8.051262835	8.19441E-16	4.75953E-15	
AGAP005101	AGAP005101	nan	828.5282682	5.561330369	0.314177259	17.70125053	4.10099E-70	1.6798E-68	
AGAP009918	AGAP009918	SGS5 [Source:UniProtKB/TrEMBL;Acc:Q5XLG6]	7.330305498	5.546120623	0.960926948	5.771636057	7.85055E-09	2.69436E-08	
AGAP009917	AGAP009917	SGS4 [Source:UniProtKB/TrEMBL;Acc:Q5XLG7]	7.641458514	5.501527096	0.991755504	5.54726147	2.90179E-08	9.41058E-08	
AGAP005072	AGAP005072	nan	28.87051263	5.47858478	0.747639945	7.327838506	2.33894E-13	1.14528E-12	
AGAP011232	AGAP011232	nan	5.109307773	5.472165276	0.983504031	5.56394799	2.63739E-08	8.59751E-08	
AGAP009916	nan	nan	2842.248885	5.410882466	0.26518758	20.4039815	1.5414E-92	1.07567E-90	
AGAP010811	AGAP010811	Fibrinogen C-terminal domain-containing protein [Source:UniProtKB	91.01407029	5.256865908	0.796529885	6.599709572	4.11964E-11	1.73885E-10	
AGAP028060	AGAP028060	glucuronosyltransferase	887.3372409	5.228176685	0.245624618	21.28523083	1.5558E-100	1.30867E-98	
AGAP028032	AGAP028032	nan	11.14647247	5.22662839	0.835531452	6.255453793	3.96362E-10	1.552E-09	
AGAP013201	AGAP013201	nan	32.2763464	5.159542477	0.608926828	8.473173193	2.38797E-17	1.51089E-16	
AGAP011578	nan	nan	408.1797303	5.113309696	0.232704283	21.97342322	5.172E-107	5.1835E-105	
AGAP010398	AGAP010398	Flavin-containing monooxygenase FMO GS-OX-like 1	2219.565421	5.04210753	0.295949076	17.03707813	4.35976E-65	1.51005E-63	
AGAP000745	AGAP000745	nan	12.33594826	5.017490393	0.784368753	6.396851448	1.58614E-10	6.39135E-10	
AGAP013059	AGAP013059	nan	312.6951851	4.983082365	0.225695342	22.07880018	5.0532E-108	5.2315E-106	
AGAP008235	AGAP008235	nan	4.826954054	4.979070018	0.993874755	5.009755999	5.44991E-07	1.56297E-06	
AGAP008851	AGAP008851	E3 ubiquitin-protein ligase mind-bomb [Source:UniProtKB/TrEMBL;A	12042.35188	4.958656949	0.145571218	34.06344342	2.5668E-254	1.8601E-251	
AGAP013480	AGAP013480	nan	3.590374652	4.891248243	1.070640044	4.568527277	4.91163E-06	1.27192E-05	
AGAP011576	nan	nan	172.8423044	4.884975144	0.273106829	17.88668252	1.49763E-71	6.327E-70	
AGAP028432	AGAP028432	nan	29.99478111	4.852627814	0.697149222	6.960673072	3.38651E-12	1.54351E-11	
AGAP028138	AGAP028138	nan	5559.34555	4.838569559	0.154181625	31.38227105	3.532E-216	1.4467E-213	
AGAP002291	AGAP002291	ebony	1221.910971	4.821937032	0.298908838	16.1317981	1.52515E-58	4.64997E-57	
AGAP001767	AGAP001767	Peptidase (mitochondrial processing) beta	29.30456531	4.808103681	0.539067204	8.919302909	4.69232E-19	3.25526E-18	
AGAP004382	GSTD3	glutathione S-transferase delta class 3	301.6395523	4.782964611	0.392783217	12.17711043	4.11608E-34	5.64448E-33	
AGAP001763	Fatp	fatty acid transporter protein 1	1430.266221	4.763243002	0.168815063	28.21574645	3.7483E-175	9.5439E-173	
AGAP029077	AGAP029077	nan	20.54793606	4.731097678	0.610346367	7.75149642	9.08159E-15	4.96274E-14	
AGAP007216	AGAP007216	DE-cadherin	328.681905	4.712111296	0.212535955	22.17089008	6.56E-109	6.8669E-107	
AGAP004316	AGAP004316	nan	4851.502155	4.668543972	0.296069202	15.76842148	5.13164E-56	1.44746E-54	
AGAP012581	AGAP012581	nan	30.44937246	4.647732107	0.491782187	9.450793934	3.3627E-21	2.61602E-20	
AGAP007666	AGAP007666	calcyphosin-like protein	10259.11802	4.629661893	0.250552256	18.47930466	3.03062E-76	1.47935E-74	
AGAP012529	GALE8	galectin 8	209.4838637	4.614028629	0.248138641	18.59455914	3.55625E-77	1.80126E-75	
AGAP001753	AGAP001753	15-hydroxyprostaglandin dehydrogenase (NAD)	34.74159678	4.54898947	0.497561631	9.142564826	6.09884E-20	4.46443E-19	
AGAP005205	PGRPLA	peptidoglycan recognition protein (long)	4109.111356	4.519663807	0.212616761	21.257326	2.8204E-100	2.35137E-98	
AGAP011225	AGAP011225	nan	57.3460484	4.513355285	0.364459668	12.38368927	3.20275E-35	4.57862E-34	
AGAP010385	AGAP010385	nan	86.07016609	4.50518505	0.344460126	13.07897406	4.34262E-39	7.05376E-38	
AGAP010390	COE12O	carboxylesterase	1082.615231	4.50345105	0.216708186	20.78117642	6.40693E-96	4.79045E-94	
AGAP007684	AGAP007684	Tubulointerstitial nephritis antigen	2986.014541	4.500908187	0.167961969	26.79718631	3.4847E-158	6.6998E-156	
AGAP013179	AGAP013179	nan	1393.535639	4.500873941	0.178477963	25.21809346	2.5367E-140	3.9831E-138	
AGAP001509	AGAP001509	nan	15.66755972	4.473477738	0.763041733	5.862690789	4.55426E-09	1.60515E-08	
AGAP006345	AGAP006345	nan	50.6959971	4.40142724	0.408312501	10.77955544	4.29959E-27	4.40287E-26	
AGAP001679	nan	nan	75.51096568	4.393964211	0.371476076	11.82839082	2.78428E-32	3.56396E-31	
AGAP013382	AGAP013382	nan	4.610872597	4.379260006	0.988667687	4.42945599	9.44711E-06	2.36391E-05	
AGAP000667	AGAP000667	G_PROTEIN_RECEP_F1_2 domain-containing protein [Source:UniPro	10.966911	4.375489321	0.821273441	5.327688808	9.94704E-08	3.06145E-07	
AGAP000133	AGAP000133	nan	26.74337643	4.372513068	0.550486435	7.942998761	1.97351E-15	1.11868E-14	
AGAP029075	AGAP029075	nan	6.608415866	4.331558838	0.97505347	4.443280822	8.89689E-06	2.23394E-05	
AGAP001061	AGAP001061	nan	12.8658239	4.323205349	0.69351603	6.233749703	4.5540E-10	1.7736E-09	
AGAP001705	AGAP001705	nan	598.5040026	4.270835173	0.189637716	22.52102205	2.5834E-112	2.7657E-110	
AGAP002232	GPR5HT2A	putative serotonin 5HT-2a receptor	4.627635348	4.25586234	0.980578749	4.340153551	1.42383E-05	3.47781E-05	
AGAP010818	AGAP010818	nan	263.0759335	4.253454758	0.304341039	13.97594874	2.18581E-44	4.25466E-43	
AGAP006367	AGAP006367	nan	7339.224631	4.186676762	0.12803169	32.70031628	1.5457E-234	9.1011E-232	Prohemocytes and Megacytes
AGAP028652	AGAP028652	nan	83.33450069	4.180241485	0.305182657	13.69750671	1.05071E-42	1.92957E-41	
AGAP013194	AGAP013194	nan	26.73183862	4.179948626	0.514950267	8.117188975	4.77106E-16	2.79702E-15	
AGAP028742	AGAP028742	nan	5.526065886	4.171738628	0.936050441	4.456745541	8.32133E-06	2.09781E-05	
AGAP010816	TEP3	thioester-containing protein 3	62660.7236	4.153502512	0.220728572	18.81724002	5.45532E-79	2.90365E-77	AM granulocytes
AGAP010709	CTL2	C-type lectin (CTL)	6.962910679	4.149323731	0.815225457	5.089786753	3.58466E-07	1.05108E-06	
AGAP012787	AGAP012787	nan	4.25996281	4.141323136	1.098656544	3.769442923	0.000163612	0.000351819	
AGAP001004	TOLL1A	TOLL-like receptor 1A	757.4906654	4.105939711	0.211676876	19.39720481	8.1483E-84	4.95259E-82	
AGAP004181	AGAP004181	Fibroblast growth factor [Source:UniProtKB/TrEMBL;Acc:A0NDD8]	108.3931144	4.082026573	0.282219388	14.46401892	2.045E-47	4.37863E-46	
AGAP012748	AGAP012748	nan	226.2312456	4.076905591	0.198811373	20.50640021	1.88758E-93	1.34719E-91	
AGAP001048	AGAP001048	nan	8.569616286	4.073769288	0.777939014	5.236617796	1.63546E-07	4.9431E-07	
AGAP009590	AGAP009590	amiloride-sensitive sodium channel, other	25.08986149	4.027708717	0.489815124	8.222916195	1.98614E-16	1.19029E-15	
AGAP010617	AGAP010617	nan	5.187413678	4.014771016	1.081080162	3.713666346	0.000204278	0.000434229	
AGAP010869	AGAP010869	fibrinogen	211.8191342	4.01427125	0.50467447	7.954179717	1.80322E-15	1.0271E-14	
AGAP002591	AGAP002591	nan	68.18572522	4.009709645	0.350556533	11.43812558	2.69648E-30	3.21564E-29	
AGAP028424	AGAP028424	nan	12.44339884	3.950739816	0.655786976	6.024425553	1.69711E-09	6.2309E-09	
AGAP012172	nan	nan	61.20090705	3.942407848	0.357271542	11.03476597	2.59727E-28	2.80606E-27	
AGAP004170	AGAP004170	nan	861.686701	3.936937407	0.203077887	19.3863422	1.00645E-83	6.07804E-82	
AGAP028574	AGAP028574	nan	25.15266406	3.914226008	0.46645047	8.391514769	4.79918E-17	2.9765E-16	
AGAP012011	AGAP012011	nan	608.3912712	3.909853698	0.186469643	20.96777594	1.29162E-97	9.893E-96	
AGAP004837	nan	nan	911.9044456	3.905203598	0.209913931	18.60383244	2.99138E-77	1.52334E-75	
AGAP010387	AGAP010387	alanine-glyoxylate aminotransferase	208.9900095	3.898506459	0.71001505	5.490737779	4.00258E-08	1.28566E-07	
AGAP000835	AGAP000835	nan	14.19801452	3.891478334	0.789899311	4.92654985	8.36943E-07	2.35298E-06	
AGAP013005	AGAP013005	nan	48169.71659	3.889840306	0.269699084	14.42289031	3.71455E-47	7.88171E-46	
AGAP009155	AGAP009155	nan	28.75046445	3.875752747	0.429856158	9.016394617	1.94381E-19	1.38105E-18	
AGAP012171	nan	nan	322.3687888	3.864774626	0.211464148	18.27626418	1.27892E-74	5.87741E-73	
AGAP011654	AGAP011654	membrane dipeptidase	317.542632	3.864620461	0.36441992	10.60485514	2.82902E-26	2.77338E-25	
AGAP006520	AGAP006520	Fatty acid elongase 2	285.4705459	3.795738454	0.20123076	18.86261554	2.3148E-79	1.25332E-77	
AGAP010855	AGAP010855	solute carrier family 45, member 1/2/4	26.94987032	3.767997156	0.456747421	8.249629853	1.58886E-16	9.55852E-16	
AGAP010542	dpr6	defective proboscis extension response 6	13.87282103	3.765043673	0.579086417	6.501695713	7.94196E-11	3.26588E-10	
AGAP006986	AGAP006986	nan	63.95069943	3.760568818	0.528657152	7.113435999	1.13189E-12	5.30788E-12	
AGAP010851	GPRLKK	putative leukokinin receptor	19.02684305	3.753645357	0.506382831	7.412663164	1.23788E-13	6.19006E-13	
AGAP009050	AGAP009050	cyclic nucleotide gated channel, invertebrate	4.971353142	3.751865174	0.968715484	3.873031076	0.00010749	0.000236936	
AGAP004574	AGAP004574	nan	181.2982478	3.734529071	0.27437419	13.61108009	3.4412E-42	6.22257E-41	
AGAP010240	ESP	late trypsin	7.684845367	3.70010401	0.72645855	5.093344983	3.51801E-07	1.0325E-06	
AGAP012588	AGAP012588	nan	4.070845174	3.699617854	0.907309853	4.077568256	4.55092E-05	0.000104929	
AGAP006449	AGAP006449	nan	6.577349064	3.697748192	0.773326834	4.781611122	1.73896E-06	4.72397E-06	
AGAP005949	AGAP005949	2-acylglycerol O-acyltransferase 2	1869.718015	3.689835743	0.154001684	23.9597103	7.3195E-127	9.9938E-125	
AGAP001376	SRPN17	serine protease inhibitor (serpin) 17	2134.989079	3.685525524	0.244477096	15.07513619	2.36029E-51	5.67252E-50	
AGAP009467	ABCG16	ATP-binding cassette transporter (ABC transporter) family G membe	162.6789378	3.658598516	0.277057569	13.20519244	8.18902E-40	1.36065E-38	
AGAP007356	AGAP007356	CRAL-TRIO domain-containing protein [Source:UniProtKB/TrEMBL;A	7.428289046	3.650557961	0.796475364	4.583390935	4.57496E-06	1.1899E-05	
AGAP011355	AGAP011355	nan	1146.688915	3.632880017	0.329790955	11.01570544	3.21012E-28	3.44841E-27	
AGAP010294	AGAP010294	nan	8.978569735	3.631947615	0.691394661	5.253074433	1.49581E-07	4.53557E-07	
AGAP003627	AGAP003627	nan	312.5971806	3.591767533	0.332455278	10.80376151	3.30385E-27	3.39799E-26	
AGAP007858	AGAP007858	lysyl-tRNA synthetase, class II	435.1658098	3.585353666	0.198879698	18.02775091	1.17995E-72	5.17035E-71	
AGAP007262	AGAP007262	chymotrypsin-like protease	3.017637292	3.583170245	1.00830931	3.553641932	0.000379936	0.00077392	
AGAP010759	AGAP010759	nan	9550.050842	3.581034892	0.227030083	15.77339376	4.74312E-56	1.34189E-54	Megacytes
AGAP028541	AGAP028541	nan	41.48900921	3.576155379	0.389605454	9.178915079	4.35456E-20	3.20503E-19	
AGAP005285	AGAP005285	nan	388.9666566	3.566213826	0.164646555	21.65981441	4.9121E-104	4.5819E-102	
AGAP010760	AGAP010760	nan	12109.61415	3.52948473	0.223693646	15.77820738	4.39494E-56	1.24713E-54	
AGAP005742	AGAP005742	semaphorin	54.73561392	3.529220116	0.331256398	10.65404362	1.66952E-26	1.65216E-25	
AGAP003139	SRPN9	serine protease inhibitor (serpin) 9	3098.83565	3.528515234	0.1217241	28.98781114	9.3726E-185	2.6757E-182	
AGAP013487	AGAP013487	nan	95.5750241	3.52552181	0.378350519	9.318136572	1.18401E-20	8.96672E-20	
AGAP006985	AGAP006985	nan	98.6841087	3.525303596	0.447248609	7.882201363	3.21663E-15	1.80273E-14	
AGAP007318	TM7318	Transmembrane protein - megacyte marker	7478.159662	3.519945262	0.22981957	15.31612502	5.96704E-53	1.52346E-51	Megacytes

AGAP006343	PGRPS2	peptidoglycan recognition protein (short)	19.36251327	3.509206816	0.504347815	6.957910224	3.45357E-12	1.57179E-11	
AGAP005756	COEAE1D	carboxylesterase	287.5124919	3.505892189	0.253240293	13.84413257	1.38037E-43	2.63248E-42	
AGAP003892	AGAP003892	solute carrier family 29 (equilibrative nucleoside transporter), memt	7735.653319	3.505463334	0.180513216	19.41942763	5.28759E-84	3.2347E-82	
AGAP028094	AGAP028094	nan	102.5874086	3.482743526	0.328566226	10.59982203	2.98548E-26	2.92372E-25	
AGAP012321	OBP26	odorant-binding protein 26	8.069470565	3.459364058	0.707432684	4.890025776	1.00823E-06	2.80855E-06	
AGAP000976	AGAP000976	nan	20.96702416	3.456514724	0.483776496	7.144858731	9.00885E-13	4.26923E-12	
AGAP006603	AGAP006603	nan	253.6852551	3.454719664	0.226954278	15.22209536	2.52318E-52	6.35586E-51	
AGAP001652	AGAP001652	lipase	33397.88846	3.446083482	0.120094935	28.69466134	4.4477E-181	1.2324E-178	Megacytes
AGAP005440	AGAP005440	nan	11.53728419	3.441455479	0.637010503	5.402509792	6.57149E-08	2.06298E-07	
AGAP010762	nan	nan	723.8389244	3.438150439	0.21566802	15.94186494	3.24522E-57	9.55415E-56	
AGAP010675	LRIM18	leucine-rich immune protein (Coil-less)	554.0630047	3.394752947	0.219684695	15.45284232	7.21887E-54	1.88914E-52	
AGAP008100	AGAP008100	Spire [Source:UniProtKB/TrEMBL;Acc:A0A1S4GX95]	465.3383139	3.388809853	0.215974124	15.69081421	1.74799E-55	4.83674E-54	
AGAP011063	AGAP011063	nan	11.66403047	3.376061995	0.565508515	5.969957847	2.37315E-09	8.58251E-09	
AGAP013117	AGAP013117	nan	4832.055875	3.37436503	0.226525766	14.89616429	3.49051E-50	8.05982E-49	
AGAP002643	AGAP002643	nan	8.926780993	3.366014173	0.953295628	3.53092375	0.000414111	0.000838998	
AGAP008403	AGAP008403	nan	307.8027194	3.346911517	0.247522516	13.5216447	1.16541E-41	2.05605E-40	
AGAP001005	AGAP001005	nan	10.89803658	3.344267139	0.744617998	4.491252087	7.08057E-06	1.79898E-05	
AGAP003318	AGAP003318	nan	146.408358	3.33645302	0.220070341	15.16084812	6.42345E-52	1.58003E-50	
AGAP003319	AGAP003319	nan	10632.10269	3.327043033	0.13845288	24.03014675	1.3465E-127	1.8655E-125	Megacytes
AGAP028531	AGAP028531	nan	83.38038377	3.324423113	0.237709119	13.98525695	1.91783E-44	3.74076E-43	
AGAP009424	AGAP009424	nan	709.9146119	3.314407578	0.138854208	23.86969491	6.3243E-126	8.2752E-124	
AGAP007290	AGAP007290	nan	35.66227852	3.311507228	0.513620037	6.447387149	1.13795E-10	4.63494E-10	
AGAP003626	AGAP003626	nan	86.15910223	3.304448947	0.291439478	11.33837105	8.47065E-30	9.80368E-29	
AGAP013166	Cht5-1	chitinase	464.379508	3.295251224	0.327529936	10.06091615	8.22295E-24	7.19967E-23	
AGAP001648	CLIPB17	CLIP-domain serine protease	9264.846222	3.29031506	0.30899714	10.64836735	1.7745E-26	1.7542E-25	
AGAP004243	AGAP004243	nan	16.50408841	3.289421142	0.589621426	5.57886976	2.42086E-08	7.92734E-08	
AGAP004920	CASPS6	short caspase 6	720.3876092	3.26116271	0.175039789	18.63097946	1.80196E-77	9.27666E-76	
AGAP010027	AGAP010027	nan	15.31748505	3.253123128	0.495850555	6.560692722	5.35584E-11	2.24056E-10	
AGAP006641	nan	nan	46.0072813	3.252011142	0.293969843	11.06239712	1.90926E-28	2.07464E-27	
AGAP004309	AGAP004309	solute carrier family 22	1105.673549	3.237728565	0.138468626	23.38239827	6.4555E-121	8.0022E-119	
AGAP011667	AGAP011667	nan	17.1722601	3.202296789	0.615962563	5.198849706	2.00526E-07	6.01641E-07	
AGAP001704	AGAP001704	isopentenyl-diphosphate delta-isomerase	1108.654866	3.194506374	0.094113214	33.94322909	1.5353E-252	1.0331E-249	
AGAP011560	AGAP011560	nan	7031.969228	3.186375928	0.119727501	26.61356748	4.7288E-156	8.25E-154	
AGAP005755	AGAP005755	DNA-binding protein D-ETS-3	17.09583769	3.167032606	0.487523736	6.496160843	8.23956E-11	3.38382E-10	
AGAP003496	AGAP003496	nan	11011.69344	3.154169972	0.118490752	26.61954549	4.0323E-156	7.1676E-154	
AGAP006689	AGAP006689	BTB (POZ) domain containing 9	269.5604966	3.138907034	0.204997953	15.31189453	6.36816E-53	1.62147E-51	
AGAP009490	AGAP009490	Neccdin-like 2	456.0357986	3.135336635	0.100399436	31.22862801	4.3556E-214	1.7097E-211	
AGAP004335	AGAP004335	filamin	17572.09317	3.132381678	0.143729188	21.79363651	2.6661E-105	2.6164E-103	
AGAP006642	nan	nan	158.541787	3.122376973	0.201035871	15.53144199	2.12546E-54	5.65649E-53	
AGAP028005	AGAP028005	nan	24.09103098	3.111365845	0.431623752	7.208513975	5.65658E-13	2.71614E-12	
AGAP003839	AGAP003839	Fem-1 homolog c	2390.28197	3.10470337	0.075717415	41.0038216	0	0	
AGAP008671	AGAP008671	nan	138.1995901	3.09377269	0.215079967	14.38429032	6.49408E-47	1.3626E-45	
AGAP000235	AGAP000235	Thymosin	39370.31323	3.090485049	0.078616245	39.31102347	0	0	Megacytes
AGAP002677	AGAP002677	coiled-coil domain-containing protein lobo homolog	5.832111103	3.090367103	0.726377629	4.254491025	2.09525E-05	5.01126E-05	
AGAP029047	CTL5	C-type lectin	8.473021694	3.083190214	0.680354664	4.531739657	5.84999E-06	1.50335E-05	
AGAP013197	AGAP013197	nan	16.19845417	3.076212214	0.468490176	6.566225652	5.16066E-11	2.16371E-10	
AGAP007289	OBP46	odorant-binding protein 46	59.83945933	3.065679524	0.296011218	10.35663291	3.90466E-25	3.64939E-24	
AGAP007287	OBP47	odorant-binding protein 47	16.24857223	3.065551738	0.551290808	5.56079941	2.68726E-08	8.74193E-08	
AGAP009184	AGAP009184	nan	731.5342998	3.063042997	0.272885531	11.2246442	3.08626E-29	3.47795E-28	
AGAP011389	AGAP011389	nan	31.10288838	3.052289506	0.396559049	7.696935705	1.39368E-14	7.46015E-14	
AGAP005713	AGAP005713	nan	15.10544587	3.051343247	0.452592633	6.741919826	1.56307E-11	6.76733E-11	
AGAP003249	CLIPB3	CLIP-domain serine protease	699.1854621	3.050823047	0.238996434	12.76514047	2.56687E-37	3.93211E-36	
AGAP007207	AGAP007207	nan	76.68301283	3.049419766	0.257618134	11.83697637	2.51352E-32	3.22614E-31	
AGAP028615	AGAP028615	nan	129.3585815	3.04496956	0.293550926	10.37288351	3.29431E-25	3.082E-24	
AGAP004707	para	voltage-gated sodium channel	55.99610076	3.042386927	0.302148911	10.06916398	7.56181E-24	6.63313E-23	
AGAP013034	IAP8	inhibitor of apoptosis 8	19.73609989	3.020611559	0.390511598	7.735011126	1.03394E-14	5.62399E-14	
AGAP003186	AGAP003186	upstream stimulatory factor	79.93399687	3.004181712	0.264086101	11.37576608	5.52159E-30	6.48615E-29	
AGAP003495	AGAP003495	nan	7.878124946	2.999308208	0.664596658	4.512975156	6.39245E-06	1.63158E-05	
AGAP006215	GPRMTH1	methuselah receptor 1	282.8197377	2.980383514	0.199087966	14.97018413	1.15002E-50	2.71538E-49	
AGAP010571	AGAP010571	nan	102.0622474	2.972367263	0.209646622	14.17798785	1.25391E-45	2.53499E-44	
AGAP003656	AGAP003656	Terribly reduced optic lobes, isoform B [Source:UniProtKB/TrEMBL;A	33382.07926	2.969547437	0.233294818	12.72873295	4.09429E-37	6.22135E-36	
AGAP029166	AGAP029166	nan	14302.24015	2.953223582	0.236675158	12.4779618	9.84752E-36	1.43169E-34	
AGAP009576	AGAP009576	collagen alpha 1	5.519976201	2.949676701	0.807847551	3.651278879	0.000260938	0.000545321	
AGAP001169	Gr49	gustatory receptor 49	34.47423754	2.94746034	0.330978616	8.905289344	5.3247E-19	1.68311E-18	
AGAP005729	AGAP005729	cyclin-dependent kinase 14	722.6162693	2.94622387	0.136867615	21.52608467	8.872E-103	7.9603E-101	
AGAP006690	AGAP006690	BTB (POZ) domain containing 9	6099.788427	2.943786111	0.171740485	17.14089784	7.35068E-66	2.64316E-64	
AGAP008366	TEP2	thioester-containing protein 2	2622.051057	2.943343731	0.0858671	34.27789849	1.6754E-257	1.5784E-254	
AGAP010272	IR25a	ionotropic receptor IR25a	24.4642251	2.942145602	0.369958492	7.952637038	1.82583E-15	1.03934E-14	
AGAP000786	AGAP000786	ZP domain-containing protein [Source:UniProtKB/TrEMBL;Acc:Q7QE	22.87413715	2.929738135	0.448887659	6.52666224	6.72515E-11	2.78617E-10	
AGAP002802	AGAP002802	neural cell adhesion molecule	308.3665291	2.924663628	0.224796015	13.01030017	1.06921E-38	1.7102E-37	
AGAP010002	AGAP010002	nan	7.904902055	2.924369934	0.632889224	4.620666336	3.8251E-06	1.00351E-05	
AGAP011294	DEF1	defensin anti-microbial peptide	9881.820375	2.922360646	0.52534384	5.562758	2.65544E-08	8.64739E-08	AM granulocytes
AGAP012991	AGAP012991	Fascin [Source:UniProtKB/TrEMBL;Acc:F5HLZ2]	1219.272325	2.912953405	0.179343014	16.2423578	2.5301E-59	7.73898E-58	
AGAP003120	AGAP003120	nan	11.14672152	2.910909881	0.538088499	5.409723281	6.31222E-08	1.98423E-07	
AGAP013430	AGAP013430	nan	97.31632396	2.905915283	0.296411448	9.803654009	1.08585E-22	9.02894E-22	
AGAP027980	ABCC10	ATP-binding cassette transporter (ABC transporter) family C membe	393.4229794	2.903222783	0.16422288	17.67855233	6.13514E-70	2.49134E-68	
AGAP009212	SRPN6	serine protease inhibitor (serpin) 6	4770.187149	2.896154957	0.163756954	17.68569143	5.40539E-70	2.20451E-68	
AGAP011391	AGAP011391	nan	67.78722763	2.890477594	0.296254065	9.75675252	1.72594E-22	1.41761E-21	
AGAP011390	AGAP011390	nan	14.99695138	2.875637539	0.573188903	5.0169107	5.2509E-07	1.50911E-06	
AGAP005194	nan	nan	10.23566919	2.867844868	0.570150093	5.029982282	4.90525E-07	1.41365E-06	
AGAP009049	Ch116	Chitinase [Source:UniProtKB/TrEMBL;Acc:A0A1S4GZY6]	18.12612964	2.866043358	0.581910521	4.925230346	8.4261E-07	2.3668E-06	
AGAP010241	AGAP010241	gamma-glutamyltranspeptidase	43.78029184	2.850909362	0.310313239	9.187198613	4.03205E-20	2.97229E-19	
AGAP012536	AGAP012536	nan	13.33931205	2.837957243	0.543014631	5.226299774	1.72936E-07	5.22022E-07	
AGAP000628	AGAP000628	nan	95.15290212	2.834890127	0.327718106	8.650392138	5.13228E-18	3.37884E-17	
AGAP012945	AGAP012945	CASPS4 protein	109.8700581	2.834189324	0.222741975	12.72409172	4.34498E-37	6.58104E-36	
AGAP013081	AGAP013081	nan	96.77306728	2.833323638	0.241521745	11.7311327	8.82695E-32	1.1029E-30	
AGAP005547	AGAP005547	alpha-crystallin B chain	52.28380792	2.828605593	0.307739465	9.191559465	3.87187E-20	2.86318E-19	
AGAP008368	TEP14	thioester-containing protein 14	9679.75662	2.826859645	0.179487146	15.74964956	6.9063E-56	1.93069E-54	
AGAP010861	nan	nan	2139.682887	2.826063415	0.268617822	10.52075918	6.93128E-26	6.65643E-25	
AGAP007917	ABCC12	ATP-binding cassette transporter (ABC transporter) family C membe	7223.949465	2.813232634	0.147885435	19.0230541	1.09892E-80	6.27449E-79	
AGAP013218	AGAP013218	sodium-independent sulfate anion transporter	1458.174905	2.812393112	0.137755861	20.41577819	1.21088E-92	8.51319E-91	
AGAP009549	AGAP009549	nan	306.909315	2.810618837	0.221389088	12.69538105	6.27239E-37	9.43965E-36	
AGAP013221	AGAP013221	nan	4538.405584	2.794497608	0.279013629	10.01563119	1.30129E-23	1.12266E-22	
AGAP010479	AGAP010479	nan	459.3921529	2.794359145	0.137435605	20.33213409	6.68316E-92	4.49729E-90	
AGAP004483	AGAP004483	Lethal giant larvae	5028.816532	2.775249543	0.149955674	18.50713265	1.80876E-76	8.92116E-75	
AGAP010417	AGAP010417	tetratricopeptide repeat protein 39B	2743.259669	2.766584334	0.159767341	17.31633212	3.54229E-67	1.29852E-65	
AGAP000868	AGAP000868	beta-1,4-mannosyltransferase egghead protein	4835.104603	2.751447317	0.202379799	13.59546422	4.26049E-42	7.65994E-41	
AGAP010328	AGAP010328	nan	36.40248963	2.748746522	0.366021245	7.509800489	5.92175E-14	3.01724E-13	
AGAP006917	Gr55	gustatory receptor 55	63.2237979	2.74278623	0.343766662	7.978627747	1.47969E-15	8.45884E-15	
AGAP006442	AGAP006442	nan	175.4100797	2.742217952	0.326780091	8.391631029	4.79444E-17	2.97552E-16	
AGAP009460	AGAP009460	c-Jun N-terminal kinase	258.877279	2.732183301	0.177903847	15.35764034	3.14826E-53	8.10377E-52	
AGAP006342	PGRPS3	peptidoglycan recognition protein (short)	17.74977137	2.729041906	0.702853207	3.882804945	0.000103258	0.00022841	
AGAP007685	AGAP007685	nan	1642.6336	2.719749888	0.128717413	21.12961975	4.2496E-99	3.33625E-97	
AGAP007203	AGAP007203	DE-cadherin	681.3832307	2.719236461	0.148617641	18.29686195	8.76545E-75	4.048E-73	
AGAP013360	AGAP013360	nan	57.65098178	2.705703525	0.43471435	6.224095252	4.84343E-10	1.87855E-09	
AGAP005162	AGAP005162	nan	2522.373747	2.702333581	0.191957742	14.07775251	5.20386E-45	1.02779E-43	
AGAP009984	AGAP009984	cell cycle control protein 50A	722.5773174	2.691292746	0.1492946	18.02672537	1.20203E-72	5.24275E-71	
AGAP001676	AGAP001676	actin, cytoplasmic	14.05968558	2.67556056	0.684284209	3.910013596	9.22909E-05	0.000205452	
AGAP005100	Vps60	vacuolar protein sorting 60	4178.014177	2.667988174	0.082652298	32.27966105	1.3498E-228	6.6929E-226	
AGAP007080	AGAP007080	hexosaminidase	1438.181274	2.651861768	0.202725883	13.08102214	4.22717E-39	6.8781E-38	
AGAP004281	AGAP004281	nan	17.30103525	2.65113093	0.48407829	5.476657365	4.33435E-08	1.38608E-07	
AGAP005408	AGAP005408	nan	14.93859068	2.643982323	0.425276781	6.217086002	5.06472E-10	1.95954E-09	
AGAP013066	AGAP013066	nan	12.67584015	2.629542872	0.493623819	5.327017808	9.98384E-08	3.06977E-07	
AGAP005246	SRPN10	serine protease inhibitor (serpin) 10	11070.86802	2.628637134	0.086237398	30.481406	4.5966E-204	1.6039E-201	Megacytes
AGAP000784	AGAP000784	abhydrolase domain containing 4	3941.958531	2.627781415	0.086688661	30.31286183	7.7597E-202	2.6109E-199	
AGAP000307	AGAP000307	Integrin alpha-PS1	2265.810929	2.624431837	0.105589431	24.85506173	2.2797E-136	3.3558E-134	
AGAP007036	APL1A	Anopheles Plasmodium-responsive Leucine-Rich Repeat 1A	1456.477362	2.623653516	0.264571135	9.916627985	3.52463E-23	2.9888E-22	
AGAP006427	ABCC7	ATP-binding cassette transporter (ABC transporter) family C membe	5329.59177	2.623129975	0.199548049	13.14535516	1.80954E-39	2.96481E-38	
AGAP008940	AGAP008940	solute carrier family 6 (neurotransmitter transporter, GABA) membe	506.7084941	2.622706075	0.200646081	13.07130473	4.80345E-39	7.77548E-38	
AGAP012916	AGAP012916	nan	9061.550348	2.615506007	0.181322741	14.42458894	3.62423E-47	7.70741E-46	Granulocytes and Megacytes
AGAP013027	AGAP013027	Protein toll	9828.824707	2.611676022	0.210977531	12.3789297	3.39845E-35	4.84369E-34	Megacytes
AGAP005527	AGAP005527	PBPe domain-containing protein [Source:UniProtKB/TrEMBL;Acc:A0A	28.86170522	2.601288169	0.399993443	6.503327037	7.85627E-11	3.23488E-10	
AGAP007156	AGAP007156	nan	7.99232791	2.59173468	0.624807418	4.148053635	3.35314E-05	7.84648E-05	
AGAP001623	AGAP001623	nan	1089.6557	2.586344477	0.15900407	16.26590109	1.72313E-59	5.28783E-58	
AGAP001647	AGAP001647	nan	13.90756209	2.584874496	0.700825196	3.688329859	0.000225731	0.000475965	
AGAP011479	AGAP011479	hyaluronoglucosaminidase	59.91269357	2.583249954	0.256239988	10.08136934	6.67888E-24	5.87504E-23	
AGAP013496	Cht5-3	chitinase	44.57409181	2.580734555	0.339742141	7.596156741	3.05055E-14	1.58956E-13	
AGAP011653	AGAP011653	membrane dipeptidase	16.29744916	2.574841815	0.594793929	4.328964516	1.49812E-05	3.6498E-05	
AGAP003247	CLIPB19	CLIP-domain serine protease	1759.954841	2.570395939	0.274299017	9.370780717	7.1998E-21	5.51458E-20	
AGAP028842	SSU_rRNA_eukar	Eukaryotic small subunit ribosomal RNA [Source:RFAM;Acc:RF01960	90.2435724	2.55653131	0.711067906	3.595340597	0.000323967	0.000666834	
AGAP013073	AGAP013073	nan	24.81522149	2.55620036	0.336846785	7.588614392	3.23344E-14	1.68114E-13	
AGAP000163	GSTMS2	glutathione transferase microsomal 2	163.6791333	2.547582272	0.223372999	11.40505916	3.94509E-30	4.66332E-29	
AGAP003352	AGAP003352	Stomatin (EPB72)-like 3	5258.622442	2.546156399	0.186343329	13.66379149	1.67054E-42	3.05003E-41	Megacytes
AGAP007291	IAP4	inhibitor of apoptosis 4	154.2438589	2.541840917	0.260407564	9.761010314	1.65498E-22	1.3629E-21	
AGAP002326	AGAP002326	nan	10.01928458	2.541710628	0.605077704	4.200635074	2.66167E-05	6.29724E-05	
AGAP004784	AGAP004784	fatty acyl-CoA reductase 2	1301.202247	2.537466672	0.135168247	18.77265355	1.26411E-78	6.69054E-77	
AGAP012696	AGAP012696	Sulfotransferase (Sult)	300.8656569	2.523311391	0.235357097	10.72120377	8.09429E-27	8.16449E-26	
AGAP003790	ANXB9	annexin B9	7555.362031	2.513237969	0.223011904	11.26952386	1.85571E-29	2.11143E-28	

AGAP012384	AGAP012384	nan	14.70484317	2.510804297	0.40542433	6.193028178	5.90192E-10	2.26669E-09	
AGAP000651	Actin5C	Actin-5C [Source:UniProtKB/Swiss-Prot;Acc:P84185]	194466.2946	2.509401475	0.070345517	35.6725146	1.055E-278	1.66E-275	Granulocytes and Megacytes
AGAP002270	CLIPB7	CLIP-domain serine protease	659.568654	2.507618185	0.252318085	9.938321234	2.83566E-23	2.41543E-22	
AGAP007821	AGAP007821	nan	2115.812727	2.502605815	0.347010852	7.211894963	5.51785E-13	2.65765E-12	
AGAP009745	AGAP009745	Sugar transporter ERD6-like 4	1788.51531	2.501737477	0.183735738	13.61595466	3.21912E-42	5.83217E-41	
AGAP006103	AGAP006103	nan	1120.036332	2.497956821	0.229281758	10.89470372	1.22164E-27	1.27312E-26	
AGAP012677	AGAP012677	nan	683.9754154	2.49692911	0.239766617	10.41399817	2.14039E-25	2.02456E-24	
AGAP006347	AGAP006347	potassium voltage-gated channel KQT-like subfamily, invertebrate	1199.507309	2.494910391	0.18347811	13.59786399	4.123E-42	7.42691E-41	
AGAP009581	AGAP009581	collagen type I/II/III/V/XI/XXIV/XXVII alpha	15.296804	2.487902201	0.442494923	5.62244236	1.88276E-08	6.23463E-08	
AGAP007346	LYSC5	C-type lysozyme	26.59299175	2.48381085	0.358168297	6.934759072	4.06914E-12	1.84216E-11	
AGAP002262	AGAP002262	Adenylate cyclase 8 [Source:UniProtKB/TrEMBL;Acc:A0A1S4GF11]	517.9406016	2.482252938	0.239223687	10.37628409	3.17909E-25	2.98309E-24	
AGAP001021	AGAP001021	dihydropyrimidine dehydrogenase (NADP+)	6635.508297	2.481232948	0.185252959	13.3937561	6.57687E-41	1.13689E-39	
AGAP005818	AGAP005818	nurim homolog	195.8631516	2.480852224	0.165012198	15.03435656	4.37277E-51	1.04558E-49	
AGAP008133	AGAP008133	Retinaldehyde binding protein 1 [Source:UniProtKB/TrEMBL;Acc:A0A	11.84481105	2.480216817	0.483138189	5.13355573	2.84319E-07	8.40467E-07	
AGAP004636	AGAP004636	sodium-independent sulfate anion transporter	404.5886291	2.479725353	0.134483719	18.43885254	6.40869E-76	3.0493E-74	
AGAP000998	AGAP000998	insulin-like growth factor 2 receptor	366.6429897	2.475052802	0.142281523	17.39546185	8.9304E-68	3.35192E-66	
AGAP010392	AGAP010392	calumenin	17468.3635	2.466793358	0.161961667	15.23072349	2.21131E-52	5.58519E-51	
AGAP010175	AGAP010175	adenylyl cyclase-associated protein 1	10435.9944	2.460454195	0.092042101	26.73183437	2.0084E-157	3.71E-155	Megacytes
AGAP006732	nan	nan	7.476875059	2.45410562	0.695502323	3.528536914	0.000417864	0.000846237	
AGAP011276	AGAP011276	nan	103.0668338	2.445281652	0.229280843	10.66500637	1.48389E-26	1.4731E-25	
AGAP007035	APL1B	Anopheles Plasmodium-responsive Leucine-Rich Repeat 1B	1019.493622	2.443761697	0.276147234	8.849488238	8.79215E-19	5.98057E-18	
AGAP008219	CYP6Z1	cytochrome P450	96.79059141	2.441510767	0.318381888	7.668497666	1.74023E-14	9.25207E-14	
AGAP000889	AGAP000889	Coactosin-like protein	14892.6759	2.434451398	0.081819665	29.75386672	1.5455E-194	4.6968E-192	
AGAP013184	CLIPB36	CLIP-domain serine protease	1066.00722	2.426717555	0.273967982	8.857668471	8.17053E-19	5.57787E-18	
AGAP009991	AGAP009991	Cyclophilin B precursor	8.154525466	2.424712391	0.642102818	3.776205809	0.000159235	0.000342893	
AGAP005170	AGAP005170	nan	542.5839387	2.42262086	0.178555649	13.56787576	6.20957E-42	1.1017E-40	
AGAP010427	AGAP010427	serine palmitoyltransferase	1434.380115	2.421769689	0.140631482	17.22067963	1.85794E-66	6.70637E-65	
AGAP027986	AGAP027986	nan	5.970193469	2.42116634	0.663101131	3.651277649	0.000260939	0.000545321	
AGAP010763	AGAP010763	nan	171.5979988	2.413536367	0.287441286	8.396623872	4.59499E-17	2.8555E-16	
AGAP006455	AGAP006455	nan	16.77499917	2.409577183	0.400094243	6.022524	1.71718E-09	6.29967E-09	
AGAP007033	APL1C	Anopheles Plasmodium-responsive Leucine-Rich Repeat 1C	11735.16759	2.407308159	0.261412809	9.208837799	3.29675E-20	2.4398E-19	
AGAP010641	AGAP010641	nan	1925.659844	2.401682245	0.138090315	17.39211214	9.46799E-68	3.5396E-66	
AGAP006891	AGAP006891	NADH dehydrogenase (ubiquinone) Fe-S protein 2	11.60807987	2.399193682	0.477958742	5.019666909	5.17612E-07	1.48853E-06	
AGAP010295	AGAP010295	nan	87.26083349	2.396442608	0.352047721	6.807152739	9.95492E-12	4.3784E-11	
AGAP013492	AGAP013492	glucose dehydrogenase (acceptor)	8.615409134	2.394040751	0.573053872	4.177688813	2.94486E-05	6.93415E-05	
AGAP009194	GSTE2	glutathione S-transferase epsilon class 2	1135.33667	2.388029203	0.115530754	20.67007369	6.44178E-95	4.7045E-93	Granulocytes
AGAP010636	nan	nan	212.8105952	2.38787568	0.221887261	10.7616619	5.22198E-27	5.31278E-26	
AGAP004593	AGAP004593	EH domain-containing protein 1	5308.523884	2.387364869	0.135960009	17.55931679	5.04791E-69	1.95705E-67	
AGAP002644	AGAP002644	phospholipid-translocating ATPase	1290.995957	2.387018549	0.156822506	15.22114786	2.56E-52	6.43139E-51	
AGAP006826	AGAP006826	integrin alpha-ps	8461.448649	2.384955984	0.157677386	15.12554234	1.09892E-51	2.68906E-50	
AGAP008313	AGAP008313	nan	146.6222392	2.384647207	0.197837156	12.05358617	1.85692E-33	2.48848E-32	
AGAP007286	Obp48	odorant-binding protein 48	95.08677734	2.376598998	0.271125081	8.765692166	1.85633E-18	1.2465E-17	
AGAP011666	AGAP011666	nan	49.21896753	2.374004061	0.312428533	7.598550739	2.99465E-14	1.5613E-13	
AGAP003878	AGAP003878	nan	37837.14551	2.367149181	0.086603722	27.33311137	1.7147E-164	3.6714E-162	Oenocytes
AGAP002536	AGAP002536	nan	1726.082374	2.365798027	0.548850053	4.31046333	1.62913E-05	3.94754E-05	
AGAP003796	AGAP003796	cyclin-dependent kinases regulatory subunit 1	77.15966343	2.363815336	0.229968024	10.278887	8.77349E-25	7.95525E-24	
AGAP002165	nan	nan	9.072117212	2.350037526	0.530424579	4.430483838	9.40219E-06	2.35392E-05	
AGAP012429	NMDAR2	ionotropic receptor NMDAR2	24.05147051	2.348667404	0.379972206	6.181155802	6.3634E-10	2.43499E-09	
AGAP001678	nan	nan	1197.097733	2.343244202	0.21876871	10.71105738	9.03242E-27	9.07719E-26	
AGAP002877	AGAP002877	Tetratricopeptide repeat protein 30 homolog [Source:UniProtKB/Sw	18.09844722	2.340862278	0.361282961	6.479304403	9.21464E-11	3.77604E-10	
AGAP008835	CLIPC1	CLIP-domain serine protease	35.05362748	2.338817255	0.339891883	6.881062391	5.94078E-12	2.65882E-11	
AGAP006745	AGAP006745	nan	4198.803551	2.338674916	0.15043346	15.54624159	1.68721E-54	4.54148E-53	Megacytes
AGAP009098	AGAP009098	Protein-glutamine gamma-glutamyltransferase E	6078.06949	2.330846338	0.139367798	16.72442542	8.70113E-63	2.8662E-61	Megacytes
AGAP011064	AGAP011064	nan	326.4754085	2.30196808	0.148222163	15.5305255	2.15606E-54	5.72175E-53	
AGAP011530	AGAP011530	nan	28.33839906	2.296811726	0.326839474	7.027338835	2.1051E-12	9.7264E-12	
AGAP010160	AGAP010160	myosin I	7761.456702	2.295088071	0.087350529	26.27446115	3.7563E-152	6.4343E-150	
AGAP010260	AGAP010260	nan	14.24210831	2.294109402	0.39661208	5.784265079	7.283E-09	2.50687E-08	
AGAP005520	AGAP005520	cytochrome b-561	172.0419043	2.281209432	0.203018804	11.23644404	2.70042E-29	3.0541E-28	
AGAP010774	AGAP010774	nan	101.6516555	2.276634432	0.294695567	7.725377251	1.11523E-14	6.03824E-14	
AGAP007651	AGAP007651	growth arrest and DNA-damage-inducible protein	473.1325499	2.264883499	0.227178005	9.969642523	2.06972E-23	1.76941E-22	
AGAP002811	CLIPD4	CLIP-domain serine protease [Source:UniProtKB/TrEMBL;Acc:A0A1S4	16.51541341	2.263256704	0.377785221	5.990855598	2.0874E-09	7.61634E-09	
AGAP001761	AGAP001761	ceramide synthetase	1899.92071	2.259442539	0.172869761	13.07020107	4.87365E-39	7.87559E-38	
AGAP012802	AGAP012802	nan	117.2076668	2.250775294	0.312326253	7.206487686	5.74135E-13	2.75544E-12	
AGAP000812	AGAP000812	calcium binding protein	885.5706431	2.24680094	0.098873996	22.72388125	2.6017E-114	2.88366E-112	
AGAP010056	AGAP010056	hexosaminidase	1842.521798	2.246490786	0.236944089	9.481100788	2.51615E-21	1.98033E-20	
AGAP009154	ARC-P34	actin-related protein 2/3 complex subunit 2	7240.757708	2.243759331	0.116223402	19.30557272	4.82178E-83	2.87506E-81	
AGAP028157	AGAP028157	nan	4114.355096	2.241755919	0.143207911	15.65385536	3.12689E-55	8.56349E-54	Granulocytes, Dividing granulocytes and Megacytes
AGAP006270	AGAP006270	fyn-related kinase	1025.707773	2.234811234	0.154332825	14.48046604	1.61002E-47	3.48689E-46	
AGAP007887	AGAP007887	nan	42.77086196	2.231869475	0.254236509	8.778713509	1.65355E-18	1.11431E-17	
AGAP000204	AGAP000204	nan	23.88038773	2.230134227	0.459672195	4.851575216	1.22485E-06	3.38197E-06	
AGAP004372	AGAP004372	elongation of very long chain fatty acids protein 1	1966.839537	2.227772939	0.125738478	17.71751155	3.07204E-70	1.26937E-68	
AGAP004737	AGAP004737	Rhomboid-4, isoform B	1049.272881	2.221631193	0.120849602	18.38343815	1.78301E-75	8.39888E-74	
AGAP003716	twf	Twinfilin [Source:UniProtKB/Swiss-Prot;Acc:Q7QG28]	167.7877541	2.21446621	0.154420246	14.34051731	1.22142E-46	2.54579E-45	
AGAP011790	CLIPA2	CLIP-domain serine protease	3495.717731	2.214259384	0.266506231	8.308471353	9.69428E-17	5.90749E-16	
AGAP001424	AGAP001424	heat shock protein 90kDa beta	12691.79985	2.210098739	0.133106634	16.60397142	6.52287E-62	2.09734E-60	
AGAP008052	SAP2	sensory appendage protein 2	73.9829377	2.205111504	0.504938289	4.367091094	1.25912E-05	3.09475E-05	
AGAP004853	AGAP004853	Ral GEF with PH domain and SH3-binding motif 1	3043.468304	2.202453717	0.078606414	28.01875307	9.6025E-173	2.3807E-170	
AGAP010862	nan	nan	1779.552611	2.200882081	0.25857126	8.511704201	1.71395E-17	1.09695E-16	
AGAP028566	AGAP028566	nan	59.29647005	2.197113336	0.376133612	5.841310824	5.17917E-09	1.81184E-08	
AGAP004163	GSTD7	glutathione S-transferase delta class 7	1846.751146	2.193339829	0.104345344	21.02000675	4.30372E-98	3.35086E-96	
AGAP008176	AGAP008176	dipeptidyl-peptidase 4	7.106160326	2.19163709	0.577323251	3.79620444	0.000146928	0.000317553	
AGAP008016	AGAP008016	acyl-CoA oxidase	578.9547419	2.18355879	0.163172805	13.38187932	7.71711E-41	1.33156E-39	
AGAP007347	LYSC1	C-type lysozyme	5361.98254	2.181613896	0.242153177	9.009230936	2.07507E-19	1.46986E-18	AM granulocytes
AGAP011282	AGAP011282	Fatty acid 2-hydroxylase [Source:UniProtKB/TrEMBL;Acc:A0A1S4H68	106.8653016	2.176193005	0.22757132	9.562685688	1.1474E-21	9.16848E-21	
AGAP001022	AGAP001022	nan	17.66041077	2.169505972	0.355300312	6.106118967	1.02083E-09	3.83462E-09	
AGAP004717	AGAP004717	nan	13.75067012	2.16622655	0.481022941	4.50337471	6.68828E-06	1.70436E-05	
AGAP010530	CLIPE4	CLIP-domain serine protease [Source:UniProtKB/TrEMBL;Acc:A0A1S	5775.541263	2.162472443	0.182785362	11.83066532	2.70985E-32	3.4734E-31	
AGAP005749	GSTO1	glutathione S-transferase omega class 1	4862.243234	2.161826025	0.063184882	34.21429221	1.4823E-256	1.1637E-253	Dividing granulocytes
AGAP028448	AGAP028448	nan	16.04905571	2.160657777	0.370407885	5.833185157	5.43792E-09	1.89954E-08	
AGAP013358	AGAP013358	nan	7.400413525	2.157689653	0.540810451	3.989733644	6.61475E-05	0.000149946	
AGAP008407	TEP13	thioester-containing protein 13	83.36535265	2.151160929	0.20890573	10.29728065	7.24813E-25	6.63602E-24	
AGAP010057	AGAP010057	nicotinic acetylcholine receptor, beta-2 subunit	8.909378628	2.148743804	0.533606387	4.026832989	5.65332E-05	0.000128932	
AGAP007876	AGAP007876	nan	35.40621495	2.142008732	0.269750402	7.940706365	2.01033E-15	1.13818E-14	
AGAP013732	AGAP013732	nan	114.3835523	2.14196842	0.248318866	8.625878716	6.36024E-18	4.15821E-17	
AGAP010772	AGAP010772	nan	74.42844502	2.131014491	0.251900239	8.459755717	2.67938E-17	1.69185E-16	
AGAP001175	GPRCAL2	putative calcitonin receptor 2	44.37738034	2.130429032	0.275808013	7.724318851	1.12453E-14	6.07814E-14	
AGAP008599	AGAP008599	nan	22.04010987	2.129767992	0.346934853	6.13881244	8.31407E-10	3.15325E-09	
AGAP009091	AGAP009091	aromatic-L-amino-acid decarboxylase	617.4251181	2.124272653	0.355365929	5.977704888	2.26303E-09	8.21581E-09	
AGAP010281	GPRGBB1	Putative GABA-B receptor 1 [Source:UniProtKB/TrEMBL;Acc:A0A1S4	36.83674083	2.121555947	0.258337054	8.212356367	2.16889E-16	1.29734E-15	
AGAP010457	AGAP010457	thymidylate synthase	944.988603	2.121360635	0.159232595	13.32240195	1.715E-40	2.9217E-39	
AGAP009595	AGAP009595	sodium/potassium-transporting ATPase subunit beta	3805.376478	2.117317925	0.104448969	20.27131467	2.30419E-91	1.50748E-89	
AGAP000562	AGAP000562	nan	9218.890892	2.116685642	0.162448238	13.02990829	8.2707E-39	1.3274E-37	
AGAP008149	AGAP008149	Protein phosphatase 1B (formerly 2C) [Source:UniProtKB/TrEMBL;Ac	801.9505509	2.115960491	0.160443742	13.18817718	1.02637E-39	1.69639E-38	
AGAP028513	AGAP028513	nan	59.0244424	2.114564177	0.407679322	5.186832056	2.13901E-07	6.40549E-07	
AGAP004164	GSTD1-4	glutathione S-transferase delta class 1	9459.91605	2.110874418	0.146147076	14.44349405	2.75513E-47	5.88574E-46	Granulocytes
AGAP001534	AGAP001534	nan	11.40408659	2.110162853	0.508809793	4.147252827	3.36488E-05	7.87201E-05	
AGAP005814	AGAP005814	ecdysoneless homolog	734.854626	2.099993164	0.080076655	26.22478643	1.3864E-151	2.3323E-149	
AGAP004836	nan	nan	650.0710152	2.098146961	0.175847135	11.93165279	8.09501E-33	1.05481E-31	
AGAP005448	AGAP005448	B9 domain-containing protein 2	99.60549667	2.095463832	0.290572621	7.211497852	5.53397E-13	2.66405E-12	
AGAP012056	AGAP012056	cofilin	21864.66673	2.09271144	0.074059359	28.25721795	1.1605E-175	3.0369E-173	Granulocytes and Megacytes
AGAP012317	AGAP012317	nan	27.02636328	2.090756579	0.294743093	7.093487945	1.30773E-12	6.10513E-12	
AGAP009528	AGAP009528	nan	517.7739376	2.08733478	0.118753804	17.57699296	3.69669E-69	1.44508E-67	
AGAP009211	AGAP009211	nan	10.53782511	2.086759309	0.487911215	4.276924252	1.89493E-05	4.56554E-05	
AGAP008245	AGAP008245	nan	44.13685542	2.084210574	0.251736754	8.279325676	1.23875E-16	7.49053E-16	
AGAP002461	AGAP002461	nan	707.2169162	2.083713242	0.147056478	14.16947606	1.41553E-45	2.8495E-44	
AGAP013079	AGAP013079	nan	1464.396434	2.081746303	0.133219553	15.62643213	4.80992E-55	1.30589E-53	
AGAP003838	AGAP003838	nan	8.749472898	2.080685019	0.533941455	3.896841125	9.74555E-05	0.000216132	
AGAP003248	AGAP003248	nan	1059.751232	2.079895508	0.269283056	7.723826152	1.12889E-14	6.0982E-14	
AGAP008551	AGAP008551	mothers against decapentaplegic homolog 1	487.1543997	2.066465676	0.121255416	17.04225469	3.99046E-65	1.38724E-63	
AGAP004397	AGAP004397	alpha-1,6-mannosyl-glycoprotein beta-1,2-N-acetylglucosaminyltran	573.8103307	2.064323208	0.10145681	20.34681765	4.95411E-92	3.35775E-90	
AGAP028537	AGAP028537	nan	11.17762809	2.054944515	0.454772595	4.51861994	6.2244E-06	1.59089E-05	
AGAP010026	AGAP010026	phospholipid-translocating ATPase	1565.02341	2.0488596	0.194429848	10.53778326	5.78463E-26	5.58944E-25	
AGAP009221	SRPN5	serine protease inhibitor (serpin) 5	2214.441769	2.047353148	0.174240138	11.75018094	7.04678E-32	8.83991E-31	
AGAP003758	AGAP003758	nan	270.257497	2.041893372	0.194482168	10.49912898	8.71808E-26	8.34686E-25	
AGAP003689	CLIPC7	CLIP-domain serine protease [Source:UniProtKB/TrEMBL;Acc:A0A1S4	1211.441982	2.04098826	0.356864366	5.719226844	1.0701E-08	3.62771E-08	
AGAP011938	AGAP011938	lamin	3921.036628	2.033845313	0.120428121	16.88845846	5.4714E-64	1.85417E-62	
AGAP000748	AGAP000748	Muscular protein 20	9.564759859	2.033725044	0.465122407	4.372451238	1.22859E-05	3.02208E-05	
AGAP004958	AGAP004958	ethanolaminephosphotransferase	294.4964352	2.033487138	0.13376219	15.20225657	3.41646E-52	8.47013E-51	
AGAP008670	AGAP008670	nan	1126.615038	2.031506182	0.150608881	13.48862147	1.82481E-41	3.19545E-40	
AGAP011562	Oseg4	outer segment 4	87.84653089	2.016660354	0.214531796	9.40028654	5.44147E-21	4.18482E-20	
AGAP012386	AGAP012386	nan	68937.7028	2.006246014	0.190819364	10.51384918	7.45858E-26	7.15553E-25	
AGAP009828	AGAP009828	nan	15.00615373	2.004345543	0.575368838	3.483583768	0.000494748	0.000992552	
AGAP001886	AGAP001886	nan	2720.981628	2.004081796	0.117050849	17.12146308	1.02662E-65	3.67025E-64	

Table S2.

Downregulated genes by Cactus Knockdown

Accesion Number	Name	Description	baseMean	log2FoldChange	lfcSE	stat	pvalue	padj	Hemocyte type
AGAP004978	PPO9	prophenoloxidase 9	23777.8002	-7.931905616	0.1685	-47.063	0	0	Oenocytoids
AGAP028406	AGAP028406	nan	7750.25117	-7.799283944	0.225	-34.657	3.5436E-263	4.173E-260	Oenocytoids
AGAP002867	CYP6P4	cytochrome P450	25.5488877	-7.715952754	0.9071	-8.5057	1.80456E-17	1.15182E-16	
AGAP000144	AGAP000144	progestin and adipoQ receptor family member 3	499.855567	-7.69138119	0.3774	-20.382	2.43118E-92	1.68413E-90	
AGAP006000	CPR25	cuticular protein RR-1 family 25	15.7863562	-7.610463392	0.9184	-8.2864	1.16761E-16	7.07401E-16	
AGAP003581	AGAP003581	D-xylulose reductase A	1106.31964	-7.122975868	0.2636	-27.026	7.223E-161	1.4793E-158	
AGAP007990	AGAP007990	glucosyl/glucuronosyl transferases	52.8642935	-6.975944305	1.2596	-5.5381	3.05766E-08	9.89565E-08	
AGAP008880	AGAP008880	nan	35.973525	-6.738191478	0.7037	-9.5758	1.01035E-21	8.08712E-21	
AGAP006136	AGAP006136	monocyte to macrophage differentiation factor 2	330.163699	-6.442614237	0.3604	-17.877	1.76868E-71	7.4387E-70	
AGAP003571	AGAP003571	threonine dehydratase	1317.19158	-6.372713602	0.1958	-32.555	1.8004E-232	9.9772E-230	
AGAP000210	AGAP000210	triacylglycerol lipase	1077.16794	-6.324830509	0.2276	-27.788	6.0342E-170	1.4212E-167	
AGAP005752	AGAP005752	glucosyl/glucuronosyl transferases	2189.21022	-6.213122667	0.2718	-22.859	1.1956E-115	1.408E-113	
AGAP006327	LRIM6	leucine-rich immune protein (Short)	682.280858	-6.197194105	0.3656	-16.952	1.87318E-64	6.39394E-63	
AGAP005751	AGAP005751	glucosyl/glucuronosyl transferases	42.4611745	-6.194983424	0.5971	-10.375	3.21893E-25	3.01746E-24	
AGAP006571	AGAP006571	nuclear receptor subfamily 1 group D member 3	9.68565768	-6.143983933	0.9094	-6.7559	1.41917E-11	6.16696E-11	
AGAP002588	AGAP002588	nan	8419.60502	-6.108430513	0.182	-33.563	5.9001E-247	3.7056E-244	
AGAP008387	AGAP008387	nan	150.384514	-6.072258913	0.6293	-9.6498	4.92527E-22	3.9932E-21	
AGAP012251	AGAP012251	inorganic phosphate cotransporter	4805.26247	-6.026570224	0.2373	-25.397	2.7104E-142	4.3279E-140	
AGAP006137	nan	nan	22.8320718	-5.976841918	0.697	-8.575	9.90601E-18	6.40965E-17	
AGAP009382	AGAP009382	nan	4.77124769	-5.785400182	1.0578	-5.4691	4.52336E-08	1.44456E-07	
AGAP004449	AGAP004449	pancreatic triacylglycerol lipase	83.1501711	-5.775735305	0.5781	-9.9902	1.68237E-23	1.4435E-22	
AGAP028980	SSU_rRNA_eukary	Eukaryotic small subunit ribosomal RNA [Source:RFAM;Acc:RF01960	655.932095	-5.712182634	0.9746	-5.8608	4.60615E-09	1.62041E-08	
AGAP028554	AGAP028554	nan	1196.48986	-5.646977962	0.2079	-27.167	1.5969E-162	3.3433E-160	
AGAP002830	AGAP002830	C-1-tetrahydrofolate synthase, mitochondrial precursor	8450.48974	-5.597586948	0.2356	-23.76	8.5705E-125	1.0911E-122	
AGAP003636	AGAP003636	inositol oxygenase	2734.91946	-5.581700591	0.2222	-25.118	3.1793E-139	4.9102E-137	
AGAP008713	AGAP008713	nan	38.4404323	-5.575036836	0.5162	-10.799	3.46939E-27	3.56435E-26	
AGAP010363	AGAP010363	nan	14.7019961	-5.566885964	0.8219	-6.7732	1.25987E-11	5.49756E-11	
AGAP009385	AGAP009385	cellular retinaldehyde-binding protein	18.0446469	-5.565601097	0.6956	-8.0008	1.23646E-15	7.09424E-15	
AGAP004572	AGAP004572	nan	26.4052676	-5.542488691	0.6784	-8.1703	3.0753E-16	1.82906E-15	
AGAP003714	HPX3	heme peroxidase 3	3408.31985	-5.478975624	0.2971	-18.44	6.24116E-76	2.9999E-74	
AGAP012635	AGAP012635	nan	12.9650626	-5.472974589	0.7687	-7.1197	1.08199E-12	5.08909E-12	
AGAP000352	TWDL1	cuticular protein TWDL family (TWDL1)	16.2536187	-5.466467959	0.7143	-7.6528	1.96607E-14	1.04175E-13	
AGAP003999	AGAP003999	nan	163.64635	-5.439859124	0.3155	-17.239	1.34382E-66	4.8693E-65	
AGAP003066	CYP304B1	cytochrome P450	116.636168	-5.438909643	0.3502	-15.529	2.208E-54	5.84314E-53	
AGAP012354	AGAP012354	Syntrophin, alpha 1	60.4766239	-5.431457844	0.5406	-10.047	9.49269E-24	8.25767E-23	
AGAP011098	AGAP011098	nan	137.616454	-5.404158307	0.3614	-14.954	1.47261E-50	3.46837E-49	Oenocytoids
AGAP008714	AGAP008714	nan	60.861685	-5.374765101	0.4547	-11.82	3.07677E-32	3.92767E-31	
AGAP003582	AGAP003582	D-xylulose reductase A	17.4712129	-5.29214823	0.7554	-7.0056	2.45926E-12	1.13128E-11	
AGAP010596	AGAP010596	Alkaline phosphatase [Source:UniProtKB/TrEMBL;Acc:Q7Q8R8]	4.84641083	-5.291703832	1.0968	-4.8245	1.40358E-06	3.84842E-06	
AGAP000218	AGAP000218	nan	102.125953	-5.289965987	0.4205	-12.581	2.69796E-36	3.95911E-35	
AGAP003545	Osk	protein oskar	27.043257	-5.253269891	0.7628	-6.887	5.69752E-12	2.55358E-11	
AGAP009219	AGAP009219	nan	23.1633731	-5.226698387	0.6939	-7.5324	4.97972E-14	2.55801E-13	
AGAP006135	AGAP006135	nan	3.35151891	-5.203138233	1.0572	-4.9216	8.58324E-07	2.40878E-06	
AGAP002317	Alpha_amylase	amylase	7282.67516	-5.083876823	0.2684	-18.941	5.22851E-80	2.91466E-78	Oenocytoids
AGAP004563	ANCE9	angiotensin-converting enzyme 9	148.969171	-5.063188132	0.3802	-13.319	1.8048E-40	3.06913E-39	
AGAP012617	AGAP012617	nan	179.468881	-5.043696632	0.3593	-14.039	8.96638E-45	1.75984E-43	
AGAP005753	AGAP005753	glucosyl/glucuronosyl transferases	141.092797	-5.024762823	0.3538	-14.203	8.76391E-46	1.77941E-44	
AGAP007252	AGAP007252	Peptidase S1 domain-containing protein [Source:UniProtKB/TrEMBL;	46.288377	-5.020262381	0.4157	-12.077	1.3917E-33	1.87572E-32	
AGAP028560	AGAP028560	nan	474.462774	-5.002460802	0.2269	-22.049	9.7677E-108	1.0002E-105	
AGAP005585	AGAP005585	nan	301.522027	-4.979277064	0.2091	-23.814	2.3956E-125	3.0917E-123	
AGAP000844	AGAP000844	Progestin and adipoQ receptor family member 4	788.790571	-4.907435023	0.2318	-21.17	1.8188E-99	1.43987E-97	
AGAP011253	AGAP011253	nan	9.54328575	-4.893404448	0.8168	-5.9911	2.08486E-09	7.61001E-09	
AGAP005497	AGAP005497	SCP domain-containing protein [Source:UniProtKB/TrEMBL;Acc:A0A1	3.608338	-4.856641566	1.1163	-4.3507	1.35698E-05	3.31968E-05	
AGAP001477	AGAP001477	Innexin inx2	70.8757624	-4.795367874	0.344	-13.938	3.70678E-44	7.17075E-43	
AGAP006609	AGAP006609	nan	21.0348322	-4.786633919	0.6277	-7.6257	2.4273E-14	1.27681E-13	
AGAP002506	AGAP002506	runt-related transcription factor	324.201393	-4.758197781	0.1993	-23.879	5.1199E-126	6.7936E-124	
AGAP011230	AGAP011230	nan	543.436757	-4.734809459	0.2599	-18.219	3.6357E-74	1.64673E-72	
AGAP004450	AGAP004450	nan	134.456281	-4.713058251	0.3123	-15.091	1.85261E-51	4.48673E-50	
AGAP006001	CPR26	cuticular protein RR-1 family 26	127.926692	-4.681609602	0.3444	-13.593	4.39401E-42	7.88495E-41	
AGAP004980	PPO7	prophenoloxidase 7	13.6523774	-4.67237043	0.7342	-6.364	1.96542E-10	7.86918E-10	
AGAP003712	Ast1	allatostatin 1	7.08833786	-4.665661923	0.8559	-5.4514	4.99774E-08	1.58852E-07	
AGAP012616	PPO5	prophenoloxidase 5	21687.4741	-4.651552574	0.2342	-19.863	8.48134E-88	5.39883E-86	Oenocytoids
AGAP028480	AGAP028480	nan	3.47488169	-4.641297013	1.0865	-4.272	1.93769E-05	4.66165E-05	
AGAP007285	AGAP007285	alpha-L-fucosidase	311.378893	-4.615829479	0.2811	-16.42	1.38179E-60	4.33928E-59	
AGAP009924	AGAP009924	nan	9.66472208	-4.603626508	0.7476	-6.1582	7.35802E-10	2.80534E-09	
AGAP004981	PPO4	prophenoloxidase 4	7206.30439	-4.599210999	0.149	-30.876	2.5449E-209	9.5902E-207	Oenocytoids
AGAP010975	AGAP010975	nan	26.7616799	-4.588901081	0.7916	-5.7969	6.75457E-09	2.33436E-08	
AGAP010657	AGAP010657	nan	41.8936143	-4.566657813	0.4559	-10.016	1.29679E-23	1.1198E-22	
AGAP007075	AGAP007075	nan	19.3364744	-4.564451244	0.6107	-7.4736	7.8054E-14	3.94077E-13	
AGAP001112	AGAP001112	nan	3.13585904	-4.540052611	1.1756	-3.862	0.000112478	0.000247006	
AGAP028398	AGAP028398	nan	8.05143187	-4.528075965	0.8467	-5.3478	8.90251E-08	2.75618E-07	
AGAP012644	AGAP012644	nan	5.27808429	-4.507236925	1.0576	-4.2616	2.03004E-05	4.86394E-05	
AGAP004154	AGAP004154	jagged	857.959562	-4.503198656	0.2068	-21.78	3.6169E-105	3.5129E-103	
AGAP003767	AGAP003767	nan	5196.80068	-4.496935919	0.2348	-19.151	9.52588E-82	5.53971E-80	Oenocytoids
AGAP029126	AGAP029126	nan	18.411012	-4.443084044	0.647	-6.8671	6.55376E-12	2.92621E-11	
AGAP004249	AGAP004249	nan	51.395445	-4.437586128	0.3893	-11.399	4.20638E-30	4.95974E-29	
AGAP006385	AGAP006385	nan	283.540464	-4.43075434	0.7771	-5.7014	1.18834E-08	4.00549E-08	
AGAP000605	AGAP000605	nan	261.956624	-4.424556557	0.8846	-5.0018	5.67923E-07	1.62577E-06	
AGAP007918	AGAP007918	xanthine dehydrogenase/oxidase	4030.929	-4.421348327	0.1688	-26.191	3.3598E-151	5.5532E-149	
AGAP011603	AGAP011603	Long-chain acyl-CoA synthetase [Source:UniProtKB/TrEMBL;Acc:A0A	8573.55885	-4.420170699	0.2497	-17.703	4.00532E-70	1.64778E-68	
AGAP004510	AGAP004510	Innexin inx2	459.008065	-4.418131468	0.2672	-16.537	1.97167E-61	6.29665E-60	
AGAP028913	LSU_rRNA_eukary	Eukaryotic large subunit ribosomal RNA [Source:RFAM;Acc:RF02543]	99.0881335	-4.408960933	0.9931	-4.4394	9.02088E-06	2.26327E-05	
AGAP008141	AGAP008141	argininosuccinate lyase	6002.19367	-4.39651821	0.1751	-25.108	4.0318E-139	6.1264E-137	
AGAP007588	AGAP007588	glucosyl/glucuronosyl transferases	394.075897	-4.386813885	0.1809	-24.256	5.7273E-130	8.0533E-128	
AGAP000211	AGAP000211	triacylglycerol lipase	5103.25989	-4.384911177	0.1581	-27.739	2.34E-169	5.3769E-167	
AGAP028555	AGAP028555	nan	498.282233	-4.359203037	0.2572	-16.952	1.86432E-64	6.38683E-63	
AGAP003176	AGAP003176	solute carrier family 23 (nucleobase transporter)	76.3543813	-4.350232637	0.3338	-13.033	7.92785E-39	1.27454E-37	
AGAP013159	nan	nan	19.4741764	-4.327824047	0.5111	-8.4678	2.49991E-17	1.58065E-16	
AGAP007455	LRIM10	leucine-rich immune protein (Short)	3911.49684	-4.327593865	0.2484	-17.421	5.72668E-68	2.16671E-66	
AGAP000153	AGAP000153	nan	40.8878693	-4.315642723	0.4851	-8.8971	5.73422E-19	3.95766E-18	
AGAP004977	PPO6	prophenoloxidase 6	79083.991	-4.312821861	0.1806	-23.881	4.8665E-126	6.5496E-124	Oenocytoids
AGAP009198	AGAP009198	nan	128.734058	-4.289383195	0.3046	-14.08	5.04817E-45	9.99135E-44	

AGAP013267	AGAP013267	nan	170.044983	-4.287799532	0.3139	-13.662	1.7167E-42	3.12824E-41	
AGAP000356	AGAP000356	nan	8.52122871	-4.252587471	0.7446	-5.7116	1.11932E-08	3.78095E-08	
AGAP002518	AGAP002518	delta-1-pyrroline-5-carboxylate synthetase	37793.214	-4.207224571	0.1507	-27.914	1.8217E-171	4.4007E-169	Granulocytes
AGAP012960	AGAP012960	nan	257.301812	-4.20622211	0.2151	-19.555	3.73425E-85	2.32983E-83	
AGAP009039	AGAP009039	glucose-6-phosphate 1-epimerase	151.953295	-4.20538689	0.3275	-12.84	9.8257E-38	1.52752E-36	
AGAP009516	nan	nan	8.12600818	-4.204435416	0.8637	-4.8679	1.12799E-06	3.1246E-06	
AGAP003087	AGAP003087	nan	5.12561631	-4.202534821	0.9682	-4.3406	1.42077E-05	3.47212E-05	
AGAP001251	AGAP001251	eupolytin	11.7228522	-4.184904405	0.6219	-6.7295	1.70238E-11	7.34345E-11	
AGAP010004	AGAP010004	nan	5.07615339	-4.182754498	0.9041	-4.6262	3.72375E-06	9.78562E-06	
AGAP010725	nan	nan	174.004261	-4.178778315	0.2638	-15.838	1.70021E-56	4.88343E-55	
AGAP003086	AGAP003086	nan	7.02442114	-4.160037236	0.8685	-4.7898	1.6693E-06	4.54259E-06	
AGAP006570	AGAP006570	myo-inositol-1(or 4)-monophosphatase	8859.50488	-4.157395297	0.1789	-23.241	1.7485E-119	2.1393E-117	Oenocytoids
AGAP006134	AGAP006134	nan	6.65423033	-4.146921508	0.9373	-4.4243	9.6739E-06	2.41499E-05	
AGAP002587	AGAP002587	nan	19.6541663	-4.144652571	0.6407	-6.4688	9.87523E-11	4.04147E-10	
AGAP005972	AGAP005972	4-nitrophenylphosphatase	318.701758	-4.139715515	0.2871	-14.421	3.7963E-47	8.01904E-46	
AGAP001880	AGAP001880	bZIP factor, other	16.0847949	-4.130949948	0.7097	-5.8211	5.84686E-09	2.03409E-08	
AGAP000679	AGAP000679	Aminoacylase [Source:UniProtKB/TrEMBL;Acc:Q7QEF5]	31526.131	-4.104723825	0.1533	-26.784	4.9967E-158	9.4147E-156	Oenocytoids
AGAP001010	AGAP001010	chondroitin sulfate synthase	170.09409	-4.103161998	0.2402	-17.079	2.11983E-65	7.50785E-64	
AGAP013241	CYP4D16	cytochrome P450	5.30215358	-4.090586709	0.8342	-4.9034	9.42055E-07	2.63122E-06	
AGAP003321	AGAP003321	glycine dehydrogenase	1498.67239	-4.087626651	0.1948	-20.986	8.7899E-98	6.78768E-96	
AGAP006258	PPO2	prophenoloxidase 2	28442.0768	-4.051077734	0.2318	-17.475	2.23633E-68	8.5644E-67	Oenocytoids
AGAP009899	AGAP009899	nan	8.83590922	-4.038931909	0.7201	-5.6089	2.03628E-08	6.72407E-08	
AGAP002721	AGAP002721	Tryptophan 2,3-dioxygenase [Source:UniProtKB/Swiss-Prot;Acc:O774	2065.79253	-4.024997514	0.2225	-18.089	3.87998E-73	1.73238E-71	
AGAP010799	AGAP010799	nan	5.39154222	-4.010443217	0.988	-4.0593	4.92201E-05	0.000113098	
AGAP008359	AGAP008359	sodium-coupled monocarboxylate transporter 1	3.85256215	-4.010249167	1.0686	-3.7527	0.000174967	0.000374628	
AGAP011228	AGAP011228	nan	8413.98229	-4.009800464	0.4668	-8.5898	8.71082E-18	5.66745E-17	Granulocytes
AGAP006906	AGAP006906	Cat eye syndrome critical region protein 1	1347.74014	-4.000927267	0.1127	-35.501	4.6726E-276	6.2886E-273	
AGAP006726	COEAE5G	carboxylesterase	2201.17039	-3.997497366	0.1943	-20.57	5.05574E-94	3.63588E-92	Oenocytoids
AGAP007076	AGAP007076	nan	67.4688145	-3.987537468	0.2863	-13.93	4.15336E-44	8.01819E-43	
AGAP009874	CPR76	cuticular protein RR-1 family 76	5.80861262	-3.970946909	0.9897	-4.0121	6.01712E-05	0.000136926	
AGAP005750	AGAP005750	glucosyl/glucuronosyl transferases	1511.87594	-3.963930585	0.1739	-22.792	5.5602E-115	6.3882E-113	
AGAP009940	AGAP009940	nan	284.247524	-3.961724089	0.2689	-14.734	3.8722E-49	8.68572E-48	
AGAP006206	nan	nan	190.510737	-3.940862111	0.2233	-17.651	1.00808E-69	4.04134E-68	
AGAP007456	LRIM8B	leucine-rich immune protein (Short)	6118.40636	-3.9304415	0.2273	-17.294	5.19666E-67	1.89026E-65	Granulocytes
AGAP013029	AGAP013029	nan	140.185467	-3.929349144	0.3094	-12.698	6.04565E-37	9.11298E-36	
AGAP001252	AGAP001252	eupolytin	11.917833	-3.928480813	0.5576	-7.0447	1.85817E-12	8.61505E-12	
AGAP001962	GPRVPR1	GPCR vasopressin family receptor 1	171.2186	-3.907937459	0.1723	-22.679	7.2564E-114	7.9491E-112	
AGAP006549	AGAP006549	nan	19.9821355	-3.891416706	0.5028	-7.7395	9.98344E-15	5.44294E-14	
AGAP011617	AGAP011617	nan	4.90321474	-3.886640253	0.9136	-4.2541	2.09856E-05	5.01791E-05	
AGAP006168	AGAP006168	BMP binding endothelial regulator	694.700242	-3.877349092	0.2095	-18.511	1.69422E-76	8.40065E-75	
AGAP003067	CYP304C1	cytochrome P450	233.071707	-3.875724352	0.2526	-15.343	3.92708E-53	1.00535E-51	
AGAP009283	AGAP009283	nan	6.56033597	-3.818322579	0.9537	-4.0035	6.24064E-05	0.00014167	
AGAP028468	AGAP028468	nan	707.936092	-3.817097591	0.2165	-17.634	1.35679E-69	5.37072E-68	
AGAP003289	AGAP003289	carbonic anhydrase	6.26895793	-3.813869106	0.9956	-3.8308	0.000127742	0.000278191	
AGAP013755	AGAP013755	nan	7789.42614	-3.804581874	0.246	-15.468	5.74805E-54	1.51264E-52	
AGAP000466	ACE2	acetylcholinesterase	130.014914	-3.801941195	0.2838	-13.395	6.48728E-41	1.12554E-39	
AGAP007674	AGAP007674	GIPC PDZ domain containing family, member 2	411.415616	-3.799060491	0.2166	-17.543	6.74851E-69	2.60564E-67	
AGAP007454	LRIM8A	leucine-rich immune protein (Short)	9438.76355	-3.794200054	0.2357	-16.095	2.75087E-58	8.33309E-57	
AGAP010604	ILP6	Insulin-like peptide 6	8.52382176	-3.792948395	0.8673	-4.3732	1.22421E-05	3.01288E-05	
AGAP001415	AGAP001415	nan	3.27470474	-3.790409077	1.0779	-3.5166	0.000437106	0.000883306	
AGAP009521	AGAP009521	nan	97.5543461	-3.789954676	0.3334	-11.368	6.06949E-30	7.08559E-29	
AGAP011972	AGAP011972	Epoxide hydrolase	198.134239	-3.788799702	0.1764	-21.48	2.3734E-102	2.0897E-100	
AGAP000275	AGAP000275	epidermal retinal dehydrogenase	612.865245	-3.774113828	0.1771	-21.313	8.688E-101	7.4409E-99	
AGAP001476	AGAP001476	Innexin inx2	1293.10692	-3.773854109	0.2375	-15.89	7.46388E-57	2.17029E-55	
AGAP001281	AGAP001281	potassium inwardly-rectifying channel subfamily J	3123.47654	-3.759899628	0.1662	-22.619	2.7942E-113	3.0257E-111	
AGAP000162	AGAP000162	Cystathionine beta-synthase [Source:UniProtKB/TrEMBL;Acc:Q7QEV	12899.2081	-3.755407958	0.2193	-17.121	1.0285E-65	3.67025E-64	Oenocytoids
AGAP013329	AGAP013329	nan	58.5082405	-3.749058651	0.3876	-9.6719	3.97079E-22	3.2249E-21	
AGAP013758	AGAP013758	xanthine dehydrogenase	292.99927	-3.747835889	0.2091	-17.922	7.94971E-72	3.40428E-70	
AGAP006226	Aldehyde_oxidase	nan	176.000978	-3.746539451	0.2621	-14.293	2.4176E-46	4.98384E-45	
AGAP002593	AGAP002593	outer membrane lipoprotein Blc	2444.71449	-3.732204929	0.2577	-14.483	1.55164E-47	3.3682E-46	
AGAP004367	AGAP004367	nan	6.27641776	-3.71151124	0.7131	-5.2048	1.94256E-07	5.8376E-07	
AGAP013028	AGAP013028	nan	1117.68323	-3.710018318	0.2477	-14.978	1.01911E-50	2.41232E-49	
AGAP028641	AGAP028641	nan	56.8742437	-3.703061814	0.2931	-12.633	1.38711E-36	2.05795E-35	
AGAP007453	LRIM9	leucine-rich immune protein (Short)	4537.20231	-3.693936772	0.2772	-13.326	1.64439E-40	2.80649E-39	Granulocytes
AGAP003205	AGAP003205	nan	376.618638	-3.68920624	0.2596	-14.213	7.60358E-46	1.55387E-44	
AGAP005717	LYSC6	C-type lysozyme (multi-lysozyme domain protein)	22.5284384	-3.686764021	0.4394	-8.3901	4.85853E-17	3.00935E-16	
AGAP003730	AGAP003730	neutral ceramidase	896.204879	-3.68553131	0.2252	-16.367	3.29211E-60	1.02023E-58	
AGAP007764	AGAP007764	nan	8.99746337	-3.67369365	0.65	-5.6516	1.58993E-08	5.29658E-08	
AGAP004940	AGAP004940	nan	382.503901	-3.672119957	0.2498	-14.698	6.62693E-49	1.47246E-47	
AGAP008193	AGAP008193	Nidogen (entactin) [Source:UniProtKB/TrEMBL;Acc:A0A1S4GXK2]	462.638259	-3.671374459	0.2146	-17.105	1.35951E-65	4.8332E-64	
AGAP013403	AGAP013403	sodium-coupled monocarboxylate transporter 2	17.912668	-3.667844459	0.5948	-6.1668	6.9691E-10	2.65921E-09	
AGAP006227	AGAP006227	alpha esterase	125.043869	-3.663923834	0.2663	-13.756	4.66562E-43	8.72119E-42	
AGAP011373	AGAP011373	nan	3.74438369	-3.659337389	0.9467	-3.8654	0.000110923	0.000243818	
AGAP005645	AGAP005645	dehydrogenase/reductase SDR family member 11 precursor	302.388965	-3.652840205	0.4207	-8.6835	3.83873E-18	2.54144E-17	
AGAP011507	AGAP011507	nan	904.647956	-3.646701855	0.2315	-15.755	6.31545E-56	1.77077E-54	
AGAP006376	PDP1	PAR-domain protein 1	433.909902	-3.645096136	0.3953	-9.2217	2.92424E-20	2.17266E-19	
AGAP011349	AGAP011349	GABA-gated chloride channel	4.25918733	-3.634551722	0.8909	-4.0795	4.51267E-05	0.000104098	
AGAP013039	AGAP013039	nan	14.0975022	-3.614229167	0.5779	-6.2542	3.9963E-10	1.56313E-09	
AGAP003000	AGAP003000	MFS transporter, PCFT/HCP family, solute carrier family 46 (folate tra	2287.37878	-3.613250741	0.1782	-20.277	2.04251E-91	1.35511E-89	
AGAP000351	GPRNPY1	neuropeptide Y receptor 1	643.541009	-3.602029942	0.1974	-18.245	2.254E-74	1.02584E-72	
AGAP006183	AGAP006183	slit protein	37.8090721	-3.590155032	0.4034	-8.9004	5.56703E-19	3.84791E-18	
AGAP000728	AGAP000728	wengen	326.556965	-3.581993277	0.2455	-14.588	3.33079E-48	7.36605E-47	
AGAP002890	AGAP002890	Lipid storage droplets surface-binding protein 1	5661.5455	-3.579754393	0.2174	-16.466	6.39551E-61	2.02188E-59	Granulocytes
AGAP012957	CYP4D17	cytochrome P450	153.399151	-3.57179938	0.2777	-12.86	7.5119E-38	1.17168E-36	
AGAP009498	AGAP009498	solute carrier family 17 (anion/sugar transporter), member 5	4273.27844	-3.570169735	0.1863	-19.159	8.07499E-82	4.72513E-80	
AGAP012761	AGAP012761	Synaptic vesicle protein	182.275027	-3.56445447	0.1931	-18.458	4.5353E-76	2.20243E-74	
AGAP007599	AGAP007599	monolysocardiolipin acyltransferase	3128.34491	-3.556441965	0.1645	-21.613	1.3503E-103	1.2472E-101	
AGAP010794	AGAP010794	nan	304.73046	-3.539026458	0.2496	-14.177	1.27206E-45	2.56619E-44	
AGAP010726	nan	nan	35.5277234	-3.532529829	0.3617	-9.7655	1.58251E-22	1.30436E-21	
AGAP005459	CPR16	cuticular protein RR-1 family 16	438.759887	-3.526620378	0.2208	-15.975	1.92174E-57	5.6933E-56	
AGAP003713	AGAP003713	nan	63.6270203	-3.525856486	0.3897	-9.0467	1.47364E-19	1.05255E-18	
AGAP012570	AGAP012570	nan	53.1128837	-3.502552663	0.412	-8.5009	1.88068E-17	1.19958E-16	
AGAP001791	AGAP001791	nan	331.958159	-3.502290928	0.3097	-11.308	1.20247E-29	1.37816E-28	
AGAP005866	AGAP005866	glutamate decarboxylase	15.1689666	-3.49578152	0.5082	-6.8789	6.03302E-12	2.69882E-11	

AGAP001601	AGAP001601	Ser/Thr protein phosphatase/nucleotidase	774.104306	-3.468240411	0.1658	-20.924	3.21599E-97	2.42382E-95	
AGAP013226	AGAP013226	nan	1644.12043	-3.457137788	0.1297	-26.656	1.527E-156	2.7664E-154	
AGAP012395	AGAP012395	peptide-methionine (S)-S-oxide reductase	3850.14615	-3.449976302	0.2614	-13.2	8.71672E-40	1.44578E-38	
AGAP002629	AGAP002629	nan	1275.01367	-3.44926394	0.8126	-4.2449	2.18681E-05	5.22096E-05	
AGAP005563	Tret1	facilitated trehalose transporter Tret1	40579.9769	-3.441113178	0.204	-16.867	7.90767E-64	2.66065E-62	Granulocytes
AGAP008558	AGAP008558	nan	4.4651699	-3.436978214	0.8318	-4.1321	3.59406E-05	8.37074E-05	
AGAP000604	AGAP000604	nan	4.84913532	-3.433371312	0.9045	-3.7957	0.000147222	0.000317969	
AGAP001015	AGAP001015	notch gene homolog 1	3328.58	-3.431146181	0.2258	-15.196	3.76173E-52	9.30165E-51	
AGAP007755	AGAP007755	nan	6.01877295	-3.428871874	0.8028	-4.2713	1.94304E-05	4.67331E-05	
AGAP006729	AGAP006729	Ester hydrolase C11orf54	5111.62935	-3.413082857	0.1268	-26.924	1.1576E-159	2.3204E-157	
AGAP002625	CTL9	C-type lectin (CTL)	53.999118	-3.410111836	0.2862	-11.915	9.87787E-33	1.28181E-31	
AGAP003501	AGAP003501	Lipase [Source:UniProtKB/TrEMBL;Acc:Q5TVS6]	3.37367287	-3.398272737	0.9266	-3.6674	0.000244995	0.000513823	
AGAP010162	AGAP010162	nan	4.9842719	-3.383001571	0.8178	-4.1369	3.52016E-05	8.21282E-05	
AGAP004156	AGAP004156	synaptic vesicle protein	160.254657	-3.380372078	0.1899	-17.797	7.42866E-71	3.11046E-69	
AGAP003209	AGAP003209	C-4 methylsterol oxidase	81.4206687	-3.376664049	0.2654	-12.724	4.33271E-37	6.57303E-36	
AGAP003106	Nep4	neprilysin, neutral endopeptidase 4	217.721818	-3.374218543	0.207	-16.304	9.2798E-60	2.85703E-58	
AGAP001106	AGAP001106	Disconnected protein	138.711785	-3.372689615	0.3356	-10.05	9.14746E-24	7.98686E-23	
AGAP006396	AGAP006396	phospholipase B, plb1	9.53579431	-3.368509407	0.7363	-4.575	4.76107E-06	1.23551E-05	
AGAP009751	ANCE2	angiotensin-converting enzyme 2	1390.42849	-3.364251639	0.1747	-19.261	1.14528E-82	6.74354E-81	
AGAP004203	Vg	vitellogenin	80.8811125	-3.3527186	0.2805	-11.954	6.1595E-33	8.04836E-32	
AGAP012851	AGAP012851	Aldo-keto reductase family 1, member C3	2689.50054	-3.350926014	0.1899	-17.65	1.02133E-69	4.0771E-68	Oenocytoids
AGAP002091	AGAP002091	phosphoribosylformylglycinamidine synthase	5133.69277	-3.339265688	0.2779	-12.015	2.95805E-33	3.91402E-32	
AGAP011460	AGAP011460	salivary cysteine-rich protein	213.407015	-3.339086963	0.2451	-13.625	2.84728E-42	5.17842E-41	
AGAP012351	nan	nan	408.858941	-3.338581709	0.2222	-15.026	4.99819E-51	1.18909E-49	
AGAP012341	AGAP012341	nan	12.32807	-3.337645667	0.5395	-6.1861	6.16677E-10	2.36263E-09	
AGAP009551	AGAP009551	sulfotransferase (Sult)	13.6902857	-3.332394949	0.5482	-6.079	1.20905E-09	4.51642E-09	
AGAP011223	AGAP011223	nan	5276.54106	-3.326940033	0.1604	-20.743	1.42583E-95	1.04943E-93	
AGAP002868	CYP6P1	cytochrome P450	143.40991	-3.323546926	0.2199	-15.112	1.34727E-51	3.28824E-50	
AGAP004936	AGAP004936	nan	58521.4869	-3.319925676	0.169	-19.649	5.84364E-86	3.69483E-84	Prohemocytes
AGAP007028	AGAP007028	glucosyl/glucuronosyl transferases	366.712893	-3.317281126	0.1607	-20.644	1.11306E-94	8.06629E-93	
AGAP011106	AGAP011106	nan	136.410365	-3.303921891	0.3272	-10.099	5.60304E-24	4.94717E-23	
AGAP002347	AGAP002347	N-acetylglucosamine-6-phosphate deacetylase [Source:UniProtKB/Tr	2255.65884	-3.301828055	0.2075	-15.909	5.44952E-57	1.59441E-55	
AGAP007598	AGAP007598	nan	25.3472269	-3.275270777	0.4455	-7.3524	1.94707E-13	9.61391E-13	
AGAP028204	AGAP028204	Alpha-mannosidase [Source:UniProtKB/TrEMBL;Acc:A0A1S4HD42]	17.4900863	-3.269261159	0.5608	-5.8298	5.54826E-09	1.93522E-08	
AGAP003580	AGAP003580	nan	14020.0337	-3.260376232	0.1855	-17.58	3.48911E-69	1.36962E-67	
AGAP001124	AGAP001124	Aminomethyltransferase [Source:UniProtKB/TrEMBL;Acc:Q7PWZ1]	357.536681	-3.244512534	0.2845	-11.404	3.99122E-30	4.71193E-29	
AGAP003542	AGAP003542	Epoxide hydrolase 2, cytoplasmic	310.598056	-3.234909749	0.2424	-13.347	1.22987E-40	2.10283E-39	
AGAP028901	SSU_rRNA_eukary	Eukaryotic small subunit ribosomal RNA [Source:RFAM;Acc:RF01960	15.2663413	-3.225831598	0.712	-4.5309	5.87297E-06	1.50843E-05	
AGAP005869	AGAP005869	nan	38.8862209	-3.221163782	0.4054	-7.9458	1.9295E-15	1.09439E-14	
AGAP004107	AGAP004107	nan	5.57585964	-3.218920578	0.7526	-4.2769	1.89541E-05	4.56554E-05	
AGAP006224	AGAP006224	aldehyde oxidase	290.449108	-3.21716727	0.2071	-15.537	1.94911E-54	5.21663E-53	
AGAP004731	AGAP004731	secretory phospholipase A2	1220.10474	-3.216543734	0.2474	-13.001	1.20116E-38	1.91799E-37	
AGAP028056	AGAP028056	nan	73.6524111	-3.200180676	0.2355	-13.588	4.69321E-42	8.3899E-41	
AGAP001856	PER	period circadian protein	1765.52282	-3.184496564	0.1698	-18.755	1.76032E-78	9.26479E-77	
AGAP028649	AGAP028649	nan	161.09642	-3.178349482	0.2017	-15.76	5.86927E-56	1.65058E-54	
AGAP012394	AGAP012394	peptide-methionine (S)-S-oxide reductase	4493.91225	-3.172243861	0.2496	-12.711	5.12128E-37	7.7444E-36	Granulocytes
AGAP004160	AGAP004160	nan	172.689128	-3.163101787	0.3344	-9.4595	3.09405E-21	2.417E-20	
AGAP004531	AGAP004531	cathepsin B precursor	6.10946575	-3.158939631	0.7386	-4.2768	1.8958E-05	4.56554E-05	
AGAP011051	AGAP011051	aldehyde reductase	295.973218	-3.158326014	0.2415	-13.078	4.37039E-39	7.08665E-38	
AGAP000033	AGAP000033	Protein retinal degeneration B	370.801971	-3.15519594	0.2017	-15.645	3.58205E-55	9.78158E-54	
AGAP008304	AGAP008304	3',5'-cyclic-nucleotide phosphodiesterase	1039.83173	-3.153481463	0.2119	-14.884	4.16668E-50	9.57421E-49	
AGAP007633	AGAP007633	solute carrier family 36 (proton-coupled amino acid transporter)	14609.7054	-3.145660971	0.1572	-20.017	3.92245E-89	2.54851E-87	
AGAP012280	AGAP012280	nan	266.11271	-3.145504714	0.192	-16.387	2.37033E-60	7.41891E-59	
AGAP001554	AGAP001554	nan	202.090158	-3.126662248	0.1992	-15.695	1.63043E-55	4.53105E-54	
AGAP028956	SSU_rRNA_eukary	Eukaryotic small subunit ribosomal RNA [Source:RFAM;Acc:RF01960	1718.10723	-3.125931303	0.7941	-3.9364	8.27201E-05	0.000185284	
AGAP005009	AGAP005009	Pyrroline-5-carboxylate reductase [Source:UniProtKB/TrEMBL;Acc:Q7	2617.04663	-3.123263198	0.2089	-14.953	1.49041E-50	3.50154E-49	
AGAP011476	AGAP011476	nan	20.2689356	-3.116272616	0.489	-6.3723	1.86267E-10	7.47049E-10	
AGAP002720	AGAP002720	cathepsin O	881.741456	-3.106508609	0.2002	-15.519	2.58646E-54	6.82551E-53	
AGAP010885	AGAP010885	nan	421.508745	-3.105294624	0.2845	-10.915	9.8121E-28	1.02825E-26	
AGAP003587	AGAP003587	sodium-independent sulfate anion transporter	1718.75882	-3.097151065	0.1639	-18.901	1.12606E-79	6.16781E-78	
AGAP011462	AGAP011462	nan	4.86235738	-3.096174854	0.7421	-4.1723	3.015E-05	7.09398E-05	
AGAP006725	COEAE3H	carboxylesterase alpha esterase	407.087548	-3.091662668	0.2244	-13.779	3.41677E-43	6.43788E-42	
AGAP004095	AGAP004095	nan	174.525564	-3.075839582	0.2239	-13.736	6.14185E-43	1.14127E-41	
AGAP001635	AGAP001635	sodium-coupled monocarboxylate transporter 2	204.45657	-3.07551775	0.1827	-16.835	1.35364E-63	4.53832E-62	
AGAP005223	AGAP005223	Lipocln_cytosolic_FA-bd_dom domain-containing protein [Source:Ur	165.007244	-3.065980036	0.2315	-13.242	5.00596E-40	8.39167E-39	
AGAP007589	AGAP007589	glucosyl/glucuronosyl transferases	621.720554	-3.057865242	0.1706	-17.921	8.02864E-72	3.42253E-70	
AGAP003500	AGAP003500	Lipase [Source:UniProtKB/TrEMBL;Acc:Q7QH37]	9.20282967	-3.051704285	0.5388	-5.6644	1.47533E-08	4.92876E-08	
AGAP005456	CPR15	cuticular protein RR-1 family 15	34.5987538	-3.035623721	0.321	-9.4572	3.16299E-21	2.46677E-20	
AGAP000313	AGAP000313	alanine-glyoxylate aminotransferase 2-like	4145.07087	-3.034879671	0.1817	-16.704	1.22334E-62	4.00178E-61	
AGAP013365	AGAP013365	nan	6527.8282	-3.031818519	0.1594	-19.022	1.11373E-80	6.32073E-79	Granulocytes
AGAP013453	AGAP013453	nan	12.7575822	-3.029051293	0.5309	-5.705	1.16354E-08	3.92613E-08	
AGAP008289	AGAP008289	nan	10.3311855	-3.024651458	0.6155	-4.9139	8.92716E-07	2.49934E-06	
AGAP010633	nan	nan	1204.37305	-3.022523715	0.2197	-13.756	4.65989E-43	8.72119E-42	
AGAP008225	AGAP008225	trehalose 6-phosphate phosphatase	5167.64302	-3.021205186	0.2138	-14.128	2.54971E-45	5.11082E-44	
AGAP013231	AGAP013231	Nitrilase homolog 2	559.870424	-3.018276405	0.2323	-12.995	1.31212E-38	2.08809E-37	
AGAP011104	AGAP011104	nan	427.715002	-3.01468997	0.2914	-10.346	4.36944E-25	4.06764E-24	
AGAP008214	CYP6M4	cytochrome P450	15.9113498	-3.013627712	0.5612	-5.3704	7.85622E-08	2.44349E-07	
AGAP001597	AGAP001597	nan	4.84873071	-3.010538762	0.771	-3.905	9.42364E-05	0.000209535	
AGAP008013	AGAP008013	nan	7263.01289	-3.010012835	0.2617	-11.5	1.31937E-30	1.58543E-29	
AGAP003490	AGAP003490	alanine-glyoxylate aminotransferase	795.275596	-3.007138647	0.1399	-21.496	1.6813E-102	1.4943E-100	Oenocytoids
AGAP001410	AGAP001410	nan	15.4557166	-2.998600332	0.4252	-7.0526	1.75558E-12	8.14747E-12	
AGAP000690	AGAP000690	nan	279.405826	-2.984546954	0.242	-12.332	6.07351E-35	8.5785E-34	
AGAP012350	nan	nan	1796.16641	-2.983440327	0.1652	-18.064	6.09658E-73	2.70924E-71	
AGAP009029	AGAP009029	Protein real-time [Source:UniProtKB/TrEMBL;Acc:A0A1S4GZW6]	79.806766	-2.981978623	0.279	-10.689	1.14734E-26	1.14746E-25	
AGAP008712	AGAP008712	Solute carrier organic anion transporter family member [Source:UniF	112.559908	-2.978096348	0.2888	-10.313	6.15574E-25	5.6634E-24	
AGAP011648	AGAP011648	nan	11.7237491	-2.97673365	0.5862	-5.0782	3.81005E-07	1.11163E-06	
AGAP010968	CLIPA9	CLIP-domain serine protease	10945.0038	-2.971260035	0.2474	-12.012	3.06453E-33	4.04922E-32	Dividing Granulocytes
AGAP012352	AGAP012352	Niemann-Pick C2 protein	5006.94598	-2.970282005	0.213	-13.947	3.27275E-44	6.34416E-43	Dividing Granulocytes
AGAP005175	AGAP005175	acetyl-CoA carboxylase / biotin carboxylase	23704.2072	-2.959842964	0.2158	-13.714	8.40361E-43	1.54932E-41	
AGAP028439	AGAP028439	nan	5256.99719	-2.953650419	0.1848	-15.982	1.71359E-57	5.09267E-56	Granulocytes
AGAP001600	AGAP001600	Ser/Thr protein phosphatase/nucleotidase	104.140397	-2.952627152	0.2597	-11.37	5.91826E-30	6.9262E-29	
AGAP012953	AGAP012953	epidermal retinal dehydrogenase	1187.39227	-2.94249174	0.1982	-14.85	6.99271E-50	1.59899E-48	
AGAP013431	nan	nan	136.457476	-2.940686527	0.2337	-12.582	2.65475E-36	3.90178E-35	
AGAP002323	AGAP002323	nan	554.594019	-2.925967201	0.1587	-18.44	6.30938E-76	3.01729E-74	

AGAP003962	AGAP003962	WSCD family member AGAP003962	21.0022062	-2.917402552	0.3655	-7.9829	1.42915E-15	8.17985E-15	
AGAP009922	AGAP009922	salivary purine nucleosidase	430.34796	-2.915677883	0.1489	-19.586	2.05101E-85	1.28817E-83	
AGAP003993	AGAP003993	nan	6.7600248	-2.911199701	0.7979	-3.6488	0.00026348	0.00055002	
AGAP006369	CPR144	cuticular protein RR-2 family 144	19.9078638	-2.909985591	0.5092	-5.7152	1.09544E-08	3.70561E-08	
AGAP003453	AGAP003453	nan	5931.74076	-2.909971112	0.1682	-17.302	4.57113E-67	1.66917E-65	
AGAP009128	AGAP009128	mitochondrial carnitine/acylcarnitine carrier protein	2204.91283	-2.909484598	0.1843	-15.786	3.85496E-56	1.10053E-54	
AGAP008596	AGAP008596	long-chain-fatty-acid--CoA ligase ACSBG	10721.8263	-2.903218293	0.241	-12.048	1.98212E-33	2.64124E-32	
AGAP005674	AGAP005674	nan	2631.86204	-2.888483883	0.2026	-14.258	3.98509E-46	8.19729E-45	
AGAP003015	AGAP003015	Argininosuccinate synthase [Source:UniProtKB/Swiss-Prot;Acc:Q7PR3	905.992913	-2.883968137	0.2339	-12.329	6.3048E-35	8.87855E-34	
AGAP006740	AGAP006740	dolichyl-phosphate mannosyltransferase polypeptide 2, regulatory su	1307.9002	-2.880732197	0.2493	-11.553	7.08769E-31	8.57165E-30	
AGAP007752	AGAP007752	nan	40.4594783	-2.87946621	0.3539	-8.1358	4.09318E-16	2.41919E-15	
AGAP002610	AGAP002610	nan	5.03221191	-2.863640478	0.72	-3.9771	6.97499E-05	0.000157619	
AGAP005301	AGAP005301	nan	45.0072735	-2.856312215	0.3721	-7.6761	1.63972E-14	8.73252E-14	
AGAP008213	CYP6M3	cytochrome P450	104.606549	-2.852590248	0.3069	-9.2951	1.47038E-20	1.10819E-19	
AGAP008207	CYP6Y2	cytochrome P450	86.035535	-2.847535037	0.2449	-11.628	2.96365E-31	3.65452E-30	
AGAP008783	AGAP008783	Arginase [Source:UniProtKB/TrEMBL;Acc:A0A1S4H002]	1167.31795	-2.845130597	0.1847	-15.404	1.54982E-53	4.01123E-52	
AGAP008892	AGAP008892	nan	417.908217	-2.843210636	0.2159	-13.169	1.3275E-39	2.18643E-38	
AGAP010142	Dat	dopamine N-acetyltransferase	2530.63992	-2.838286283	0.1599	-17.747	1.82768E-70	7.58525E-69	
AGAP002789	AGAP002789	nan	5.70084052	-2.837506957	0.6762	-4.196	2.71662E-05	6.41919E-05	
AGAP003303	AGAP003303	nan	109.004999	-2.836879562	0.2309	-12.288	1.04903E-34	1.46197E-33	
AGAP002672	AGAP002672	nan	668.892011	-2.835433553	0.1838	-15.429	1.04764E-53	2.72647E-52	
AGAP006699	AGAP006699	hairy and enhancer of split, invertebrate	858.698334	-2.832903216	0.1086	-26.077	6.587E-150	1.0699E-147	
AGAP012387	TOLL6	TOLL-like receptor 6	77.3245835	-2.828099213	0.3668	-7.7112	1.24652E-14	6.70671E-14	
AGAP001590	AGAP001590	nan	302.039014	-2.823836965	0.2181	-12.949	2.37916E-38	3.76076E-37	
AGAP013189	AGAP013189	nan	3067.58971	-2.817727508	0.1822	-15.466	5.85753E-54	1.53715E-52	
AGAP008632	AGAP008632	alpha-aminoadipic semialdehyde synthase	3981.68771	-2.812682021	0.1597	-17.613	1.96282E-69	7.73712E-68	Dividing Granulocytes
AGAP011459	AGAP011459	nan	33.1253239	-2.812048835	0.3174	-8.8599	8.00967E-19	5.47598E-18	
AGAP008288	TIM	timeless	7798.30818	-2.805276006	0.1311	-21.393	1.5406E-101	1.3315E-99	
AGAP004270	AGAP004270	hexosaminidase	24.5336753	-2.795173226	0.4168	-6.7071	1.98595E-11	8.53933E-11	
AGAP028177	AGAP028177	nan	7.9695215	-2.79499991	0.609	-4.5894	4.446E-06	1.15774E-05	
AGAP009330	AGAP009330	Troponin C isoform 4"	63.4230335	-2.788674109	0.3713	-7.511	5.86569E-14	2.99192E-13	
AGAP008208	CYP6Y1	cytochrome P450	263.444328	-2.785155	0.2155	-12.922	3.36308E-38	5.27181E-37	
AGAP000262	AGAP000262	nan	12.6655084	-2.784010858	0.5806	-4.7949	1.62755E-06	4.43795E-06	
AGAP007601	AGAP007601	nan	537.939718	-2.781081293	0.2205	-12.614	1.76954E-36	2.61298E-35	
AGAP013770	AGAP013770	nan	73.4854943	-2.780319016	0.364	-7.6391	2.18759E-14	1.15523E-13	
AGAP001520	AGAP001520	protein phosphatase 1, regulatory (inhibitor) subunit 3	3229.13407	-2.778218252	0.153	-18.163	1.01454E-73	4.5514E-72	
AGAP003849	AGAP003849	nan	13.1587734	-2.777089907	0.5736	-4.8415	1.28833E-06	3.54997E-06	
AGAP029107	AGAP029107	nan	1012.84628	-2.772678791	0.237	-11.698	1.29917E-31	1.6147E-30	
AGAP005496	LRIM12	leucine-rich immune protein (Short)	203.283658	-2.766593335	0.3225	-8.5793	9.54397E-18	6.18389E-17	
AGAP028029	AGAP028029	nan	5.02626872	-2.762000872	0.7591	-3.6384	0.000274325	0.000570386	
AGAP011714	nan	nan	439.767191	-2.761655121	0.1904	-14.505	1.12542E-47	2.46572E-46	
AGAP006158	AGAP006158	nan	36.2486886	-2.760644472	0.3219	-8.5766	9.76845E-18	6.32498E-17	
AGAP008009	AGAP008009	RYK receptor-like tyrosine kinase [Source:UniProtKB/TrEMBL;Acc:A0A	4.41505268	-2.760315422	0.7329	-3.7665	0.000165534	0.000355562	
AGAP005103	AGAP005103	nan	477.425162	-2.759866256	0.2061	-13.394	6.57512E-41	1.13689E-39	
AGAP004976	PPO8	prophenoloxidase 8	43.90878	-2.747668438	0.2434	-11.287	1.5251E-29	1.74369E-28	
AGAP007801	AGAP007801	vrille	2468.89931	-2.747094542	0.0853	-32.212	1.2181E-227	5.738E-225	
AGAP028400	AGAP028400	nan	5.69646929	-2.744756716	0.7615	-3.6042	0.000313127	0.000645648	
AGAP008142	nan	nan	22.9964762	-2.744114338	0.4755	-5.7714	7.8605E-09	2.69679E-08	
AGAP001480	AGAP001480	nan	1445.71215	-2.743518159	0.097	-28.277	6.6421E-176	1.7879E-173	
AGAP012295	CYP9L1	cytochrome P450	635.65781	-2.738935645	0.1749	-15.664	2.67983E-55	7.36056E-54	
AGAP005776	PDH	pigment dispersing hormone	28.7151958	-2.738428116	0.5075	-5.3955	6.83162E-08	2.13823E-07	
AGAP002641	AGAP002641	nan	9.02264866	-2.729059706	0.6329	-4.312	1.61757E-05	3.92154E-05	
AGAP004534	AGAP004534	cathepsin B precursor	86.8145119	-2.728691805	0.2043	-13.355	1.10832E-40	1.9019E-39	
AGAP007094	AGAP007094	nan	7.26679985	-2.727472848	0.6001	-4.5451	5.49007E-06	1.41587E-05	
AGAP000968	AGAP000968	nan	94.3562328	-2.725815367	0.2311	-11.795	4.12248E-32	5.22015E-31	
AGAP002341	AGAP002341	nan	1003.57572	-2.723399398	0.1967	-13.849	1.29596E-43	2.48155E-42	
AGAP007339	AGAP007339	troponin C, isoform 3	44.4004595	-2.720632296	0.3134	-8.6813	3.91329E-18	2.58898E-17	
AGAP009176	AGAP009176	fatty acid synthase, animal type	33667.3064	-2.719926417	0.1833	-14.837	8.43178E-50	1.92338E-48	
AGAP000167	AGAP000167	Lipid storage droplets surface-binding protein 2	9070.62516	-2.714439432	0.0793	-34.228	9.2256E-257	7.9013E-254	Granulocytes
AGAP010269	AGAP010269	ANK_REP_REGION domain-containing protein [Source:UniProtKB/TrE	68.6841714	-2.713220433	0.2536	-10.698	1.0417E-26	1.04292E-25	
AGAP013400	AGAP013400	nan	5086.33564	-2.703161119	0.1731	-15.612	6.00712E-55	1.62624E-53	
AGAP005739	nan	nan	138.026837	-2.700610582	0.4011	-6.7332	1.66021E-11	7.17472E-11	
AGAP007647	AGAP007647	nan	3027.80365	-2.699881035	0.1583	-17.054	3.27409E-65	1.14241E-63	
AGAP004157	AGAP004157	synaptic vesicle protein	31.6579558	-2.699466121	0.3022	-8.9333	4.13507E-19	2.87927E-18	
AGAP005834	COEJHE2E	carboxylesterase	258.838753	-2.687648621	0.2812	-9.5594	1.18386E-21	9.45181E-21	
AGAP009218	AGAP009218	nan	526.027122	-2.686723095	0.5865	-4.5807	4.63322E-06	1.20446E-05	
AGAP002503	AGAP002503	4-coumarate:CoA ligase	3661.11725	-2.686283431	0.1765	-15.218	2.68018E-52	6.67989E-51	
AGAP010969	AGAP010969	Roundabout 1	62.0145588	-2.682168675	0.2699	-9.9381	2.84093E-23	2.41774E-22	
AGAP012216	AGAP012216	sterol O-acyltransferase	169.461239	-2.681926554	0.2115	-12.682	7.48376E-37	1.11735E-35	
AGAP007738	AGAP007738	nan	221.051401	-2.681722644	0.2178	-12.311	7.92426E-35	1.11093E-33	
AGAP005740	nan	nan	41.0247269	-2.673648343	0.4357	-6.1371	8.40181E-10	3.18525E-09	
AGAP002268	AGAP002268	nan	4372.36981	-2.664891922	0.2027	-13.149	1.72456E-39	2.83049E-38	
AGAP003934	AGAP003934	Battenin [Source:UniProtKB/TrEMBL;Acc:Q7Q2B1]	810.701736	-2.661543747	0.0961	-27.689	9.5586E-169	2.1441E-166	
AGAP001127	AGAP001127	P37NB protein	576.584241	-2.660769671	0.1794	-14.834	8.88369E-50	2.0167E-48	
AGAP005992	CYP302A1	cytochrome P450	80.4973131	-2.651850026	0.2698	-9.8275	8.56846E-23	7.15E-22	
AGAP000180	AGAP000180	phosphoribosylaminoimidazole carboxylase	5773.79183	-2.649490911	0.2247	-11.792	4.28269E-32	5.41574E-31	
AGAP004954	AGAP004954	rhythmically expressed gene 2 protein	313.42621	-2.649035701	0.2208	-11.995	3.77261E-33	4.96393E-32	
AGAP002835	AGAP002835	alpha-tocopherol transfer protein-like protein	53.4834947	-2.646952914	0.2813	-9.4099	4.96717E-21	3.82631E-20	
AGAP007754	AGAP007754	nan	1841.38919	-2.645616117	0.122	-21.68	3.2013E-104	3.0159E-102	
AGAP007165	AGAP007165	Late trypsin	9.33984706	-2.641139965	0.5333	-4.9521	7.34118E-07	2.07692E-06	
AGAP006467	AGAP006467	nan	20.2503579	-2.640444595	0.3706	-7.1241	1.04729E-12	4.93078E-12	
AGAP003097	AGAP003097	yellow protein	84.2787943	-2.636689025	0.2939	-8.9702	2.95951E-19	2.08071E-18	
AGAP011924	AGAP011924	Potassium channel subfamily K, invertebrate [Source:UniProtKB/TrEM	79.1578349	-2.634037214	0.2057	-12.805	1.52893E-37	2.3652E-36	
AGAP007711	AGAP007711	nan	6245.8815	-2.63161604	0.1939	-13.571	5.97309E-42	1.06175E-40	Dividing Granulocytes
AGAP009770	GPRCAL1	putative calcitonin receptor 1	370.072892	-2.631610182	0.2542	-10.351	4.14188E-25	3.85961E-24	
AGAP028580	AGAP028580	nan	107.348715	-2.630831885	0.2637	-9.9782	1.89803E-23	1.62557E-22	
AGAP009414	AGAP009414	1-acyl-sn-glycerol-3-phosphate acyltransferase alpha	792.162407	-2.620327636	0.1958	-13.381	7.79382E-41	1.34233E-39	
AGAP002718	AGAP002718	4-coumarate:CoA ligase isoform 2 [Source:UniProtKB/TrEMBL;Acc:Q3	1450.95555	-2.616001711	0.1703	-15.357	3.18945E-53	8.18741E-52	
AGAP007198	AGAP007198	nan	756.12112	-2.613410195	0.1623	-16.105	2.3612E-58	7.17575E-57	
AGAP003483	AGAP003483	nan	394.558751	-2.608053865	0.218	-11.965	5.40774E-33	7.08572E-32	
AGAP002069	AGAP002069	decaprenyl-diphosphate synthase subunit 1	36.9606939	-2.606488166	0.3439	-7.5801	3.45261E-14	1.78917E-13	
AGAP001779	AGAP001779	nan	200.711143	-2.606480434	0.1899	-13.728	6.92004E-43	1.28082E-41	
AGAP028646	ANCE3	angiotensin-converting enzyme 3	31.9498117	-2.60620726	0.2999	-8.6916	3.57438E-18	2.37143E-17	
AGAP000290	CLIPA27	CLIP-domain serine protease	3535.03588	-2.602632476	0.176	-14.784	1.86988E-49	4.22449E-48	Granulocytes

AGAP001524	AGAP001524	nan	71.7487177	-2.599672448	0.2849	-9.1264	7.07987E-20	5.16249E-19	
AGAP008982	AGAP008982	CzcD (Cation-efflux system membrane protein) [Source:UniProtKB/T	356.806884	-2.599164944	0.229	-11.352	7.28096E-30	8.46838E-29	
AGAP007029	AGAP007029	glucosyl/glucuronosyl transferases	527.444528	-2.597261687	0.1792	-14.493	1.35051E-47	2.93838E-46	
AGAP010860	AGAP010860	sodium-dependent nutrient amino acid transporter 2	700.333353	-2.595959467	0.219	-11.855	2.03445E-32	2.61838E-31	
AGAP008143	AGAP008143	nan	23.8458732	-2.595511659	0.4224	-6.145	7.99724E-10	3.03676E-09	
AGAP007163	AGAP007163	3',5'-cyclic-nucleotide phosphodiesterase	313.285862	-2.594609145	0.1854	-13.993	1.73114E-44	3.38362E-43	
AGAP012477	AGAP012477	gamma-butyrobetaine dioxygenase	43.7310946	-2.58874021	0.3542	-7.3092	2.68647E-13	1.31204E-12	
AGAP011322	AGAP011322	fibulin 2	10.4308474	-2.588621121	0.6504	-3.9799	6.89343E-05	0.000155926	
AGAP013537	AGAP013537	nan	15.564936	-2.586296847	0.5132	-5.0394	4.66996E-07	1.34915E-06	
AGAP006579	AGAP006579	nan	18.5285262	-2.586225151	0.5121	-5.0505	4.40577E-07	1.27595E-06	
AGAP006548	AGAP006548	glycine cleavage system H protein	3029.33721	-2.585621626	0.2382	-10.854	1.91878E-27	1.99084E-26	
AGAP002084	AGAP002084	glycerol-3-phosphate O-acyltransferase 3/4	1244.10441	-2.578332454	0.21	-12.279	1.1747E-34	1.62988E-33	
AGAP012307	AGAP012307	Spondin-1	15732.9862	-2.571529683	0.1781	-14.441	2.84551E-47	6.06505E-46	
AGAP005581	AGAP005581	3-hydroxyisobutyrate dehydrogenase [Source:UniProtKB/TrEMBL;Ac	4012.06571	-2.565208818	0.1729	-14.836	8.61132E-50	1.95959E-48	
AGAP001561	GPRNNA5	putative GPCR class a orphan receptor 5	39.8573453	-2.56234367	0.3002	-8.5357	1.3925E-17	8.95477E-17	
AGAP009364	AGAP009364	nan	32.8702336	-2.56014532	0.4466	-5.7327	9.88478E-09	3.36798E-08	
AGAP005783	AGAP005783	nan	129.288309	-2.559195545	0.2169	-11.798	4.00764E-32	5.08156E-31	
AGAP011427	nan	nan	197.796839	-2.55540795	0.2501	-10.217	1.67081E-24	1.50054E-23	
AGAP010632	nan	nan	559.977344	-2.549597648	0.2491	-10.236	1.37148E-24	1.23643E-23	
AGAP004600	nan	nan	197.437918	-2.544823074	0.1531	-16.62	4.99063E-62	1.61016E-60	
AGAP007920	AGAP007920	glucuronosyltransferase	1090.97589	-2.540702277	0.2074	-12.249	1.69933E-34	2.35087E-33	
AGAP009763	AGAP009763	nan	108.051319	-2.535435227	0.2509	-10.105	5.26959E-24	4.65711E-23	
AGAP002449	AGAP002449	3-OH androgenic UDPGT	10.2672766	-2.535213461	0.4894	-5.1807	2.21103E-07	6.60646E-07	
AGAP002156	GPRGNR1	putative gonadotrophin releasing hormone receptor 1	1190.95674	-2.535035992	0.2038	-12.439	1.60396E-35	2.31053E-34	
AGAP003759	AGAP003759	juvenile hormone-inducible protein	900.466307	-2.532817671	0.2116	-11.969	5.16558E-33	6.7873E-32	Granulocytes
AGAP006698	AGAP006698	nan	20.9079053	-2.523103693	0.371	-6.8001	1.04529E-11	4.59101E-11	
AGAP009472	ABCG20	ATP-binding cassette transporter (ABC transporter) family G membe	63.036108	-2.517693555	0.275	-9.1558	5.39325E-20	3.95407E-19	
AGAP010887	CPR113	cuticular protein RR-2 family 113	16.3552987	-2.515612185	0.5228	-4.8114	1.49864E-06	4.10428E-06	
AGAP009757	ANCE7	angiotensin-converting enzyme 7	10.4647292	-2.508544242	0.5018	-4.9994	5.75158E-07	1.64598E-06	
AGAP003422	AGAP003422	endoplasmic reticulum metallopeptidase 1	125.955835	-2.507949863	0.2339	-10.725	7.80256E-27	7.87866E-26	
AGAP006741	AGAP006741	nan	578.501361	-2.504956326	0.2433	-10.296	7.37979E-25	6.75E-24	
AGAP002250	AGAP002250	calcium/calmodulin-dependent protein kinase kinase	527.504932	-2.503700527	0.2193	-11.418	3.41461E-30	4.04642E-29	
AGAP012399	AGAP012399	maltase	3023.90855	-2.503289364	0.1176	-21.292	1.356E-100	1.1509E-98	
AGAP006569	AGAP006569	acetyl-CoA synthetase	716.52121	-2.503169264	0.1061	-23.592	4.6247E-123	5.8092E-121	
AGAP007761	AGAP007761	Complement control protein	14.786335	-2.502881112	0.5086	-4.9208	8.61892E-07	2.41807E-06	
AGAP009312	AGAP009312	nan	9.586563	-2.493802194	0.551	-4.5257	6.02074E-06	1.54368E-05	
AGAP011750	AGAP011750	alpha-N-acetylglucosaminidase	722.334084	-2.493652027	0.2349	-10.618	2.45678E-26	2.42106E-25	
AGAP009347	AGAP009347	FK506-binding protein 4/5	3624.89028	-2.484843102	0.1689	-14.711	5.48884E-49	1.22247E-47	
AGAP009556	AGAP009556	nan	559.315853	-2.47441434	0.1965	-12.595	2.26295E-36	3.33114E-35	
AGAP006819	AGAP006819	abhydrolase domain-containing protein 1/3	631.818128	-2.470024441	0.2032	-12.156	5.29825E-34	7.24453E-33	
AGAP002826	AGAP002826	nan	33.9130791	-2.469666613	0.6566	-3.7611	0.000169195	0.00036293	
AGAP009896	AGAP009896	proton-coupled amino acid transporter	69.8293157	-2.466530637	0.2596	-9.5024	2.05032E-21	1.6232E-20	
AGAP011509	COEunkn	carboxylesterase	420.334576	-2.458427804	0.3092	-7.9515	1.84278E-15	1.04836E-14	
AGAP000095	AGAP000095	anoctamin 5	4124.76665	-2.45804903	0.0772	-31.844	1.5845E-222	6.7855E-220	
AGAP008557	AGAP008557	AMP-binding domain protein	292.756205	-2.451986748	0.1995	-12.293	9.84826E-35	1.37452E-33	
AGAP000698	AGAP000698	nan	981.786796	-2.446687047	0.0813	-30.098	5.1128E-199	1.661E-196	Granulocytes
AGAP002109	AGAP002109	solute carrier family 31 (copper transporter), member 1	5710.06577	-2.444179463	0.2399	-10.19	2.18898E-24	1.95844E-23	
AGAP012813	AGAP012813	nan	152.580053	-2.439718865	0.1883	-12.958	2.1264E-38	3.36687E-37	
AGAP001884	AGAP001884	fumarate hydratase, class II	11280.3377	-2.438626332	0.1692	-14.409	4.55178E-47	9.57194E-46	Oenocytoids
AGAP007662	AGAP007662	All-trans/9-cis	11.9938402	-2.436478461	0.4515	-5.3959	6.81775E-08	2.1346E-07	
AGAP005617	AGAP005617	nan	3311.35222	-2.43499106	0.1134	-21.465	3.2861E-102	2.8665E-100	
AGAP009609	AGAP009609	homogentisate 1,2-dioxygenase	22.0763605	-2.427578942	0.3998	-6.0727	1.25793E-09	4.69501E-09	
AGAP001989	AGAP001989	nan	4244.17765	-2.419207125	0.2014	-12.009	3.18551E-33	4.20318E-32	
AGAP003927	ILP5	Insulin-like peptide 5	32.0637047	-2.41812528	0.5408	-4.4711	7.78321E-06	1.969E-05	
AGAP011197	AGAP011197	nan	15631.9393	-2.417966052	0.3117	-7.7563	8.74367E-15	4.78641E-14	Granulocytes
AGAP004802	AGAP004802	4-hydroxyphenylpyruvate dioxygenase [Source:UniProtKB/TrEMBL;A	135.189293	-2.413744061	0.2708	-8.914	4.92069E-19	3.41117E-18	
AGAP012391	AGAP012391	nan	24.8363814	-2.412875336	0.3979	-6.0641	1.32681E-09	4.93677E-09	
AGAP003579	AGAP003579	cadherin-87A	139.194367	-2.412126322	0.1743	-13.838	1.49847E-43	2.84045E-42	
AGAP004620	AGAP004620	Envelysin	15.5825335	-2.411984736	0.4254	-5.6696	1.43097E-08	4.79074E-08	
AGAP028196	AGAP028196	nan	266.574124	-2.409816791	0.2173	-11.09	1.404E-28	1.53982E-27	
AGAP002891	GPRMGL4	putative metabotropic glutamate receptor 4	373.811128	-2.407173492	0.2192	-10.979	4.80847E-28	5.11871E-27	
AGAP002738	SCRB5	Class B Scavenger Receptor (CD36 domain).	38.217221	-2.404354095	0.3112	-7.7259	1.11032E-14	6.01859E-14	
AGAP002761	AGAP002761	3-methylcrotonyl-CoA carboxylase beta subunit	1711.80514	-2.404176528	0.2023	-11.881	1.4801E-32	1.91276E-31	
AGAP000131	AGAP000131	nan	29.2004817	-2.403920305	0.3135	-7.6688	1.73551E-14	9.23222E-14	
AGAP011715	nan	nan	2052.03365	-2.403424709	0.1053	-22.815	3.2285E-115	3.755E-113	
AGAP008688	AGAP008688	nan	3288.38596	-2.402442913	0.1915	-12.544	4.30178E-36	6.29302E-35	
AGAP002925	AGAP002925	poly(U)-specific endoribonuclease	6803.74621	-2.401733656	0.2459	-9.7675	1.55225E-22	1.28504E-21	
AGAP007095	AGAP007095	nan	8.07568557	-2.400270434	0.5705	-4.2069	2.58844E-05	6.13015E-05	
AGAP011231	AGAP011231	fibrinogen	77.3634722	-2.397781425	0.3923	-6.1117	9.85592E-10	3.71262E-09	
AGAP000327	AGAP000327	tyrosine aminotransferase	1656.41281	-2.397077006	0.2245	-10.679	1.2738E-26	1.27258E-25	
AGAP003358	AGAP003358	Sugar transporter SWEET [Source:UniProtKB/TrEMBL;Acc:A0NDW1]	110.058707	-2.396761041	0.3004	-7.9789	1.47585E-15	8.44202E-15	
AGAP011052	nan	nan	857.99609	-2.396236463	0.1623	-14.767	2.39414E-49	5.38309E-48	
AGAP006637	AGAP006637	Oatp58Dc	12.5468924	-2.394554131	0.6858	-3.4915	0.000480403	0.000965212	
AGAP011830	AGAP011830	myo-inositol-1-phosphate synthase	34.555182	-2.389023549	0.3819	-6.255	3.97412E-10	1.55547E-09	
AGAP003267	AGAP003267	nan	45.6408423	-2.385621788	0.3007	-7.9344	2.11486E-15	1.19592E-14	
AGAP011158	AGAP011158	Kynurenine--oxoglutarate transaminase 3 isoform 1	2474.65055	-2.384308505	0.1095	-21.769	4.5306E-105	4.3554E-103	Oenocytoids
AGAP007664	AGAP007664	coiled-coil domain-containing protein 34	27.849818	-2.384306765	0.3838	-6.213	5.19672E-10	2.00896E-09	
AGAP007675	AGAP007675	dynein, axonemal heavy chain	6.36055081	-2.380253171	0.6441	-3.6957	0.000219288	0.000463625	
AGAP000238	AGAP000238	nan	703.056376	-2.380158991	0.2402	-9.9074	3.86679E-23	3.27305E-22	
AGAP007781	AGAP007781	eukaryotic translation initiation factor 4E-binding protein 1	14699.8994	-2.378865811	0.0693	-34.312	5.16E-258	5.4014E-255	
AGAP012000	AGAP012000	fibrinogen and fibronectin	4234.79495	-2.37771306	0.1924	-12.361	4.23122E-35	6.01242E-34	Oenocytoids
AGAP008012	AGAP008012	nan	596.141968	-2.377128217	0.2183	-10.888	1.3098E-27	1.36349E-26	
AGAP000015	AGAP000015	proto-oncogene tyrosine-protein kinase ROS	56.839972	-2.376981853	0.2965	-8.0166	1.08705E-15	6.27132E-15	
AGAP003005	AGAP003005	serine/threonine-protein kinase SIK	567.698708	-2.376750193	0.1422	-16.71	1.10866E-62	3.63925E-61	
AGAP012742	AGAP012742	nan	8.2364549	-2.373141712	0.5079	-4.6725	2.97616E-06	7.89368E-06	
AGAP010645	AGAP010645	nan	625.912603	-2.372574179	0.2409	-9.8491	6.91789E-23	5.77778E-22	
AGAP006743	AGAP006743	nan	1458.16669	-2.372151238	0.1901	-12.479	9.73705E-36	1.41782E-34	Oenocytoids
AGAP005302	AGAP005302	DIRAS family, GTP-binding Ras-like 2	68.5889576	-2.368684796	0.2906	-8.15	3.63803E-16	2.15288E-15	
AGAP001293	AGAP001293	nan	24.530601	-2.36509304	0.3108	-7.6086	2.77013E-14	1.44825E-13	
AGAP009405	CPAP3-E	cuticular protein	75.4477584	-2.363863534	0.2379	-9.9369	2.87681E-23	2.44607E-22	
AGAP000278	OBP9	odorant-binding protein 9	136.522372	-2.361210706	0.2298	-10.276	9.01486E-25	8.16625E-24	
AGAP009381	AGAP009381	Cellular retinaldehyde-binding protein [Source:UniProtKB/TrEMBL;A	25.722645	-2.359419209	0.5046	-4.6756	2.93042E-06	7.77675E-06	
AGAP007692	SRPN14	serine protease inhibitor (serpin) 14	234.911196	-2.359105557	0.2157	-10.937	7.67766E-28	8.08171E-27	
AGAP006018	AGAP006018	nan	82.4562232	-2.358385416	0.2127	-11.087	1.45341E-28	1.59031E-27	

AGAP004106	AGAP004106	nan	155.190438	-2.355642662	0.2036	-11.568	5.97053E-31	7.2485E-30	
AGAP002457	AGAP002457	nan	22.7808396	-2.355336707	0.4475	-5.2637	1.41202E-07	4.28979E-07	
AGAP008582	AGAP008582	Alpha-mannosidase [Source:UniProtKB/TrEMBL;Acc:A0A1S4GYP5]	44.6842384	-2.352787645	0.251	-9.3718	7.13126E-21	5.47098E-20	
AGAP006728	AGAP006728	nan	27.5540987	-2.352718202	0.42	-5.6017	2.12274E-08	6.99488E-08	
AGAP000553	white	protein white	69.5525027	-2.350714155	0.3416	-6.882	5.90298E-12	2.64316E-11	
AGAP009635	AGAP009635	nan	15.4947577	-2.344111236	0.536	-4.3735	1.22252E-05	3.01028E-05	
AGAP006724	COEAE3G	carboxylesterase	47.2679065	-2.337800547	0.3693	-6.33	2.45154E-10	9.74511E-10	
AGAP001717	AGAP001717	nan	21.0105193	-2.337232131	0.4685	-4.9889	6.07266E-07	1.73313E-06	
AGAP028648	AGAP028648	nan	510.247443	-2.333370386	0.2169	-10.758	5.43989E-27	5.52255E-26	
AGAP010766	AGAP010766	nan	17.7400371	-2.332750466	0.4366	-5.3425	9.16865E-08	2.83299E-07	
AGAP003238	AGAP003238	N-myc downstream regulated	1764.02464	-2.331890497	0.21	-11.103	1.21359E-28	1.33566E-27	
AGAP007525	AGAP007525	coronin homolog	483.016816	-2.330480232	0.1292	-18.034	1.06008E-72	4.66682E-71	
AGAP009109	AGAP009109	nan	656.568432	-2.32919262	0.1171	-19.894	4.56758E-88	2.92729E-86	
AGAP005095	AGAP005095	actin beta/gamma 1	571.590763	-2.32903806	0.2336	-9.9721	2.01957E-23	1.7281E-22	
AGAP009415	AGAP009415	lysophosphatidate acyltransferase	191.787636	-2.327522704	0.218	-10.675	1.33206E-26	1.32797E-25	
AGAP012052	nan	nan	10.0520965	-2.326512702	0.5746	-4.0491	5.14087E-05	0.000117754	
AGAP009688	AGAP009688	Leucine-rich repeats and immunoglobulin-like domains protein 3	74.0276439	-2.325611898	0.2811	-8.2738	1.29807E-16	7.83919E-16	
AGAP011948	AGAP011948	threonine 3-dehydrogenase	947.615608	-2.319896367	0.1697	-13.673	1.4782E-42	2.7041E-41	
AGAP009848	nan	nan	6.61977499	-2.318913746	0.6367	-3.6421	0.000270373	0.000562913	
AGAP003030	AGAP003030	Pyruvate dehydrogenase E1 component subunit alpha [Source:UniPr	1193.86372	-2.313211468	0.1672	-13.835	1.57042E-43	2.97087E-42	
AGAP011523	AGAP011523	nan	58.4287778	-2.312625646	0.3869	-5.9779	2.26011E-09	8.20836E-09	
AGAP013439	AGAP013439	nan	32.3701908	-2.311477393	0.3233	-7.1502	8.66827E-13	4.11197E-12	
AGAP004119	AGAP004119	cGMP-specific 3', 5'-cyclic phosphodiesterase	135.308647	-2.311172394	0.1737	-13.305	2.16381E-40	3.66642E-39	
AGAP010508	AGAP010508	proton-coupled amino acid transporter	82.2617448	-2.306618937	0.2546	-9.0608	1.29533E-19	9.29737E-19	
AGAP012019	AGAP012019	nan	257.54224	-2.306162464	0.1967	-11.723	9.77371E-32	1.21958E-30	
AGAP012662	AGAP012662	omega-amidase	919.738534	-2.305791851	0.2436	-9.467	2.87909E-21	2.25657E-20	
AGAP002663	AGAP002663	nan	76.0958659	-2.301545809	0.2791	-8.2454	1.64551E-16	9.89302E-16	
AGAP011940	AGAP011940	nan	23493.8308	-2.300702471	0.1589	-14.475	1.73554E-47	3.733E-46	Granulocytes
AGAP028892	LSU_rRNA_eukary	Eukaryotic large subunit ribosomal RNA [Source:RFAM;Acc:RF02543]	383.839363	-2.300185518	0.386	-5.9591	2.53662E-09	9.13512E-09	
AGAP005564	AGAP005564	CP2 domain-containing protein [Source:UniProtKB/TrEMBL;Acc:A7U	11.7002051	-2.299782375	0.4128	-5.5709	2.53403E-08	8.27777E-08	
AGAP001659	AGAP001659	hexamerin	13.2905745	-2.298331936	0.4735	-4.8539	1.21073E-06	3.34497E-06	
AGAP012954	AGAP012954	nan	72.053172	-2.294932598	0.296	-7.7532	8.95762E-15	4.89784E-14	
AGAP005370	COEBE4C	carboxylesterase beta esterase	16.5310695	-2.291844587	0.4735	-4.8406	1.2946E-06	3.56517E-06	
AGAP008704	AGAP008704	Juvenile hormone-inducible protein [Source:UniProtKB/TrEMBL;Acc:	421.928565	-2.28767662	0.2088	-10.957	6.12395E-28	6.48244E-27	
AGAP004318	CLIPC3	CLIP-domain serine protease	1204.74386	-2.287218806	0.2052	-11.144	7.6366E-29	8.47402E-28	
AGAP004262	TO3	takeout 3	29.1144885	-2.286912991	0.3274	-6.9845	2.85881E-12	1.30805E-11	
AGAP006047	CYP4J9	cytochrome P450	102.844225	-2.284419971	0.1975	-11.565	6.18441E-31	7.4985E-30	
AGAP011503	AGAP011503	nan	642.360089	-2.282940118	0.2205	-10.351	4.13535E-25	3.85734E-24	
AGAP012577	AGAP012577	nan	3224.89105	-2.281795555	0.2424	-9.4125	4.84298E-21	3.73369E-20	
AGAP003578	AGAP003578	aldehyde dehydrogenase (NAD+)	2418.49943	-2.281313782	0.0916	-24.907	6.3135E-137	9.4412E-135	Granulocytes
AGAP004762	AGAP004762	alpha-tocopherol transfer protein-like protein	85.5034718	-2.281133253	0.2467	-9.2472	2.30543E-20	1.71967E-19	
AGAP001470	AGAP001470	nan	17971.8688	-2.281092055	0.1994	-11.439	2.68319E-30	3.20385E-29	Granulocytes
AGAP003168	AGAP003168	Isocitrate dehydrogenase [NADP] [Source:UniProtKB/TrEMBL;Acc:Q7	6440.11392	-2.275208578	0.1805	-12.604	1.99719E-36	2.94453E-35	
AGAP007334	AGAP007334	Tektin [Source:UniProtKB/TrEMBL;Acc:Q7QJ75]	29.2657475	-2.27501447	0.3021	-7.5315	5.01499E-14	2.57472E-13	
AGAP008889	ABCG15	ATP-binding cassette transporter (ABC transporter) family G membe	182.714194	-2.265786564	0.2511	-9.0235	1.82163E-19	1.29619E-18	
AGAP003773	AGAP003773	nan	703.878338	-2.265195948	0.2323	-9.7522	1.80474E-22	1.47847E-21	
AGAP003301	AGAP003301	M-phase inducer phosphatase	714.854198	-2.260530545	0.2052	-11.019	3.10743E-28	3.34191E-27	
AGAP001116	AGAP001116	D-amino-acid oxidase	916.292957	-2.260425193	0.2041	-11.077	1.63119E-28	1.7807E-27	
AGAP012165	nan	nan	7.09811052	-2.25837811	0.5328	-4.2386	2.24916E-05	5.36302E-05	
AGAP028764	aga-mir-34	nan	9.22155097	-2.25816415	0.4525	-4.99	6.03724E-07	1.72406E-06	
AGAP001657	AGAP001657	hexamerin	23.7940774	-2.25530474	0.3638	-6.1989	5.685E-10	2.18606E-09	
AGAP013540	AGAP013540	nan	99.607894	-2.255033994	0.2446	-9.2187	3.0078E-20	2.23298E-19	
AGAP007279	AGAP007279	nan	293.691065	-2.250852654	0.2131	-10.561	4.51074E-26	4.381E-25	
AGAP011984	AGAP011984	UDP-N-acetyl-alpha-D-galactosamine:polypeptide N-acetylgalactosar	4104.57233	-2.248194125	0.1976	-11.378	5.38698E-30	6.33592E-29	Granulocytes
AGAP008614	AGAP008614	nan	116.770244	-2.242769973	0.2087	-10.747	6.12674E-27	6.21313E-26	
AGAP001987	AGAP001987	nan	91.8940082	-2.241147168	0.2601	-8.615	6.99526E-18	4.56387E-17	
AGAP009115	AGAP009115	phosphatidylinositol phospholipase C, beta	121.799069	-2.240868083	0.1531	-14.638	1.61471E-48	3.57934E-47	
AGAP029185	AGAP029185	nan	6259.02738	-2.240571367	0.2081	-10.768	4.85248E-27	4.94219E-26	
AGAP007881	AGAP007881	Steroid dehydrogenase	75.5187113	-2.240117035	0.2082	-10.76	5.31949E-27	5.40614E-26	
AGAP000128	AGAP000128	MFS transporter, VNT family, synaptic vesicle glycoprotein 2	190.229327	-2.239006767	0.2558	-8.7539	2.0619E-18	1.37767E-17	
AGAP003449	AGAP003449	rootletin	132.804659	-2.238462492	0.2285	-9.7942	1.1924E-22	9.8887E-22	
AGAP010640	AGAP010640	nan	3865.77393	-2.238179986	0.183	-12.229	2.16425E-34	2.98527E-33	
AGAP013036	AGAP013036	nan	47.3192495	-2.236496656	0.28	-7.9881	1.37024E-15	7.85219E-15	
AGAP009131	AGAP009131	nan	27.7632898	-2.234811024	0.3467	-6.4465	1.14452E-10	4.65967E-10	
AGAP000156	AGAP000156	nan	28.4121895	-2.231484108	0.315	-7.0843	1.39724E-12	6.5133E-12	
AGAP003328	AGAP003328	NADH dehydrogenase (ubiquinone) 1 alpha subcomplex 6	105.32323	-2.230101589	0.3969	-5.6186	1.92548E-08	6.36714E-08	
AGAP007014	AGAP007014	Amino_oxidase domain-containing protein [Source:UniProtKB/TrEMI	31.9757341	-2.225944393	0.4408	-5.05	4.41757E-07	1.27898E-06	
AGAP013290	LRIM27	leucine-rich immune protein (Coil-less)	401.682148	-2.225568481	0.2364	-9.4164	4.66818E-21	3.60188E-20	
AGAP028564	AGAP028564	nan	1831.46812	-2.224442565	0.1833	-12.138	6.6206E-34	8.97448E-33	
AGAP012008	AGAP012008	nan	207.211918	-2.219825262	0.2262	-9.8122	9.97317E-23	8.30011E-22	
AGAP012053	AGAP012053	alpha,alpha-trehalase	4513.24466	-2.219554737	0.1444	-15.372	2.53072E-53	6.53202E-52	
AGAP009144	AGAP009144	nan	360.441606	-2.218211654	0.1419	-15.635	4.18545E-55	1.13963E-53	
AGAP004376	AGAP004376	aldose 1-epimerase	454.806495	-2.217002701	0.2047	-10.829	2.51583E-27	2.59602E-26	Oenocytoids
AGAP004306	AGAP004306	nan	6.12836441	-2.215525833	0.593	-3.7362	0.000186819	0.000398737	
AGAP006907	AGAP006907	Cat eye syndrome chromosome region, candidate 1a	1136.7432	-2.212906822	0.117	-18.921	7.64914E-80	4.21418E-78	
AGAP010473	AGAP010473	Pleckstrin-like proteiny domain-containing family G member 5	18.2736161	-2.212106507	0.4326	-5.1137	3.1588E-07	9.2997E-07	
AGAP002324	AGAP002324	mitochondrial sodium/hydrogen exchanger NHA2	498.561816	-2.210831099	0.2296	-9.6301	5.96462E-22	4.8234E-21	
AGAP000299	AGAP000299	nan	255.253733	-2.205293292	0.1263	-17.455	3.17072E-68	1.20449E-66	
AGAP012290	AGAP012290	nan	131.239237	-2.203350671	0.188	-11.721	1.00038E-31	1.24664E-30	
AGAP004118	SCRAL1	Class A Scavenger Receptor (SRCR domain) with Lysyl Oxidase domai	14.0255715	-2.202704126	0.442	-4.9831	6.25627E-07	1.78391E-06	
AGAP007790	AGAP007790	Sodium/potassium-transporting ATPase subunit beta [Source:UniPro	5685.58683	-2.202668102	0.106	-20.78	6.54492E-96	4.85509E-94	
AGAP001713	AGAP001713	stearoyl-CoA desaturase (delta-9 desaturase)	24038.5132	-2.200516903	0.2207	-9.9689	2.08606E-23	1.78175E-22	
AGAP003751	CPAP1-C	cuticular protein	107.406582	-2.19811333	0.1952	-11.258	2.10985E-29	2.39481E-28	
AGAP012679	AGAP012679	nan	23.4968382	-2.197140641	0.4351	-5.0497	4.42501E-07	1.28074E-06	
AGAP012275	AGAP012275	nan	113.518995	-2.194052528	0.2382	-9.2126	3.18275E-20	2.361E-19	
AGAP007049	AGAP007049	nan	3830.83849	-2.193460503	0.2469	-8.8836	6.47324E-19	4.44817E-18	Megacytes
AGAP001283	AGAP001283	potassium inwardly-rectifying channel subfamily J	22.1943654	-2.193404679	0.3257	-6.735	1.63985E-11	7.08994E-11	
AGAP003441	AGAP003441	nan	14.2669086	-2.192601287	0.3697	-5.9306	3.01748E-09	1.08131E-08	
AGAP000097	AGAP000097	solute carrier family 25	2876.95234	-2.189979922	0.2078	-10.541	5.60827E-26	5.42459E-25	
AGAP006756	AGAP006756	nan	103.630912	-2.189459005	0.1996	-10.968	5.436E-28	5.76069E-27	
AGAP027997	LRIM5	leucine-rich immune protein (Short)	1455.95722	-2.188307329	0.196	-11.166	6.00569E-29	6.68789E-28	
AGAP011643	AGAP011643	nan	10.6236155	-2.188271772	0.6175	-3.544	0.00039417	0.000800836	
AGAP028636	AGAP028636	nan	1573.60888	-2.185494737	0.2674	-8.1742	2.97744E-16	1.7731E-15	
AGAP010365	AGAP010365	nan	8.4200103	-2.181281288	0.4973	-4.3866	1.15145E-05	2.84645E-05	

AGAP000023	AGAP000023	nan	18.0493725	-2.178246081	0.5402	-4.0324	5.52155E-05	0.000126075	
AGAP002178	AGAP002178	homeobox protein homothorax	44.5424978	-2.174738692	0.2413	-9.0134	1.99778E-19	1.41832E-18	
AGAP013476	AGAP013476	nan	14.4147151	-2.173877245	0.5294	-4.1062	4.02251E-05	9.31794E-05	
AGAP006638	AGAP006638	Oatp58Dc	12.6633594	-2.170027724	0.5634	-3.8517	0.000117306	0.000257068	
AGAP000571	CLIPC5	CLIP-domain serine protease	10.8570501	-2.165583685	0.5998	-3.6106	0.000305454	0.000630656	
AGAP002377	AGAP002377	fatty-acid amide hydrolase 2	68.9084911	-2.163506379	0.3091	-6.9998	2.5633E-12	1.17684E-11	
AGAP008311	AGAP008311	acylphosphatase	7988.93375	-2.161992961	0.2504	-8.6338	5.93622E-18	3.89722E-17	
AGAP002419	CYP4D22	cytochrome P450	1923.83179	-2.160518349	0.0876	-24.671	2.1876E-134	3.1707E-132	
AGAP004730	AGAP004730	phospholipase A2, venom	19.4809999	-2.159578666	0.3953	-5.463	4.68228E-08	1.49228E-07	
AGAP001111	AGAP001111	nan	471.415494	-2.158151069	0.205	-10.528	6.44399E-26	6.20745E-25	
AGAP007400	AGAP007400	nan	755.641709	-2.15537651	0.1853	-11.634	2.75536E-31	3.40213E-30	
AGAP012320	OBP25	odorant-binding protein 25	77.2698096	-2.154520754	0.2584	-8.3378	7.56694E-17	4.64115E-16	
AGAP000419	nan	nan	29.8116697	-2.1542553	0.3554	-6.0611	1.35205E-09	5.02273E-09	
AGAP007843	nan	nan	2508.82842	-2.146932903	0.1011	-21.226	5.4709E-100	4.5212E-98	
AGAP001264	AGAP001264	Plasma glutamate carboxypeptidase	9682.13789	-2.139077005	0.1423	-15.037	4.20384E-51	1.00775E-49	Granulocytes
AGAP028393	ssu rRNA	nan	17124.0786	-2.137588739	0.2965	-7.2087	5.65039E-13	2.71455E-12	
AGAP000300	AGAP000300	Bifunctional pyrimidine biosynthesis protein (PyrABCN)	3883.62761	-2.13416748	0.0795	-26.828	1.5227E-158	2.9887E-156	
AGAP000881	AGAP000881	aldehyde dehydrogenase family 7 member A1	4456.34368	-2.133098404	0.0716	-29.786	5.9931E-195	1.882E-192	Granulocytes
AGAP002620	MISO	mating-induced stimulator of oogenesis MISO	13.3059206	-2.127162419	0.4494	-4.733	2.21264E-06	5.95579E-06	
AGAP001650	AGAP001650	cation transport regulator-like protein 2	1404.09983	-2.124739553	0.2002	-10.611	2.65818E-26	2.61406E-25	
AGAP009285	AGAP009285	nan	575.172146	-2.12378252	0.1703	-12.471	1.07776E-35	1.56209E-34	
AGAP028491	AQP2	aquaporin	2622.49654	-2.123261447	0.2287	-9.2834	1.64145E-20	1.23318E-19	
AGAP003931	AGAP003931	nan	89.0536391	-2.12050679	0.2109	-10.056	8.66738E-24	7.57471E-23	
AGAP006009	CPR30	cuticular protein RR-1 family 30	17.0728277	-2.119690384	0.3787	-5.5974	2.176E-08	7.16284E-08	
AGAP008113	AGAP008113	nan	1100.17195	-2.119589278	0.2139	-9.9107	3.73952E-23	3.16817E-22	
AGAP000834	AGAP000834	nan	15.6386385	-2.118096973	0.4258	-4.9747	6.53363E-07	1.85962E-06	
AGAP012900	AGAP012900	nan	109.39396	-2.11366951	0.2964	-7.1317	9.91026E-13	4.6729E-12	
AGAP028653	AGAP028653	nan	16.7094924	-2.113573078	0.4028	-5.2473	1.54356E-07	4.67583E-07	
AGAP012223	nan	nan	428.887679	-2.112026931	0.1719	-12.285	1.09582E-34	1.52267E-33	
AGAP012034	AGAP012034	nan	298.621047	-2.110518824	0.2595	-8.1338	4.15994E-16	2.45556E-15	
AGAP004742	AGAP004742	Pyruvate carboxylase [Source:UniProtKB/TrEMBL;Acc:A7UUW7]	9558.43452	-2.106403767	0.1597	-13.187	1.03766E-39	1.71205E-38	AM granulocytes
AGAP010066	AGAP010066	nan	558.200174	-2.104753471	0.2562	-8.2155	2.11199E-16	1.26491E-15	
AGAP028470	AGAP028470	nan	8.91645284	-2.103492404	0.5561	-3.7827	0.000155167	0.000334515	
AGAP006821	AGAP006821	acetyl-CoA acyltransferase 2	7478.7622	-2.098850418	0.1901	-11.042	2.40893E-28	2.60557E-27	
AGAP013078	AGAP013078	Plasma glutamate carboxypeptidase precursor	71.6591333	-2.097192675	0.2216	-9.4634	2.97979E-21	2.32968E-20	
AGAP001991	nan	nan	10.2003167	-2.094781512	0.586	-3.575	0.000350277	0.00071707	
AGAP007315	AGAP007315	nan	753.192575	-2.09397512	0.2065	-10.139	3.71041E-24	3.30083E-23	
AGAP004700	AGAP004700	nan	416.744629	-2.093142641	0.2482	-8.4324	3.38527E-17	2.12476E-16	
AGAP000130	nan	nan	5.44505255	-2.092342209	0.5987	-3.4948	0.000474493	0.000953743	
AGAP006278	AGAP006278	nan	13581.1932	-2.086522229	0.0655	-31.854	1.1709E-222	5.2528E-220	Granulocytes
AGAP008967	AGAP008967	calcium/calmodulin-dependent 3',5'-cyclic nucleotide phosphodieste	107.393113	-2.086261108	0.2924	-7.1353	9.66081E-13	4.55756E-12	
AGAP013192	AGAP013192	venom allergen	17.0219767	-2.085497543	0.3864	-5.3973	6.76602E-08	2.11911E-07	
AGAP005586	AGAP005586	nan	11.1820093	-2.085485398	0.5688	-3.6664	0.000245949	0.00051571	
AGAP012006	AGAP012006	Protein phosphatase 1 regulatory subunit 16A [Source:UniProtKB/Trl	173.707427	-2.084268535	0.1802	-11.569	5.92785E-31	7.20598E-30	
AGAP004890	AGAP004890	ribose-phosphate pyrophosphokinase	8852.92536	-2.083813712	0.158	-13.191	9.92841E-40	1.64386E-38	
AGAP012435	AGAP012435	nan	15.6197647	-2.08339812	0.3835	-5.4323	5.56293E-08	1.7569E-07	
AGAP000629	AGAP000629	nan	23.8618019	-2.083250723	0.3235	-6.4401	1.19419E-10	4.85561E-10	
AGAP008717	AGAP008717	hydroxymethylglutaryl-CoA lyase	520.615658	-2.082417529	0.1793	-11.613	3.55499E-31	4.36088E-30	
AGAP000090	AGAP000090	adenylate cyclase	1948.60327	-2.080296444	0.207	-10.049	9.31266E-24	8.12248E-23	
AGAP003167	AGAP003167	NAD(P) transhydrogenase	1535.80979	-2.080269361	0.1178	-17.661	8.34232E-70	3.35868E-68	
AGAP002992	AGAP002992	Carbonic anhydrase [Source:UniProtKB/TrEMBL;Acc:Q5TU56]	1392.54205	-2.079466438	0.1968	-10.566	4.27788E-26	4.15913E-25	
AGAP011518	AGAP011518	nan	24.3270571	-2.077310625	0.3884	-5.349	8.84174E-08	2.73917E-07	
AGAP008051	SAP1	sensory appendage protein 1	5638.92957	-2.076512063	0.2105	-9.8655	5.87431E-23	4.92804E-22	
AGAP005507	nSyb	synaptic vesicle-associated integral membrane protein	79.0111676	-2.074773617	0.181	-11.465	1.98279E-30	2.37355E-29	
AGAP006512	nan	nan	110.440291	-2.074064219	0.2843	-7.2943	3.00213E-13	1.46015E-12	
AGAP009433	AGAP009433	arylformamidase	907.898295	-2.07304017	0.2937	-7.0572	1.6988E-12	7.89173E-12	
AGAP001936	AGAP001936	phosphatidylinositol phospholipase C, beta	237.607847	-2.072051026	0.1885	-10.992	4.15409E-28	4.43212E-27	
AGAP000129	AGAP000129	nan	69.638292	-2.071984736	0.1994	-10.391	2.71112E-25	2.55415E-24	
AGAP013443	AGAP013443	Plasma glutamate carboxypeptidase	108.119815	-2.071928878	0.1693	-12.236	2.00547E-34	2.77031E-33	
AGAP006132	AGAP006132	ganglioside-induced differentiation-associated-protein 1	111.53105	-2.070212766	0.1752	-11.814	3.29319E-32	4.19826E-31	
AGAP002632	AGAP002632	nan	10674.1222	-2.068286741	0.2431	-8.5067	1.7888E-17	1.1433E-16	AM granulocytes
AGAP006731	nan	nan	8.65256326	-2.066824188	0.5161	-4.0043	6.21956E-05	0.000141294	
AGAP003283	AGAP003283	atrial natriuretic peptide receptor A	24.3287584	-2.066317297	0.3369	-6.1331	8.61977E-10	3.26525E-09	
AGAP005865	AGAP005865	fumarylacetoacetase	3370.03313	-2.063049793	0.1288	-16.022	8.92832E-58	2.67028E-56	Oenocytoids
AGAP010367	nan	nan	140.777242	-2.062172048	0.2229	-9.2509	2.22549E-20	1.66268E-19	
AGAP007636	AGAP007636	phosphatidate phosphatase LPIN	2381.53633	-2.062107291	0.1664	-12.393	2.85874E-35	4.09304E-34	
AGAP011317	AGAP011317	nan	7508.68761	-2.061480433	0.2178	-9.4641	2.96155E-21	2.31926E-20	
AGAP006908	AGAP006908	nan	276.466364	-2.060194817	0.2114	-9.7458	1.92275E-22	1.57378E-21	
AGAP002194	AGAP002194	1D-myo-inositol-triphosphate 3-kinase	1155.23353	-2.060069468	0.0836	-24.651	3.5995E-134	5.138E-132	
AGAP011062	AGAP011062	GLOBIN domain-containing protein [Source:UniProtKB/TrEMBL;Acc:(	35.0196878	-2.059952927	0.2494	-8.26	1.45708E-16	8.77695E-16	
AGAP005183	AGAP005183	nan	451.147516	-2.057479912	0.2324	-8.8523	8.57642E-19	5.84226E-18	
AGAP000249	AGAP000249	mannosyl-glycoprotein endo-beta-N-acetylglucosaminidase	24190.3946	-2.05668358	0.1607	-12.796	1.73325E-37	2.67687E-36	Oenocytoids
AGAP009417	AGAP009417	nan	7.27352313	-2.052987884	0.5719	-3.5901	0.0003306	0.000679001	
AGAP004232	AGAP004232	pellino	1462.74894	-2.050918804	0.258	-7.9499	1.86699E-15	1.06149E-14	
AGAP009648	AGAP009648	2-oxo-4-hydroxy-4-carboxy-5-ureidoimidazoline decarboxylase	1149.88975	-2.046919414	0.2289	-8.9438	3.75945E-19	2.62743E-18	
AGAP001690	AGAP001690	nan	12.1928332	-2.046676305	0.4324	-4.7336	2.20626E-06	5.94031E-06	
AGAP002378	AGAP002378	Adenylosuccinate lyase [Source:UniProtKB/TrEMBL;Acc:Q7QBZ6]	3550.03286	-2.046063833	0.2044	-10.011	1.36952E-23	1.18045E-22	
AGAP000768	AGAP000768	Septin 4 [Source:UniProtKB/TrEMBL;Acc:A0A1S4G9T6]	54.721443	-2.042753052	0.2127	-9.6045	7.65258E-22	6.1778E-21	
AGAP001257	AGAP001257	UTP--glucose-1-phosphate uridylyltransferase	7912.21303	-2.041670623	0.156	-13.084	4.06898E-39	6.63215E-38	
AGAP003239	AGAP003239	nan	593.849156	-2.041349275	0.2561	-7.9721	1.55975E-15	8.89495E-15	
AGAP000806	AGAP000806	Angiopoietin-like 1	4950.15451	-2.039105955	0.0944	-21.601	1.7461E-103	1.5971E-101	
AGAP008138	AGAP008138	nan	8.29291267	-2.038910263	0.5414	-3.7663	0.000165684	0.000355723	
AGAP007757	AGAP007757	Gustatory receptor [Source:UniProtKB/TrEMBL;Acc:Q7PIY0]	42.4383324	-2.038875842	0.2814	-7.2444	4.34501E-13	2.10027E-12	
AGAP002068	AGAP002068	nan	111.485108	-2.034382171	0.2654	-7.6667	1.76426E-14	9.3693E-14	
AGAP009786	AGAP009786	phosphoribosylamine--glycine ligase / phosphoribosylglycinamide fo	3517.44325	-2.034314259	0.1794	-11.339	8.4086E-30	9.75583E-29	
AGAP000481	AGAP000481	cyanogenic beta-glucosidase	308.242708	-2.033760652	0.1819	-11.183	4.96101E-29	5.54421E-28	
AGAP007304	AGAP007304	nan	12.5422352	-2.030801082	0.459	-4.4243	9.67432E-06	2.41499E-05	
AGAP001065	AGAP001065	glycine hydroxymethyltransferase	6907.60554	-2.030513674	0.1874	-10.835	2.35607E-27	2.43383E-26	
AGAP010733	AGAP010733	Vanin-like protein 1	976.750068	-2.023907092	0.1783	-11.35	7.40834E-30	8.60592E-29	
AGAP012557	AGAP012557	nan	141.642617	-2.020568992	0.1793	-11.269	1.87319E-29	2.12875E-28	
AGAP000366	AGAP000366	nan	21.0535763	-2.018835092	0.3807	-5.3036	1.1351E-07	3.47765E-07	
AGAP000198	Cht5-5	Chitinase [Source:UniProtKB/TrEMBL;Acc:A0A1S4G846]	8.17446088	-2.017481331	0.5173	-3.9001	9.61601E-05	0.00021351	
AGAP003586	AGAP003586	Phosphate carrier, mitochondrial	5065.702	-2.017271645	0.2432	-8.2937	1.09798E-16	6.6693E-16	
AGAP003141	AGAP003141	Insulin-related peptide binding protein	349.295186	-2.01487268	0.1762	-11.436	2.77389E-30	3.30377E-29	

AGAP010042	AGAP010042	solute carrier organic anion transporter family member	21.0389471	-2.013165455	0.3254	-6.1858	6.17889E-10	2.36631E-09
AGAP001515	AGAP001515	nan	423.014864	-2.012263574	0.2512	-8.0115	1.13334E-15	6.52239E-15
AGAP001200	AGAP001200	glycogen debranching enzyme	2019.46101	-2.008162939	0.1894	-10.605	2.82763E-26	2.77338E-25
AGAP004793	AGAP004793	ornithine--oxo-acid transaminase	92.9537762	-2.006348426	0.2092	-9.5893	8.86788E-22	7.14054E-21
AGAP005662	AGAP005662	acyl-CoA dehydrogenase	10248.125	-2.004762998	0.177	-11.326	9.73147E-30	1.12079E-28
AGAP006513	nan	nan	210.228167	-2.004080989	0.1764	-11.364	6.3446E-30	7.39758E-29
AGAP002429	CYP314A1	cytochrome P450	38.4907408	-2.003366386	0.2933	-6.8304	8.46568E-12	3.74437E-11
AGAP001550	AGAP001550	sodium-coupled monocarboxylate transporter 1	198.112491	-2.001364547	0.2249	-8.8995	5.61224E-19	3.87631E-18